Prostasin regulates PD-L1 expression in human lung cancer cells

Li-Mei Chen[1]*, Julius C. Chai[1], Bin Liu[3], Tara M. Strutt[2], K. Kai McKinstry[2] and Karl X. Chai[1]

Burnett School of Biomedical Sciences

[1]Division of Cancer Research

[2]Division of Immunity and Pathogenesis

University of Central Florida College of Medicine, Orlando, FL, USA

[3]Department of Epigenetics and Molecular Carcinogenesis, Division of Basic Science Research, The University of Texas MD Anderson Cancer Center, Smithville, TX, USA

*Corresponding author:

Li-Mei Chen, M.D., Ph.D.

Burnette School of Biomedical Sciences

Division of Cancer Research,

College of Medicine

University of Central Florida

Orlando, FL 32816-2364, USA

E-mail address: Limei.Chen@ucf.edu

Phone: 407-823-3585

Abstract

The serine protease prostasin is a negative regulator of lipopolysaccharide-induced inflammation and has a role in the regulation of cellular immunity. Prostasin expression in cancer cells inhibits migration and metastasis, and reduces epithelial-mesenchymal transition. Programmed death-ligand 1 (PD-L1) is a negative regulator of the immune response and its expression in cancer cells interferes with immune surveillance. The aim of this study was to investigate if prostasin regulates PD-L1 expression. We established sublines over-expressing various forms of prostasin as well as a subline deficient for the prostasin gene from the Calu-3 human lung cancer cells. We report here that PD-L1 expression induced by interferon-gamma (IFNγ) is further enhanced in cells over-expressing the wild-type membrane-anchored prostasin. The PD-L1 protein was localized on the cell surface and released into the culture medium in extracellular vesicles (EVs) with the protease-active prostasin. The epidermal growth factor-epidermal growth factor receptor (EGF-EGFR), protein kinase C (PKC), and mitogen-activated protein kinase (MAPK) participated in the prostasin-mediated up-regulation of PD-L1 expression. A Gene Set Enrichment Analysis (GSEA) of patient lung tumors in The Cancer Genome Atlas (TCGA) database revealed that prostasin and PD-L1 regulate common signaling pathways during tumorigenesis and tumor progression.

Keywords: PRSS8, CD274, extracellular vesicles, interferon-gamma, immune checkpoint.

Introduction

Lung cancer remains as the second most diagnosed cancer for both men and women, and the leading cause of cancer-related death in the US, with 235,760 new cases and 131,880 deaths estimated for 2021 [1]. These current facts and figures represent an annual decrease of 2% in incidents since the mid-2000s, and a greater decline in percent deaths since 1990, as a result of smoking cessation campaigns and improved diagnosis and treatments. Non-small cell lung cancers (NSCLCs) constitute the majority of lung cancers, at 84%. Surgery, chemotherapy and radiation are the treatment options for early-stage NSCLCs. Advanced-stage patients are treated with chemotherapy, molecular-targeting drugs and/or immunotherapy. Despite the efforts and advances, the 5-year survival rate for lung cancer remains low at 21% overall and 25% for NSCLCs. Localized lung cancers have a 59% 5-year survival rate but only 17% of lung cancers are diagnosed at this stage. New drug targets and treatment strategies are required to further improve lung cancer survival.

Immunotherapy regimes targeting the immune checkpoint molecules programmed cell death protein 1 (PD-1) and programmed death-ligand 1 (PD-L1, CD274) are showing great promises in treating lung cancers, especially in patients with pretreated advanced NSCLC. The main functions of PD-L1 are the inhibition of T cell proliferation, induction of immune cell apoptosis, and suppression of T cell cytokine secretion. These actions are mediated by PD-L1 binding to its receptor PD-1, which is expressed on activated T cells, B cells, and myeloid cells. This mechanism normally acts in tissues to limit autoimmune reactions or immune destruction that could be caused by overly robust inflammatory responses [2-4]. However, this pathway is also used by tumor cells to evade immune elimination and can promote tumor progression [5,6]. The cytokine interferon gamma (IFNγ) is a strong inducer of PD-L1 expression [7]. Tumor-infiltrating lymphocytes present in the tumor microenvironment are a major source of IFNγ to increase tumor cell PD-L1 expression [8,9].

Nivolumab (targeting PD-1), pembrolizumab (targeting PD-1) and atezolizumab (targeting PD-L1) are examples of blocking antibodies to overcome this regulatory blockade during cancer treatment, in combination with other regimens. Clinical trials in pretreated advanced NSCLC patients indicated a longer median overall survival (OS), a higher median duration of response (DOR), a longer median progression-free survival (PFS), and a higher median overall response rate (ORR) when compared with the standard-of-care chemotherapy, e.g., docetaxel [10].

The trypsin-like serine protease prostasin (PRSS8) is extracellularly tethered on the epithelial cell membrane via a glycosylphosphatidylinositol (GPI) anchor [11-13]. Prostasin is expressed in all normal epithelial cells and low-grade tumors, but often down-regulated in high-grade tumors [14] and during inflammation [15]. We have previously established a role for prostasin in reducing inflammation [15-17], suppressing tumor cell invasion and metastasis [18-20], and in inhibiting the epithelial-mesenchymal transition [21]. We have also identified prostasin as a regulator of cytokine and reactive oxygen species production including IFNγ, tumor necrosis factor alpha (TNF-α), and the inducible nitric oxide synthase (iNOS), all of which are implicated for a role in the tumor microenvironment and progression [22].

In this study, we intended to investigate if prostasin, as a regulator of the inflammatory cytokines, has a role in the regulation of PD-L1 expression. A human NSCLC cell line, Calu-3, was used as a model to establish stable sublines expressing the human prostasin or its functional variants via lentiviral transduction. A stable subline with the prostasin gene knocked-out via gene editing

was also established. In these stable Calu-3 sublines we evaluated PD-L1 expression changes with or without IFNγ stimulation. The signaling pathways mediating prostasin regulation of PD-L1 expression were investigated, including the epidermal growth factor (EGF)-epidermal growth factor receptor (EGFR) axis, protein kinase C (PKC), and the mitogen-activated protein kinase (MAPK). The relationship of prostasin and PD-L1 in lung tumors was further explored in patient specimens using data from The Cancer Genome Atlas (TCGA).

Materials and Methods

Cell culture

The Calu-3 (ATCC® HTB-55™) human lung adenocarcinoma cell line, the Beas-2B (ATCC® CRL-9609™) human normal lung epithelial cell line, and the PC-3 (ATCC® CRL-1435™) and DU-145 (ATCC® HTB-81™) human prostate carcinoma cell lines were purchased from the ATCC (American Type Culture Collection, Manassas, VA). The human telomerase reverse transcriptase (hTERT)-immortalized B6Tert-1 normal human trophoblast cell line was a gift of Dr. Yanling Wang (Institute of Zoology, Beijing, China) [23]. Tissue culture flasks and dishes were purchased from Sarstedt, Inc. (Newton, NC). Transwell® inserts for air-liquid cell cultures were purchased from Corning Inc. (Corning, NY). Fetal bovine serum (FBS) was purchased from Sigma-Aldrich (St. Louis, MO). Other cell culture media and reagents were purchased from Thermo Fisher Scientific (Waltham, MA). The parent Calu-3 cells and the genetically-engineered sublines were cultured in Eagle's minimum essential medium (EMEM) supplemented with 10% FBS and sodium pyruvate. The Beas-2B cells were cultured in the bronchial epithelial cell growth basal medium (BEBM, Cat. No. CC-3171, Lonza/Clonetics Corporation, Basel, Switzerland) supplemented with the additives from the BEGM Kit (Cat. No. CC-3130, Lonza/Clonetics). The PC-3 and DU-145 cells were maintained as described previously [18]. All cells were incubated at 37ºC in a humidified atmosphere of 5% CO_2 in air.

Chemicals and antibodies

The PKC inhibitor Gö 6976 (selective for PKCα and PKCβ1, Product No. 365253-1ML) and MEK inhibitor U0126 (Product No. 19-147) were purchased from Calbiochem/MilliporeSigma (St. Louis, MO). The tyrosine kinase inhibitor lapatinib was purchased from Santa Cruz Biotechnology (Dallas, TX, Cat. No. sc-202205).

The commercial antibodies were purchased from Cell Signaling Technology, Inc. (Danvers, MA): PD-L1 (Cat. No. 13684P), pSTAT1 (Cat. No. 8826S, 7649S), total STAT1 (Cat. No. 9175S), pERK1/2 (Cat. No. 9101S); or Santa Cruz Biotechnology: GAPDH (Cat. No. sc-32233), EGFR (Cat. No. sc-03), total ERK (Cat. No. sc-94), CD63 (Cat. No. sc-5275), Alix (Cat. No. sc-53540), Tsg101 (Cat. No. sc-7964), HSP70 (Cat. No. sc-24); or MilliporeSigma (St. Louis, MO): CMTM6 (Cat. No. HPA026980), beta-tubulin (Cat. No. T4026); pPKCα (Cat. No. 06-822); or BD Biosciences (San Jose, CA): PKCα (Cat. No. 610107). The human prostasin antibody was described previously [13]. The anti-EGFR monoclonal antibody cetuximab/Erbitux was generously provided by ImClone Systems (Bridgewater, New Jersey) and the anti-Her2 monoclonal antibody trastuzumab/Herceptin was generously provided by Genentech (South San Francisco, CA). For all Western blots the antibodies were used at the dilution ratio of 1:1,000.

Antibodies used for flow cytometry: Allophycocyanin (APC)-conjugated mouse anti-human CD274 (B7-H1 PD-L1) antibody (BioLegend, San Diego, CA; #329708, clone 29E.2A3, mouse IgG2b, *k*), APC mouse IgG2b, *k* isotype control antibody (BioLegend, #400322, clone MPC-11), goat anti-rabbit IgG-cyanine Cy™2 fluorophore-conjugated secondary antibody (Jackson ImmunoResearch Laboratories, Inc., West Grove, PA; Code: 111-225-144).

Establishment of Calu-3 sublines

The cDNAs coding for the wild-type human prostasin and the protease-dead variant were described previously [23]. The prostasin cDNA in the lentiviral vector contained only the coding sequence (nucleotides 230-1261 in NM_002773). The cDNA coding for the GPI-anchor-free prostasin variant was engineered via PCR-mediated deletion of the GPI-anchor signal coding sequence (nucleotides 1196-1258). The cDNAs coding for prostasin and the variants were subcloned into the pLVX-Puro vector (Clontech laboratories, Inc., Mountain View, CA) to produce lentiviruses for transduction of the Calu-3 cells. The CRISPR/Cas9 All-in-One Lentivector set with a PRSS8 gRNA (Cat. No. K1733205) or a Scrambled gRNA (Cat. No. K010) was purchased from Applied Biological Materials Inc. (Richmond, BC Canada) for knocking out the prostasin gene in the Calu-3 cells. Lentiviral production and transduction of cells were carried out as described previously [23]. Each subline was established by culturing the transduced cells in puromycin (5 µg/ml) for two weeks, and maintained as a polyclonal mixture from an initial 50-100 drug-resistant colonies.

Reverse-transcription and real-time quantitative polymerase chain reaction (RT-qPCR)

Total cellular RNA was extracted using the Trizol reagent (Invitrogen, Carlsbad, CA) according to the manufacturer's protocol. One microgram of total RNA from each sample was subjected to reverse-transcription using the iScript cDNA Synthesis Kit (Cat. No. 170-8891, Bio-Rad, Hercules, CA) and one-fifth of the iScript product was used for each gene-specific qPCR, using the iQ SYBR Green Supermix (Cat. No. 170-8882, Bio-Rad). For quantitative comparisons between samples the relative expression levels were used with either glyceraldehyde 3-phosphate dehydrogenase (GAPDH) or beta-actin copy numbers as the reference. The PCR primers for GAPDH and beta-actin were described previously [15,16]. The PCR primers for human PD-L1 and PD-L2 were adopted from previous reports [24,25].

SDS-polyacrylamide gel electrophoresis (PAGE) and Western blot analysis

Cells were lysed in a lysis buffer (20 mM Tris-Base at pH 7.6, 150 mM NaCl, 1% NP-40, 10% glycerol) containing a cocktail of inhibitors, or subjected to Triton™ X-114 detergent-phase separation as described previously [13]. Triton™ X-114 extraction is a common method used to enrich for GPI-anchored membrane proteins [26], such as prostasin. Briefly, $5x10^5$ cells were lysed in 0.2 ml of lysis buffer prepared with TBS (10 mM Tris-HCl at pH 7.5 and 150 mM NaCl) containing 1% Triton™ X-114 and a protease inhibitor cocktail. The cells were extracted for 30 minutes at 4°C with gentle shaking, then spun at 12,000 x g for 15 minutes to clear the debris. The Triton™ X-114 detergent was clouded out from the lysate supernatant during an incubation at 37°C for 3 minutes. The detergent phase (containing membrane-anchored proteins) was then separated from the aqueous phase (containing soluble proteins) via a brief centrifugation at 300 x g for 3 minutes at the room temperature. The clouding procedure was repeated to further purify the detergent phase free of the aqueous phase. The detergent phase was then resuspended in the original volume of TBS for further analysis. The total protein concentrations were determined using the Pierce™ BCA Protein Assay Kit (Thermo Fisher Scientific).

Samples (20-40 micrograms per sample) were mixed with the sample buffer, resolved on polyacrylamide gels, transferred to a nitrocellulose membrane (Thermo Fisher Scientific), and blotted with the appropriate antibodies. To blot for prostasin and CD63, the samples were mixed with a sample buffer without reducing agents for the electrophoresis.

Extracellular vesicle (EV) isolation, detergent-phase separation and protease activity binding assay

Equal numbers of cells ($5x10^5$) were cultured and the conditioned media were collected for EV isolation. Three methods were carried out for EV isolation. First, the Invitrogen Total Exosome Isolation Reagent (Cat. No. 4478359) was used following the manufacturer's protocol. Briefly, conditioned media were centrifuged at 2,000 x g for 30 minutes to remove cell debris and large vesicles. The supernatant was then mixed with the reagent at 4°C overnight. The EV pellet was collected by centrifugation at 10,000 x g for 1 hour at 4°C. The pellet was washed briefly and gently with phosphate-buffered saline (PBS) once and resuspended in PBS at 1/10th of the starting medium volume. Second, polyethylene glycol (PEG, Thermo Fisher Scientific) was used as described [27] with modifications. Spun media were mixed with a PEG solution to reach a final concentration of 8.3 percent. The mixture was incubated at 4°C overnight and taken through the same centrifugation procedures described above. Third, the PEG-precipitated EVs were resuspended in PBS and subjected to ultracentrifugation at 100,000 x g for 90 minutes to further eliminate protein carryover from the culture medium. The isolated EVs were subjected to the protease activity binding assay or detergent-phase separation [13], followed by analysis using SDS-PAGE and Western blotting. The integrity of the isolated EVs was examined by Western blotting using antibodies against EV markers, i.e., CD63, Alix, Tsg101 and HSP70 [28,29] and by flow cytometry [30]. We did not find significant differences in the properties of EVs in the binding assay and the phase separation experiments using EVs isolated from the three different methods. We used both FBS-containing and FBS-free conditioned media for EV isolation and we observed similar results in our experiments.

Flow cytometry

Cell surface labeling: Membrane-surface protein staining was performed according to suggestions from the manufacturers of the antibodies, or as described previously [31]. Briefly, cells were detached from culturing plates with 0.05% trypsin and 0.53 mM EDTA, washed with the growth medium containing 10% FBS and resuspended in the labeling buffer (PBS plus 10% FBS and 0.09% sodium azide). The PD-L1-APC or isotype-APC antibodies were added to the cell suspension at a ratio of $1x10^6$ cells per 5 µl of the antibody in 100 µl of the staining buffer. Cells were incubated on ice for 20 minutes in the dark, followed by washing in the labeling buffer twice, resuspending in fluorescence-activated cell sorting (FACS) buffer (PBS containing 0.2% BSA and 0.02% sodium azide) and flow cytometry analysis. For cell-surface staining of prostasin, the prostasin antibody was added into the cell suspension at a ratio of $1x10^6$ cells per 1 µl of the antibody in 100 µl of the staining buffer. Cells were incubated on ice for 30 minutes, washed with the labeling buffer twice, and then resuspended in the labeling buffer containing the Cy™2-labeled secondary antibody (at 1:100 dilution) for another 30 minutes on ice in the dark. For double antibody cell-surface staining, cells were labeled, in sequence, with the

prostasin antibody, a goat anti-rabbit IgG-Cy2, and then PD-L1-APC or isotype-APC. Cells were washed in between the antibody staining steps, and then washed at the end of the staining, resuspended in the FACS buffer before flow cytometry analysis. A pre-immune rabbit serum was used as a control for cell-surface labeling of prostasin. A mock staining with the Cy™2-labeled secondary antibody alone (omitting the primary antibody) was also performed on cells as a control.

EV labeling: The isolated EVs were labeled with CellTrace™Violet (Cat. No. C34557, Thermo Fisher Scientific). The labeling procedure was performed as suggested by the manufacturer. Briefly, the isolated EVs were incubated with the CellTrace reagent at a final concentration of 5 μM for 20 minutes at 37°C. The mixture was diluted with PBS or the FACS buffer and subjected to flow cytometry analysis.

Flow cytometry was performed using a CytoFLEX S Flow Cytometer with the laser configuration of V2B2Y3R2 and operated by the CytExpert Software v2.3 (Beckman Coulter, Brea, CA). The violet side scatter (VSSC) detector configuration was set for the detection of EVs [31].

Gene Set Enrichment Analysis (GSEA) and Pathway Analysis

The RNA-seq Firehose data for lung squamous cell carcinoma (LUSC) and lung adenocarcinoma (LUAD) in The Cancer Genome Atlas (TCGA) Research Network (https://www.cancer.gov/tcga) were downloaded by using the Bioconductor package "RTCGAToolbox" [32]. We extracted the normalized raw counts from the datasets with the FirehoseAnalyzeDates as "20160128". An R script developed in-house classified the majority of the RNA-seq samples into three groups: samples with high PRSS8 expression (top 25%), high CD274 expression (top 25%), and low expression of both PRSS8 and CD274 (bottom 50% for both PRSS8 and CD274). The gene set enrichment analysis (GSEA) version 4.0.2 developed by the Broad Institute and the Hallmark gene sets from the Molecular Signatures Database (MSigDB) were utilized. Further comparisons of the enriched gene sets with <25% false discovery rate (FDR) for the PRSS8-high and CD274-high groups were performed and represented with Venn diagrams.

The rank ordered gene lists from GSEA with the ranking score threshold as 0.25 were further subjected to pathway analysis. Data were analyzed with the Ingenuity Pathway Analysis (IPA) developed by QIAGEN Inc. [33]. The hierarchical clustering heatmap of the identified pathways was generated with a z-score cutoff of 2.

Statistical analysis

Data were expressed as mean ± standard deviations (SD). Student *t* test was used to compare the mean fluorescence intensities (MFI) before and after treatments, in which, a *p* value less than 0.05 is considered statistically significant. One-way Analysis of variance (ANOVA) coupled with Tukey's HSD (Honestly Significant Difference) post hoc test was used to determine statistical significance when comparing three or more independent groups, in which, a *p* value less than 0.05 was considered statistically significant.

Results

Generation of Calu-3 human lung cancer cell sublines expressing prostasin variants or with prostasin knockout (KO)

To determine the effect of prostasin expression changes on the expression of PD-L1, we established Calu-3 sublines over-expressing a wild-type human prostasin (P), an active-site mutant prostasin (M), a secreted active prostasin variant lacking the GPI-anchor (G), or the lentiviral vector-alone (V) as a control. We also established a Calu-3 subline with the prostasin gene knocked-out (KO) via CRISPR/Cas9 editing using a lentiviral vector and a control subline (CC) with a scrambled guide RNA. The differential prostasin/variant expression was ascertained in the Calu-3 sublines by Western blotting, and the results are shown in Figure 1A. The over-expressed prostasin protein can be readily detected in the sublines over-expressing the wild-type prostasin (P, Lane 5) or the protease-dead mutant prostasin (M, Lane 6). The subline over-expressing the secreted prostasin (G, Lane 7) has a moderate level of the prostasin protein in the cell lysate. Prostasin protein expression was not detected in the subline with the prostasin gene knocked out (KO, Lane 3) while baseline levels were detected in the parent Calu-3 cells (Lane 1) and in the vector control sublines (CC and V, Lanes 2 and 4).

The P and M forms of prostasin could be extracted from the cell membrane by means of Triton™ X-114 detergent-phase separation [13], confirming their membrane anchorage (Figure 1A, middle panel). As GPI-anchored proteins can be released from cells in the form of extracellular vesicles (EVs) [34,35], we analyzed and show in Figure 1A (bottom panel) the presence of prostasin in the isolated EVs. In Figure 1B, the CD63 protein was used as a marker for the Triton™ X-114-extracted membrane fractions and for the isolated EV fractions. The amount of beta-tubulin protein was used as a loading control for the total cell lysate analyzed in each sample.

Prostasin potentiates IFNγ-induced PD-L1 expression in the Calu-3 lung cancer cells

Inflammatory cytokines such as IFNγ can induce PD-L1 expression [36,37], while prostasin is a negative regulator of IFNγ expression [15]. With the Calu-3 sublines expressing various functional forms of prostasin we investigated the expression of PD-L1 with or without IFNγ stimulation. The Calu-3 cells do not express detectable amounts of PD-L1, but an over-expression of the wild-type prostasin in the Calu-3 cells induced PD-L1 protein expression without any IFNγ treatment (Figure 2A, top panel, Lane 5). Similar results were also observed with normal human lung epithelial cells (Beas-2B) when prostasin was constitutively over-expressed (Supplementary Figure 1A, Lanes 2 and 5) and with normal human trophoblast cells (B6Tert-1) (Supplementary Figure 1B, Lane 5) when prostasin over-expression was induced by tetracycline (tet). The Beas-2B and B6Tert-1 cells express readily detectable endogenous PD-L1, which was enhanced by the over-expression of the wild-type prostasin. The active-site mutant prostasin (M) and the secreted active prostasin lacking the GPI-anchor (G) were unable to induce PD-L1 expression in the Calu-3 cells (Figure 2A, top panel, Lanes 6 and 7).

The PD-L1 protein became readily detected in all the cell types when treated with IFNγ, as shown in Figure 2A (middle three panels). The increased PD-L1 protein expression in the treated cells lasted for at least 96 hours after the IFNγ stimulation (Figure 2B), indicating a low

turnover rate [38,39]. PD-L1 expression was further increased in the Calu-3 subline over-expressing the wild-type prostasin as a GPI-anchored active membrane protease (Lane 5). But this enhancement was not observed in the sublines expressing either the inactive (M, Lane 6), or the GPI-anchor-free prostasin (G, Lane 7). Along with the up-regulation of the PD-L1 protein, the PD-L1 mRNA expression was also up-regulated by the IFNγ treatment, and was further increased only in the Calu-3P subline (Figure 2C, filled bars). The mRNA of another PD-1 ligand, PD-L2 (PDCD1LG2, programmed cell death 1 ligand 2) was also up-regulated by the IFNγ treatment (Figure 2C, unfilled bars), but the overall expression level was very low. PD-L2 protein expression was not detected by means of Western blotting under any experimental conditions.

We evaluated PD-L1 expression in the Calu-3 sublines cultured in Transwell air-liquid interface conditions to mimic the physiological context of lung epithelial cells and to allow the Calu-3 lung cells to differentiate before the IFNγ treatment [17]. For air-liquid Transwell cultures, the differentiation state of the Calu-3 cells was verified by confirming a high transepithelial electrical resistance (TEER>1,000 Ω-cm^2) measured with an Epithelial Volt/Ohm Meter (EVOM). We observed that prostasin is able to induce PD-L1 mRNA expression in the air-liquid cultures (Supplementary Figure 1C).

The IFNγ-induced over-expressed PD-L1 protein is localized on the surface of Calu-3 cells with prostasin

We performed flow cytometry to determine if the induced PD-L1 protein was on the plasma membrane of live Calu-3 cells and to quantify the cell-surface PD-L1 expression. The cells were also analyzed for the cell-surface prostasin. We first analyzed the parent Calu-3 cells treated with IFNγ. The analysis was restricted to live-gated Calu-3 cells identified by propidium iodide staining to avoid artifacts caused by non-specific staining of dead or dying cells. Live cells were further gated by FSC/SSC to discriminate doublets/cell aggregates from singlets. Double-staining for PD-L1 and prostasin revealed a uniform co-expression of these proteins, as shown in Figure 3A (Q2-UR). The double-staining signals for PD-L1 and prostasin were clearly separated from the control signals (Q2-LL), as well as the signals of single-staining for either prostasin (Q2-UL) or PD-L1 (Q2-LR).

Analysis of the cell-surface prostasin expression in the Calu-3 sublines is shown in Figure 3B. The sublines over-expressing the wild-type active prostasin (P) or the inactive mutant (M) had the strongest expression levels, while the vector controls (V and CC) and the secreted prostasin subline had moderate expression levels that fell between the KO and P/M populations. The relative levels of prostasin protein on the cell surface determined by flow cytometry were similar to those observed in the Western blot analysis of the total cell lysate (Figure 1).

We then analyzed PD-L1 expression in the Calu-3 sublines. Before the IFNγ treatment, all sublines had a background staining (Figure 3C). After the IFNγ treatment, PD-L1 expression was dramatically increased in all sublines, but the increase was the highest in the subline expressing the wild-type active prostasin (Figure 3D, Peak P). Figure 3E shows the mean fluorescent intensity (MFI) for the cell-surface PD-L1 levels from duplicate wells of each subline, along with the signal from isotype control staining (IgG), which was low across the board.

Extracellular vehicles (EVs) contain prostasin and PD-L1

By means of Western blot analysis, we detected both PD-L1 (Figure 4A, top two panels) and prostasin (Figure 4C, top panel) in the EVs isolated from the conditioned media of IFNγ-treated Calu-3 sublines. The Tsg101, Alix, CD63 and HSP70 proteins were used as markers for the EVs [29]. Similar to prostasin (Figure 1), the PD-L1 protein can also be extracted and detected in the Triton™ X-114 detergent phase (Figure 4A, second panel from top), indicating a membrane anchorage in the EVs.

The EVs were labeled with CellTrace™Violet [40] for flow cytometry and were determined to be in the size range of 0.1-0.2 μM (Figure 4B, brown box) using green-fluorescent non-violet microsphere beads as the sizing reference. The active esterases inside the exosomes would cleave and convert the non-fluorescent violet dye to the fluorescent violet dye, which subsequently reacts with amine-containing proteins in the exosomes. The covalently-bonded fluorescent dye-protein adducts were then detected in the PB450 violet channel in flow cytometry. Internalization of the membrane-permeable violet dye indicated that the membranous structures were maintained in the exosomes, and they were within the expected sizes [41,42].

The protease activity of prostasin in the EVs was ascertained by an established binding assay [13,43]. When incubated with the cognate prostasin inhibitor protease nexin-1 (PN-1), a higher molecular weight complex was formed via the binding of the prostasin active-site serine to the suicide substrate inhibitor PN-1 (Figure 4C, top panel). The over-expressed wild-type prostasin (P) in the EVs showed a strong binding activity, while the inactive mutant prostasin (M) had no binding activity. The low-level endogenous prostasin in Calu-3 and the other sublines exhibited a basal binding activity, except in the KO subline with the prostasin gene knocked out.

Prostasin increases PD-L1 expression via the EGF-EGFR axis

To investigate the signaling pathways involved in the prostasin-mediated PD-L1 up-regulation, we first assessed the role of the EGF-EGFR pathway. Previously, we showed that prostasin regulates EGFR activity [23,44] and others have shown that the activated EGFR promotes PD-L1 expression [45]. We show in Figure 5A that activation of the EGF-EGFR axis by EGF up-regulated PD-L1 expression only in the subline over-expressing the wild-type prostasin (Calu-3P, Lane 5). This up-regulation was also observed at the mRNA level (Figure 5B), indicating a transcriptional mechanism.

The Calu-3 cells express ErbB1/EGFR and ErbB2/Her2, and are sensitive to EGFR tyrosine kinase inhibitors (TKIs) and the EGFR-targeting antibody cetuximab/Erbitux [46-48]. We show in Figure 5C and D that the EGF-induced PD-L1 expression in the Calu-3P subline (Lane 1) can be partially blocked by the dual-EGFR/Her2 TKI lapatinib (Lane 2), cetuximab/Erbitux (Lane 3), and the Her2-targeting antibody trastuzumab/Herceptin (Lane 4). The programmed cell death 6-interacting protein (Alix) and the chemokine-like factor-like (CKLF) MARVEL transmembrane domain containing family member 6 (CMTM6) protein are also involved in the up-regulation of PD-L1 [49-51]. But as shown in Figure 5E, we did not observe significant changes of

expression for either Alix or CMTM6 in the Calu-3 sublines treated with EGF. We observed an increased EGFR expression in the Calu-3P cells (Figure 5E, Lane 5, and Figure 5F).

The PKC and MAPK pathways contribute to prostasin-induced PD-L1 expression

The Janus kinase/signal transducer and activator of transcription 1 (JAK/STAT1) signaling pathway is a major regulator of IFNγ-induced PD-L1 expression in many cell lines and patient samples [7,52]. In Figure 6A, we show that Stat1 was phosphorylated at both Ser727 and Tyr701 in the IFNγ-treated cells. The phosphorylation at Tyr701 diminished within 48 hours, but the phosphorylation at Ser727 remained after 48 hours. No statistically significant changes of Stat1 phosphorylation was observed across the different cell types (Figure 6B and 6C). On the other hand, phosphorylation of the extracellular signal-regulated kinases (pERK1/2) was the highest in the cells over-expressing the wild-type prostasin (Figure 6A, Lane 5; Figure 6D).

The mechanism of PD-L1 expression regulation by IFNγ is complex. An initial screening of a panel of inhibitors identified the protein kinase C (PKC) inhibitor Gö 6976 as being able to attenuate PD-L1 expression in the prostasin over-expressing cells treated with IFNγ. PKC can be activated by diacylglycerol (DAG), a product of the IFNγ-activated phospholipase C gamma 2 (PLCγ-2) [53]. In Figure 7A, we show that inhibition of PKCα by Gö 6976 greatly reduced PD-L1 expression in all Calu-3 sublines treated with IFNγ, but the expression of PD-L1 remained high only in the Calu-3P cells (top panel, Lane 8). The PKCα inhibitor was shown to have promoted ERK phosphorylation (pERK1/2) in the Calu-3P cells (Figure 7A, middle panel, Lane 8). The MEK inhibitor U0126 further inhibited the IFNγ-induced PD-L1 expression in these cells, synergistically with the PKCα inhibition by Gö 6976, as shown in Figure 7B.

We evaluated the status of the PKCα protein in the Calu-3 sublines and show that the prostasin over-expression reduced the level of total PKCα in the Calu-3P cells (Figure 8A and B), with a corresponding reduction in the phosphorylation of Ser657 in PKCα (Figure 8C). We have also observed a PKCα down-regulation by prostasin re-expression in human prostate cancer cell lines PC-3 and DU-145 (Supplementary Figure 2). The Calu-3 subline with the prostasin gene knockout (KO) had a significant increase of the phosphorylation of Ser657 in PKCα (Figure 8C).

The gene set enrichment analysis (GSEA)

To explore the functional relationships of prostasin (PRSS8) and PD-L1 (CD274), we performed GSEA to identify enriched gene sets in PRSS8-high (top 25%) or CD274-high (top 25%) patients with lung squamous cell carcinoma (LUSC). The normalized read counts of RNA-seq data were retrieved from the TCGA database [54]. We defined a patient group with a low expression (bottom 50%) of both PRSS8 and PD-L1 as the control group in the GSEA. The hypothesis that PRSS8 and CD274 may be involved in some common pathways can be supported if we observe overlapping enriched gene sets. The GSEA results with the LUSC datasets have shown that the enriched gene sets from the PRSS8-high group and the CD274-high group are substantially overlapped (Figure 9, Panel a). A total of 33 functional gene clusters were up-regulated in the CD274-high group, and among them, 31 matched the up-regulated gene sets in the PRSS8-high group. Likewise, the down-regulated gene clusters in the PRSS8-high and CD274-high groups showed a significant overlap as well (Figure 9, Panel

b). All eight down-regulated gene sets from the CD274-high group were found on the down-regulated list from the PRSS8-high group.

The common enriched gene sets suggest multiple shared signaling pathways in the patient groups with high PRSS8 or high CD274 expression. These include the IL6_JAK_Stat3 signaling and IFNγ response pathways (Figure 9, Panel c). In addition, a hierarchical clustering heatmap of pathways identified by using the Ingenuity Pathway Analysis (IPA) revealed that the ERK/MAPK signaling is shared by the PRSS8-high and the CD274-high groups (Supplementary Figure 4). These findings support our experimental results that PRSS8 is involved in the MAPK pathway. To further test the potential clinical relevance of the relationship between prostasin and PD-L1 we performed GSEA for lung adenocarcinoma (LUAD) patients (Figure 9, Panels d-e). The same common gene enrichment patterns were observed for the LUAD tumors with high expression for both PRSS8 and CD274 among the multiple signaling pathways identified in the LUSC tumors.

Discussion

PD-L1 is a major player in tumor cell evasion of immune surveillance and has been exploited as a target and a marker for cancer immunotherapy. In epithelial cancers, tumor cell PD-L1 expression is a critical factor of consideration for achieving and improving efficacy. It had been well established that the inflammatory cytokines, such as IFNγ, abundant in the tumor microenvironment, boost tumor cell PD-L1 expression. The membrane-associated extracellular serine protease prostasin is a major player in epithelial homeostasis and has a role in regulating the innate immune response and the expression of inflammatory cytokines, including IFNγ [15]. Prostasin is also involved in transcriptional and post-translational regulation of membrane proteins, in particular, growth factor receptors such as EGFR, and cytokine receptors, such as the TLR4 (toll-like receptor 4) [55]. In this study, we aimed to determine if there is a cross-talk between the cell signaling pathways regulated by prostasin and the mechanisms that regulate PD-L1 expression.

Using human NSCLC cell line Calu-3 sublines expressing various forms of prostasin or with a prostasin gene knockout, we first demonstrated the responsiveness of the PD-L1 gene to the prostasin over-expression. Without any external stimuli, the PD-L1 protein expression was induced from a null background by the wild-type prostasin, but not the protease-dead or the membrane-anchor-free, secreted prostasin variant (Figure 2). This result suggests that the prostasin-mediated up-regulation of PD-L1 requires its serine protease function, as well as the membrane anchorage. We then employed a known positive regulator of PD-L1 expression, IFNγ, to investigate if the membrane-associated prostasin could have an impact on an IFNγ induction of PD-L1 expression. Indeed, the IFNγ up-regulation of PD-L1 was greatly enhanced, also by only the wild-type prostasin and involved a transcriptional mechanism (Figure 2). In this context, an outside-in mechanism of signal intervention is postulated for prostasin, likely involving its interactions with relevant membrane proteins, i.e., growth factor receptors and cytokine receptors.

Our focus turned to the MAPK signaling pathway at first, because an activation of this pathway stabilizes the PD-L1 mRNA [56] and prostasin regulates a direct upstream growth factor receptor, EGFR [23,44]. We stimulated the cells with EGF, and a robust transcriptional up-regulation of PD-L1 was observed in the cells over-expressing the wild-type prostasin (Figure 5). The use of EGF independently of IFNγ allowed us to tease out the involvement of the MAPK signaling pathway. On the other hand, we did not observe a statistically significant change in the phosphorylation of Stat1 (Figure 6), a signal relay downstream of the IFNγ receptors. Alternatively, IFNγ signaling can activate phospholipase C gamma 2 (PLCγ-2) [53], which hydrolyzes phosphatidylinositol (3,4,5)-trisphosphate (PIP3) and generates diacylglycerol (DAG) to activate protein kinase C (PKC). The PKCα inhibitor Gö 6976 was able to tame the IFNγ induction of PD-L1 expression, but the effect was incomplete in the cells expressing the wild-type prostasin (Figure 7A). A synergistic suppression of IFNγ induction of PD-L1 was observed when the MEK inhibitor U0126 was used in combination with Gö 6976 (Figure 7B). PKCα has been shown to regulate EGFR activation and internalization [57,58]. Herein we showed that PKCα was significantly down-regulated by the wild-type prostasin (Figure 8). We postulate that the down-regulation of PKCα by prostasin could reduce EGFR internalization and ubiquitination [59], contributing to the increased PD-L1 expression in response to IFNγ via such a cross-talk to the EGFR signaling pathway. In support of this, the EGFR level in the Calu-3P subline expressing the wild-type prostasin was increased (Figure 5F).

Physiologically, prostasin protects the integrity of the epithelium by down-regulating inflammatory cytokine production, e.g., IFNγ [15,16] and by enhancing tight junction formation [17]. The endogenously expressed PD-L1 in normal epithelial cells can be viewed as a mechanism for increasing the tolerance of normal cells during an immune attack or for preventing damage caused by an overly aggressive local inflammatory response. In tumors, PD-L1 expression is up-regulated by IFNγ and other cytokines in the tumor microenvironment. The expression of PD-L1 could be further enhanced and sustained by the presence of prostasin in tumor cells. It is possible that the co-expression of prostasin in PD-L1-positive tumor cells may sensitize the cells to the anti-PD-L1 antibodies in immunotherapy targeting the PD-1/PD-L1 checkpoint. Indeed, reports have shown that higher PD-L1 staining in tumor cells is associated with a higher response rate and improved efficacy in PD-1/PD-L1 blockade therapy [60,61]. Whether PD-L1 expression is up-regulated in prostasin-positive tumor cells in patients would then warrant further investigation.

An interrogation into the TCGA database revealed that prostasin (PRSS8) and PD-L1 (CD274) are involved in common pathways in both lung squamous cell carcinoma (LUSC) and lung adenocarcinoma (LUAD) (Figure 9). The IL6_JAK_Stat3 signaling and IFNγ response pathways are shared in PRSS8-high and CD274-high patients. It is possible that prostasin participates in the IL-6_JAK-Stat3 pathway via activation of the MAPK pathway as it cross-talks with the IL-6-JAK/STAT pathway [62]. We have also observed shared pathways in both LUSC and LUAD patient groups with low PRSS8 expression and low CD274 expression. The E2F_targets related pathway is among the shared pathways in the low expressors. This finding is consistent with our result that PKCα was down-regulated by PRSS8 over-expression, as PKC activation increases E2F-1 expression [63].

PD-L1 is released by metastatic melanoma and glioblastoma cancer cells in extracellular vesicles (EVs), though the physiological outcome or significance remains unclear. The dynamically changing amounts of circulating exosomes carrying PD-L1 in patients was suggested as a predictor for anti-PD-1 therapy [64,65]. In addition, antibodies can be neutralized in patient blood by the corresponding antigen in the exosomes released by cancer cells during an antibody-based immunotherapy. This competition can result in a reduced treatment efficacy, as in the case of rituximab for treating lymphoma [66]. In this study, we showed that the protease-active prostasin and PD-L1 co-localized in the EVs released by lung cancer cells. It will be interesting to learn in future studies if the active prostasin in the EVs could interfere with the PD-L1 function in immune surveillance or immune editing.

Conclusion

Prostasin is identified as a potent regulator of PD-L1 expression induced by the inflammatory cytokine IFNγ in human lung epithelial and cancer cells. This action requires the serine protease activity and the membrane anchorage and is mediated by the cross-talk between IFNγ signaling and EGF-EGFR signaling, involving PKCα, as illustrated by Nodes 1 and 2 in Figure 10. Prostasin and PD-L1 co-localize in exosomes shed from lung epithelial or cancer cells, as illustrated by Node 3 in Figure 10. Understanding the roles played by prostasin in the tumor microenvironment could provide information on if and how prostasin can be explored and developed as therapeutics or a marker for immune editing.

Data Availability

The TCGA datasets of LUSC and LUAD (Level 3) used in current study are publicly available at the TCGA Research Network (https://www.cancer.gov/tcga).

Conflicts of Interest

The authors declare no conflict of interest.

Acknowledgement

The B6Tert-1 normal human trophoblast cell line was a gift of Dr. Yanling Wang (Institute of Zoology, Beijing, China). This work was assisted by the BMS Core Facility of the BSBS/College of Medicine at University of Central Florida. This work was partially supported by the Florida Department of Health Live Like Bella Pediatric Cancer Research Initiative (20L06, on the exosomal protease analysis), Public Health Research, Biomedical Research Program; and by University of Central Florida College of Medicine to L.M.C and K.X.C. The funders had no role in the manuscript preparation and writing including the study design and data collection and analyses.

Author Contributions

L.M.C., conceptualization, investigation, formal analysis, funding acquisition, writing – original draft, review and editing. **J.C.C.,** investigation. **B.L.,** GSEA and IPA analysis, writing – review and editing. **T.M.S.,** formal analysis, writing – review and editing**. K.K.M.,** formal analysis, writing – review and editing. **K.X.C.,** conceptualization, investigation, formal analysis, funding acquisition, writing – review and editing.

Abbreviations

Beas-2B, human normal lung epithelial cell line; B6Tert-1, human telomerase reverse transcriptase (hTERT)-immortalized normal human trophoblast cell line; Calu-3, human lung adenocarcinoma cell line; CD274, cluster of differentiation 274 (PD-L1); DU145, human prostate carcinoma cell line; EGF-EGFR, epidermal growth factor-epidermal growth factor receptor; EV, extracellular vesicle; GPI, glycosylphosphatidylinositol; GSEA, Gene Set Enrichment Analysis; IFNγ, interferon-gamma; IFNGR1/2, interferon-gamma receptor protein complex; IPA, Ingenuity Pathway Analysis; LUAD: lung adenocarcinoma; LUSC, lung squamous cell carcinoma; MAPK, mitogen activated protein kinase; MEK, the MAPK/ERK kinase; NSCLC, non-small cell lung cancer; PC-3, human prostate carcinoma cell line; PD-1, programmed cell death protein 1; PD-L1, programmed death-ligand 1; PKC, protein kinase C; PRSS8, serine protease 8 (prostasin); TCGA: The Cancer Genome Atlas.

References

1. Siegel, R.L.; Miller, K.D.; Fuchs, H.E.; Jemal, A. Cancer Statistics, 2021. CA Cancer J. Clin. 2021, 71(1), 7-33.
2. Ishida, Y.; Agata, Y.; Shibahara, K.; Honjo, T. Induced expression of PD-1, a novel member of the immunoglobulin gene superfamily, upon programmed cell death. EMBO J. 1992, 11(11), 3887-95.
3. Shinohara, T.; Taniwaki, M.; Ishida, Y.; Kawaichi, M.; Honjo, T. Structure and chromosomal localization of the human PD-1 gene (PDCD1). Genomics. 1994, 23(3), 704-6.
4. Sharpe, A.H.; Wherry, E.J.; Ahmed, R.; Freeman, G.J. The function of programmed cell death 1 and its ligands in regulating autoimmunity and infection. Nat. Immunol. 2007, 8(3), 239-45.
5. Flies, D.B.; Chen, L. The new B7s: playing a pivotal role in tumor immunity. J. Immunother. 2007, 30(3), 251-60.
6. Chen, L.; Han, X. Anti-PD-1/PD-L1 therapy of human cancer: past, present, and future. J. Clin. Invest. 2015, 125(9), 3384-91.
7. Garcia-Diaz, A.; Shin, D.S.; Moreno, B.H.; Saco, J.; Escuin-Ordinas, H.; Rodriguez, G.A.; Zaretsky, J.M.; Sun, L.; Hugo, W.; Wang, X.; et al. Interferon Receptor Signaling Pathways Regulating PD-L1 and PD-L2 Expression. Cell Rep. 2017, 19(6), 1189-1201.
8. Dong, H., Zhu, G.; Tamada, K.; Chen, L. B7-H1, a third member of the B7 family, co-stimulates T-cell proliferation and inter-leukin-10 secretion. Nat. Med. 1999, 5(12), 1365-1369.
9. Loke, P.; Allison, J.P. PD-L1 and PD-L2 are differentially regulated by Th1 and Th2 cells. Proc. Natl. Acad. Sci. U. S. A. 2003, 100(9), 5336-41.
10. Somasundaram, A.; Burns, T.F. The next generation of immunotherapy: keeping lung cancer in check. J. Hematol. Oncol. 2017, 10(1), 87-98.
11. Yu, J.X.; Chao, L.; Chao, J. Prostasin is a novel human serine proteinase from seminal fluid. Purification, tissue distribution, and localization in prostate gland. J. Biol. Chem. 1994, 269(29), 18843-8.
12. Yu, J.X.; Chao, L., Chao, J. Molecular cloning, tissue-specific expression, and cellular localization of human prostasin mRNA. J. Biol. Chem. 1995, 270(22), 13483-9.
13. Chen, L.M.; Skinner, M.L.; Kauffman, S.W.; Chao, J.; Chao, L.; Thaler, C.D.; Chai, K.X. Prostasin is a glycosylphosphatidyl-inositol-anchored active serine protease. J. Biol. Chem. 2001, 276(24), 21434-42.
14. Chen, L.M.; Chai, K.X. PRSS8 (protease, serine, 8). Atlas Genet. Cytogenet. Oncol. Haematol. 2012; 16(9), 658-664.
15. Chen, L.M.; Wang, C.; Chen, M.; Marcello, M.R.; Chao, J.; Chao, L.; Chai, K.X. Prostasin attenuates inducible nitric oxide synthase expression in lipopolysaccharide-induced urinary bladder inflammation. Am J Physiol Renal Physiol. 2006, 291(3), F567-F577.
16. Chen, L.M.; Hatfield, M.L.; Fu, Y.Y.; Chai, K.X. Prostasin regulates iNOS and cyclin D1 expression by modulating protease-activated receptor-2 signaling in prostate epithelial cells. Prostate. 2009, 69(16), 1790-801.
17. Chai, A.C.; Robinson, A.L., Chai, K.X.; Chen, L.M. Ibuprofen regulates the expression and function of membrane-associated serine proteases prostasin and matriptase. BMC Cancer. 2015, 15, 1025-1038.

18. Chen, L.M.; Hodge, G.B.; Guarda, L.A.; Welch, J.L.; Greenberg, N.M.; Chai, K.X. Down-regulation of prostasin serine protease: a potential invasion suppressor in prostate cancer. Prostate. 2001, 48(2), 93-103.
19. Chen, L.M.; Chai, K.X. Prostasin serine protease inhibits breast cancer invasiveness and is transcriptionally regulated by promoter DNA methylation. Int J Cancer. 2002, 97(3), 323-9.
20. Ma, X.J.; Fu, Y.Y.; Li, Y.X.; Chen, L.M.; Chai, K.; Wang, Y.L. Prostasin inhibits cell invasion in human choriocarcinomal JEG-3 cells. Histochem. Cell Biol. 2009, 132(6), 639-46.
21. Chen, L.M.; Verity, N.J.; Chai, K.X. Loss of prostasin (PRSS8) in human bladder transitional cell carcinoma cell lines is associated with epithelial-mesenchymal transition (EMT). BMC Cancer. 2009, 9:377-388.
22. Vyas, D.; Laput, D.; Vyas, A.K. Chemotherapy-enhanced inflammation may lead to the failure of therapy and metastasis. Onco Targets Ther. 2014, 7,1015-1023.
23. Fu, Y.Y.; Gao, W.L.; Chen, M.; Chai, K.X., Wang, Y.L., Chen, L.M. Prostasin regulates human placental trophoblast cell proliferation via the epidermal growth factor receptor signaling pathway. Hum. Reprod. 2010, 25(3), 623-32.
24. Fang, M.; Meng, Q.; Guo, H.; Wang, L.; Zhao, Z.; Zhang, L.; Kuang, J.; Cui, Y.; Mai, L., Zhu, J. Programmed Death 1 (PD-1) is involved in the development of proliferative diabetic retinopathy by mediating activation-induced apoptosis. Mol Vis. 2015, 21, 901-10.
25. Meng, Q.; Yang, P.; Guo, H.; Zhang, L.; Chen, X.; Jiang, Z.; Hou, S.; Fang, M.; Cui, Y. Characteristic expression of PD-1 and its ligands mRNAs in patients with noninfectious uveitis. Int. J. Clin. Exp. Med. 2016, 9(1), 323-329.
26. Ko, Y.G.; Thompson, G.A. Jr. Purification of glycosylphosphatidylinositol-anchored proteins by modified triton X-114 partitioning and preparative gel electrophoresis. Anal. Biochem. 1995, 224(1), 166-72.
27. Weng, Y.; Sui, Z.; Shan, Y.; Hu, Y.; Chen, Y.; Zhang, L.; Zhang, Y. Effective isolation of exosomes with polyethylene glycol from cell culture supernatant for in-depth proteome profiling. Analyst. 2016, 141(15), 4640-4646.
28. Kowal, J.; Arras, G.; Colombo, M.; Jouve, M.; Morath, J.P.; Primdal-Bengtson, B.; Dingli, F.; Loew, D.; Tkach, M.; Théry ,C. Proteomic comparison defines novel markers to characterize heterogeneous populations of extracellular vesicle subtypes. Proc Natl Acad Sci U S A. 2016, 113(8), E968-77.
29. Willms, E.; Johansson, H.J.; Mäger, I.; Lee, Y.; Blomberg, K.E.; Sadik, M.; Alaarg, A.; Smith, C.I.; Lehtiö, J., El Andaloussi, S.; et al. Cells release subpopulations of exosomes with distinct molecular and biological properties. Sci Rep. 2016, 6, 22519-22530.
30. Brittain, G.C.; Chen, Y.Q.; Martinez, E.; Tang, V.A.; Renner, T.M.; Langlois, M.A.; Gulnik, S. A Novel Semiconductor-Based Flow Cytometer with Enhanced Light-Scatter Sensitivity for the Analysis of Biological Nanoparticles. Sci Rep. 2019, 9(1), 16039.
31. Tejero, J.D.; Armand, N.C.; Finn, C.M.; Dhume, K.; Strutt, T.M.; Chai, K.X.; Chen, L.M.; McKinstry, K.K. Cigarette smoke extract acts directly on CD4 T cells to enhance Th1 polarization and reduce memory potential. Cell. Immunol. 2018, 331, 121-129.
32. Samur, M.K. RTCGAToolbox: a new tool for exporting TCGA Firehose data. PLoS ONE, 2014, 9(9), e106397-106404.
33. Krämer, A.; Green, J.; Pollard, J. Jr.; Tugendreich, S. Causal analysis approaches in Ingenuity Pathway Analysis. Bioinformatics. 2014, 30(4), 523-30.
34. Chatterjee, S.; Smith, E.R.; Hanada, K.; Stevens, V.L.; Mayor, S. GPI anchoring leads to sphingolipid dependent retention of endocytosed proteins in the recycling endosomal compartment. EMBO J. 2001, 20(7), 1583-92.

35. de Gassart, A.; Geminard, C.; Fevrier, B.; Raposo, G.;Vidal, M. Lipid raft-associated protein sorting in exosomes. Blood. 2003, 102(13), 4336-44.
36. Bridge, J.A.; Lee, J.C.; Daud, A.; Wells, J.W.; Bluestone, J.A. Cytokines, Chemokines, and Other Biomarkers of Response for Checkpoint Inhibitor Therapy in Skin Cancer. Front. Med. (Lausanne). 2018, 5, 351-368.
37. Chen, S.; Crabill, G.A.; Pritchard, T.S.; McMiller, T.L.; Wei, P.; Pardoll, D.M.; Pan, F.; Topalian, S.L. Mechanisms regulating PD-L1 expression on tumor and immune cells. J. Immunother. Cancer. 2019, 7(1), 305-317.
38. Li, C.W.; Lim, S.O.; Xia, W.; Lee, H.H.; Chan, L.C.; Kuo, C.W.; Khoo, K.H.; Chang, S.S.; Cha, J.H.; Kim, T.; et al. Glycosylation and stabilization of programmed death ligand-1 suppresses T-cell activity. Nat. Commun. 2016, 7, 1263212641.
39. Wang, Y.N.; Lee, H.H.; Hsu, J.L.; Yu, D.; Hung, M.C. The impact of PD-L1 N-linked glycosylation on cancer therapy and clinical diagnosis. J. Biomed. Sci. 2020, 27(1), 77-87.
40. Morales-Kastresana, A.; Telford, B.; Musich, T.A.; McKinnon, K.; Clayborne, C.; Braig, Z.; Rosner, A.; Demberg, T.; Watson, D.C.; Karpova, T.S.; et al. Labeling Extracellular Vesicles for Nanoscale Flow Cytometry. Sci Rep. 2017, 7(1), 1878.
41. Zhang, H.; Freitas, D.; Kim, H.S.; Fabijanic, K.; Li, Z.; Chen, H.; Mark, M.T.; Molina, H.; Martin, A.B.; Bojmar, L.; et al. Identification of distinct nanoparticles and subsets of extracellular vesicles by asymmetric flow field-flow fractionation. Nat. Cell Biol. 2018, 20, 332-343.
42. Doyle, L.M.; Wang, M.Z. Overview of Extracellular Vesicles, Their Origin, Composition, Purpose, and Methods for Exosome Isolation and Analysis. Cells. 2019, 8(7), 727.
43. Chen, L.M., Zhang, X., Chai, K.X. Regulation of prostasin expression and function in the prostate. Prostate. 2004, 59(1), 1-12.
44. Chen, M.; Chen, L.M.; Lin, C.Y.; Chai, K.X. The epidermal growth factor receptor (EGFR) is proteolytically modified by the Matriptase-Prostasin serine protease cascade in cultured epithelial cells. Biochim Biophys Acta. 2008, 1783(5), 896-903.
45. Akbay, E.A., Koyama, S.; Carretero, J.; Altabef, A.; Tchaicha, J.H.; Christensen, C.L.; Mikse, O.R.; Cherniack, A.D.; Beauchamp E.M.; Pugh, T.J.; et al. Activation of the PD-1 pathway contributes to immune escape in EGFR-driven lung tumors. Cancer Discov. 2013, 3(12), 1355-63.
46. Baselga, J. The EGFR as a target for anticancer therapy-focus on cetuximab. Eur. J. Cancer 2001, 37 Suppl 4, S16-22.
47. Johnston, S.R.D.; Leary, A. Lapatinib: a novel EGFR/HER2 tyrosine kinase inhibitor for cancer. Drugs Today (Barc). 2006, 42(7), 441-53.
48. O'Donovan, N.; Crown, J. EGFR and HER-2 antagonists in breast cancer. Anticancer Res. 2007, 27(3A), 1285-94.
49. Monypenny, J.; Milewicz, H.; Flores-Borja, F.; Weitsman, G.; Cheung, A.; Chowdhury, R.; Burgoyne, T.; Arulappu, A.; Lawler, K.; Barber, P.R.; et al. ALIX Regulates Tumor-Mediated Immunosuppression by Controlling EGFR Activity and PD-L1 Presentation. Cell Rep. 2018, 24(3), 630-641.
50. Burr, M.L.; Sparbier, C.E.; Chan, Y.C.; Williamson, J.C.; Woods, K.; Beavis, P.A.; Lam, E.Y.N.; Henderson, M.A.; Bell, C.C.; Stolzenburg, S.; et al. CMTM6 maintains the expression of PD-L1 and regulates anti-tumour immunity. Nature. 2017, 549(7670), 101-105.
51. Mezzadra, R.; Sun, C.; Jae, L.T.; Gomez-Eerland, R.; de Vries, E.; Wu, W.; Logtenberg, M.E.W.; Slagter, M.; Rozeman, E.A.; Hofland, I.; et al. Identification of CMTM6 and CMTM4 as PD-L1 protein regulators. Nature. 2017, 549(7670), 106-110.

52. Gough, D.J.; Levy, D.E.; Johnstone, R.W.; Clarke, C.J. IFNgamma signaling-does it mean JAK-STAT? Cytokine Growth Factor Rev. 2008, 19(5-6), 383-94.
53. Chang, Y.J.; Holtzman, M.J.; Chen, C.C. Interferon-gamma-induced epithelial ICAM-1 expression and monocyte adhesion. Involvement of protein kinase C-dependent c-Src tyrosine kinase activation pathway. J. Biol. Chem. 2002, 277(9), 7118-26.
54. Grossman, R.L.; Heath, A.P.; Ferretti, V.; Varmus, H.E.; Lowy, D.R.; Kibbe, W.A.; Staudt, L.M. Toward a Shared Vision for Cancer Genomic Data. New Eng. J. Med. 2016, 375(12), 1109-12.
55. Uchimura, K.; Hayata, M.; Mizumoto, T.; Miyasato, Y.; Kakizoe, Y.; Morinaga, J.; Onoue, T.; Yamazoe, R.; Ueda, M.; Adachi, M.; et al. The serine protease prostasin regulates hepatic insulin sensitivity by modulating TLR4 signalling. Nat Commun. 2014, 5, 3428.
56. Stutvoet, T.S.; Kol, A.; de Vries, E.G.; de Bruyn, M.; Fehrmann, R.S.; Terwisscha van Scheltinga A.G.; de Jong S. MAPK pathway activity plays a key role in PD-L1 expression of lung adenocarcinoma cells. J. Pathol. 2019, 249(1), 52-64.
57. Stewart, J.R.; O'Brian, C.A. Protein kinase C-{alpha} mediates epidermal growth factor receptor transactivation in human prostate cancer cells. Mol. Cancer Ther. 2005, 4(5), 726-32.
58. Heckman, C.A.; Biswas, T.; Dimick, D.M.; Cayer, M.L. Activated Protein Kinase C (PKC) Is Persistently Trafficked with Epidermal Growth Factor (EGF) Receptor. Biomolecules. 2020, 10(9), 1288-1304.
59. Lei, C.T.; Wei,Y.H.; Tang, H.; Wen, Q.; Ye, C.; Zhang, C.; Su, H. PKC-α Triggers EGFR Ubiquitination, Endocytosis and ERK Activation in Podocytes Stimulated with High Glucose. Cell. Physiol. Biochem. 2017, 42, 281-294.
60. Shukuya T, Carbone DP. Predictive Markers for the Efficacy of Anti-PD-1/PD-L1 Antibodies in Lung Cancer. J. Thorac. Oncol. 2016, 11(7), 976-88.
61. Ribas, A.; Hu-Lieskovan, S. What does PD-L1 positive or negative mean? J. Exp. Med. 2016, 213(13), 2835-2840.
62. Costa-Pereira, A.P. Regulation of IL-6-type cytokine responses by MAPKs. Biochem. Soc. Trans. 2014, 42(1), 59-62.
63. Pintus, G.; Tadolini, B.; Posadino, A.M.; Sanna, B.; Debidda, M.; Carru, C.; Deiana, L.; Ventura. PKC/Raf/MEK/ERK signaling pathway modulates native-LDL-induced E2F-1 gene expression and endothelial cell proliferation Cardiovasc. Res. 2003, 59(4), 934-44.
64. Chen, G.; Huang, A.C.; Zhang, W.; Zhang, G.; Wu, M.; Xu, W.; Yu, Z.; Yang, J.; Wang, B.; Sun, H.; et al. Exosomal PD-L1 contributes to immunosuppression and is associated with anti-PD-1 response. Nature. 2018, 560(7718), 382-386.
65. Ricklefs, F.L.; Alayo. Q.; Krenzlin, H.; Mahmoud, A.B.; Speranza, M.C.; Nakashima, H; Hayes, J.L.; Lee, K; Balaj, L; Passaro, C.; et al. Immune evasion mediated by PD-L1 on glioblastoma-derived extracellular vesicles. Sci. Adv. 2018, 4(3):eaar2766-2779.
66. Aung, T., Chapuy, B.; Vogel, D.; Wenzel, D.; Oppermann, M.; Lahmann, M.; Weinhage, T.; Menck, K.; Hupfeld, T.; Koch, R. Exosomal evasion of humoral immunotherapy in aggressive B-cell lymphoma modulated by ATP-binding cassette transporter A3. Proc. Natl. Acad. Sci. U. S. A. 2011, 108(37), 15336-15341.

Figure 1

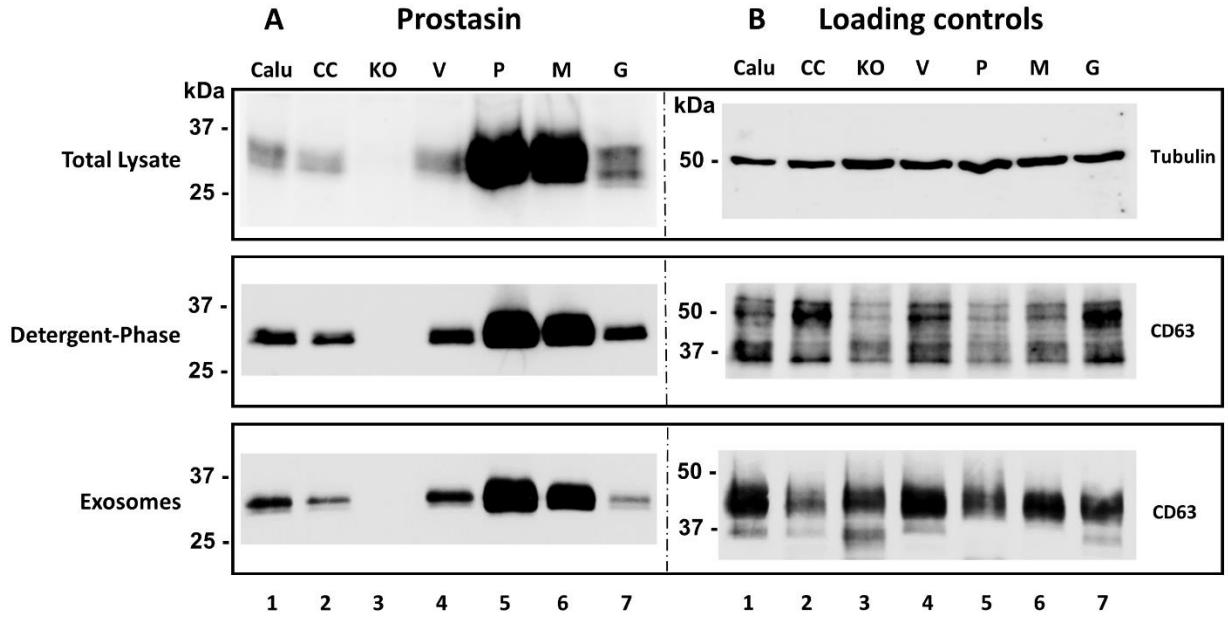

Figure 1. Western blot analysis of prostasin expression in Calu-3 sublines.

Top panel: total cell lysate, 40 µg/lane; **middle panel:** Triton™ X-114-extracted membrane fractions from 40 µg of total cell lysate; **bottom panel:** isolated exosomes from 0.5 ml conditioned-medium per sample ($2.5x10^5$ cells). **A:** Samples were immunoblotted with an antibody against human prostasin. **B:** Samples were immunoblotted with antibodies against β-tubulin (total lysate) or CD63 (membrane fractions and exosomes) as loading controls. Calu: Calu-3 parent cells, CC: Calu-3 control subline with scrambled gRNAs, KO: Calu-3 knockout subline with prostasin-specific gRNAs, V: Calu-3 subline with vector alone, P: Calu-3 subline over-expressing the wild-type prostasin, M: Calu-3 subline over-expressing an active-site mutant prostasin, G: Calu-3 over-expressing an active prostasin without the GPI-anchor.

Figure 2

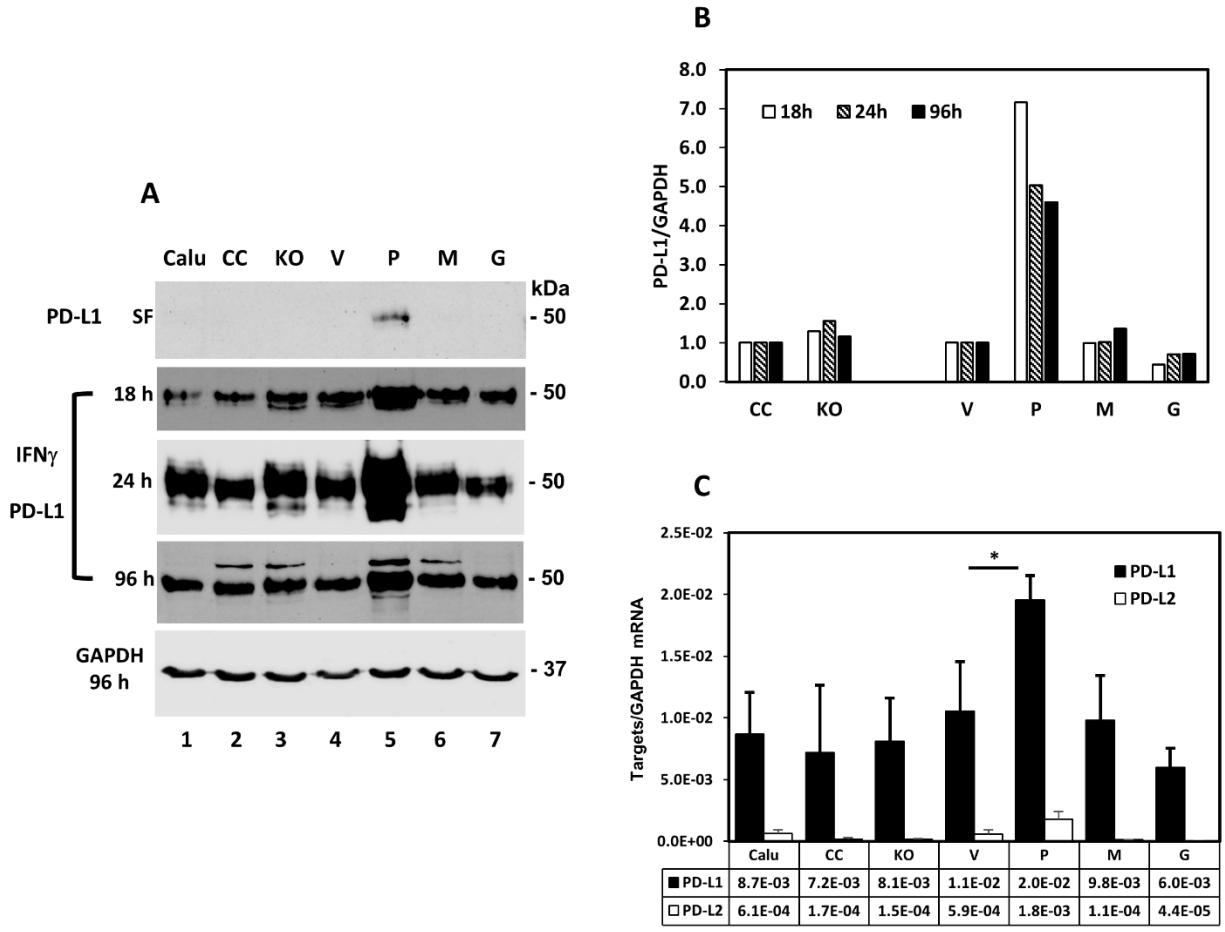

	Calu	CC	KO	V	P	M	G
PD-L1	8.7E-03	7.2E-03	8.1E-03	1.1E-02	2.0E-02	9.8E-03	6.0E-03
PD-L2	6.1E-04	1.7E-04	1.5E-04	5.9E-04	1.8E-03	1.1E-04	4.4E-05

Figure 2. Prostasin increases PD-L1 expression.

A: Western blot analysis of PD-L1 expression in Calu-3 sublines in serum free cultures (SF) or treated with IFNγ at 100 ng/ml for various times as indicated. **B:** Bar graph of IFNγ-induced PD-L1 expression in Calu-3 sublines normalized against GAPDH expression at various times shown in A. **C:** RT-qPCR analysis of PD-L1 and PD-L2 expressions normalized against the GAPDH expression. Data are presented as mean ± SD (n=3). ANOVA $p < 0.05$, * denotes $p < 0.05$ as compared to the vector control (V).

Figure 3

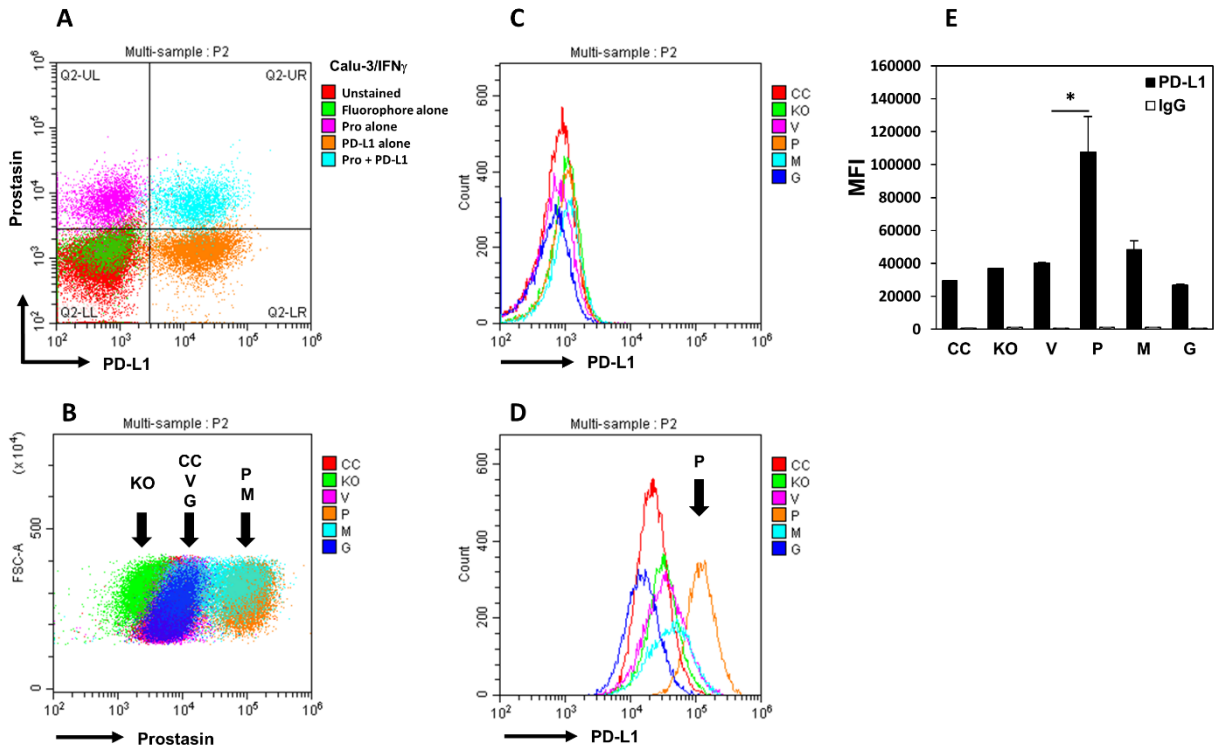

Figure 3. Flow cytometry analysis of PD-L1 and prostasin expressions in Calu-3 sublines.

A: Representative dot plot of PD-L1 (x-axis) and prostasin expressions (y-axis) in Calu-3 cells treated with IFNγ (100 ng/ml for 24 hours). Red: unstained cells. Green: secondary antibody (anti-rabbit-Cy2) and isotype IgG-APC. Magenta: prostasin antibody-labeled cells. Orange: PD-L1-APC antibody labeled-cells. Sky blue: prostasin and PD-L1 antibodies double-labeled cells. **B:** Representative dot plot of prostasin expression in Calu-3 sublines. CC (red): Calu-3 control subline with scrambled gRNAs, KO (green): Calu-3 knockout subline with prostasin-specific gRNAs, V (magenta): Calu-3 subline with vector alone, P (orange): Calu-3 subline over-expressing the wild-type prostasin, M (sky blue): Calu-3 subline over-expressing an active-site mutant prostasin, G (blue): Calu-3 over-expressing an active prostasin without the GPI-anchor. **C-D:** Histogram of PD-L1 expression in Calu-3 sublines without IFNγ treatment (**C**) or with IFNγ treatment (**D**). **E:** Mean fluorescent intensity (MFI) of PD-L1 (filled boxes) and isotype antibody (open boxes) from duplicate settings were quantified and presented in bar graphs. Data are presented as mean ± SD. ANOVA $p < 0.05$, * denotes $p < 0.05$ as compared to the vector control (V).

Figure 4

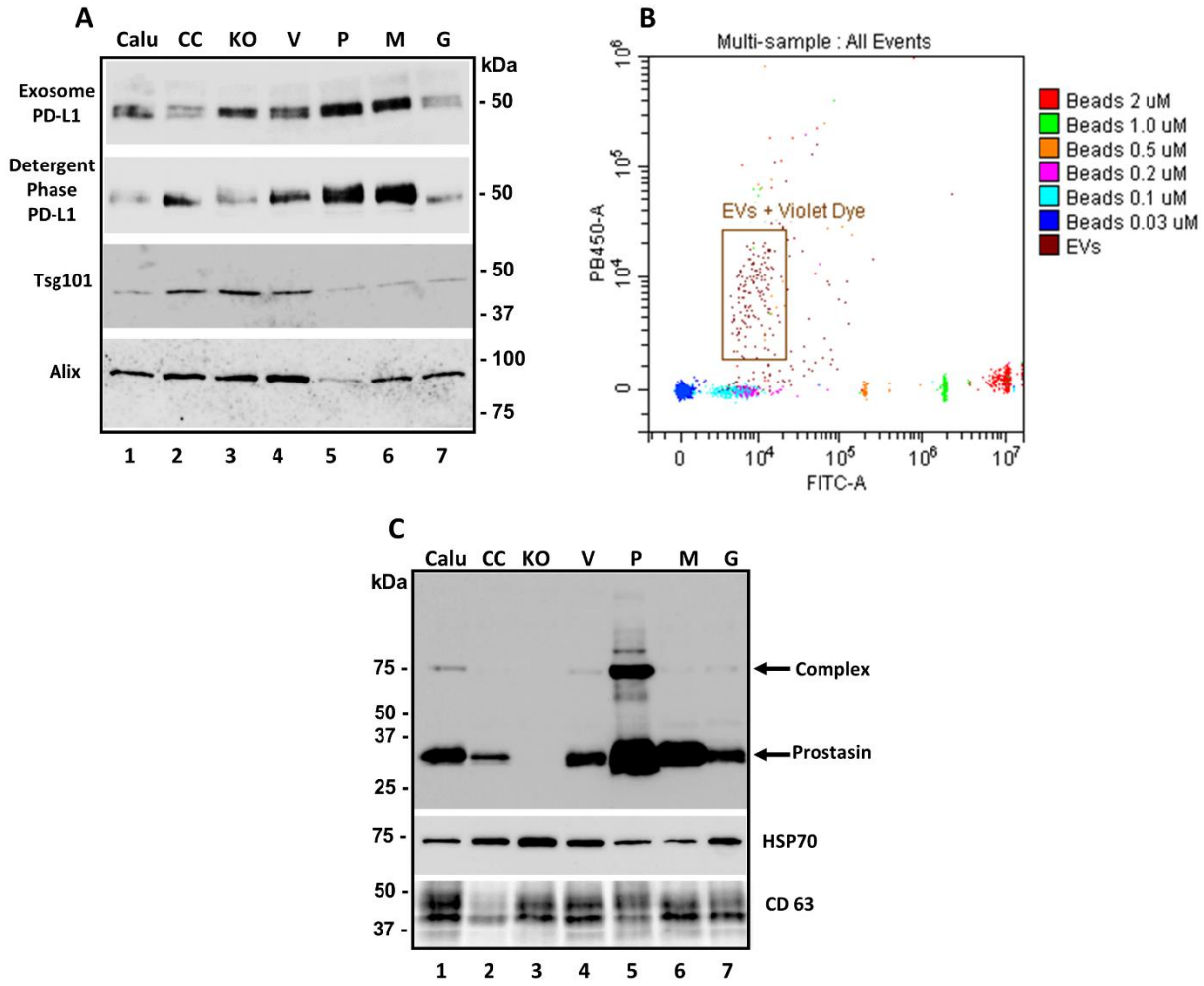

Figure 4. Identification of PD-L1 and active prostasin in exosomes (EVs) and membrane fractions.

A: Western blot analysis of PD-L1 expression in exosomes (top panel) and membrane extractions (detergent phase). Exosome markers (Tsg101 and Alix) were blotted as loading controls. **B:** Flow cytometry analysis of isolated exosomes (in brown box) labeled with a violet dye (PB450 channel) and sizing beads (0.03 µm to 2.0 µm) labeled with a green dye (FITC channel). **C:** Western blot analysis of the binding assay of exosomes with purified PN-1 [43]. The wild-type prostasin in exosomes is active and able to form a covalent bound with its cognitive inhibitor PN-1 shifting the molecular weight of prostasin from 35 kDa (prostasin alone) to 75 kDa (prostasin and PN-1 complex). HSP 70 and CD63 were blotted as loading controls for exosomes.

Figure 5

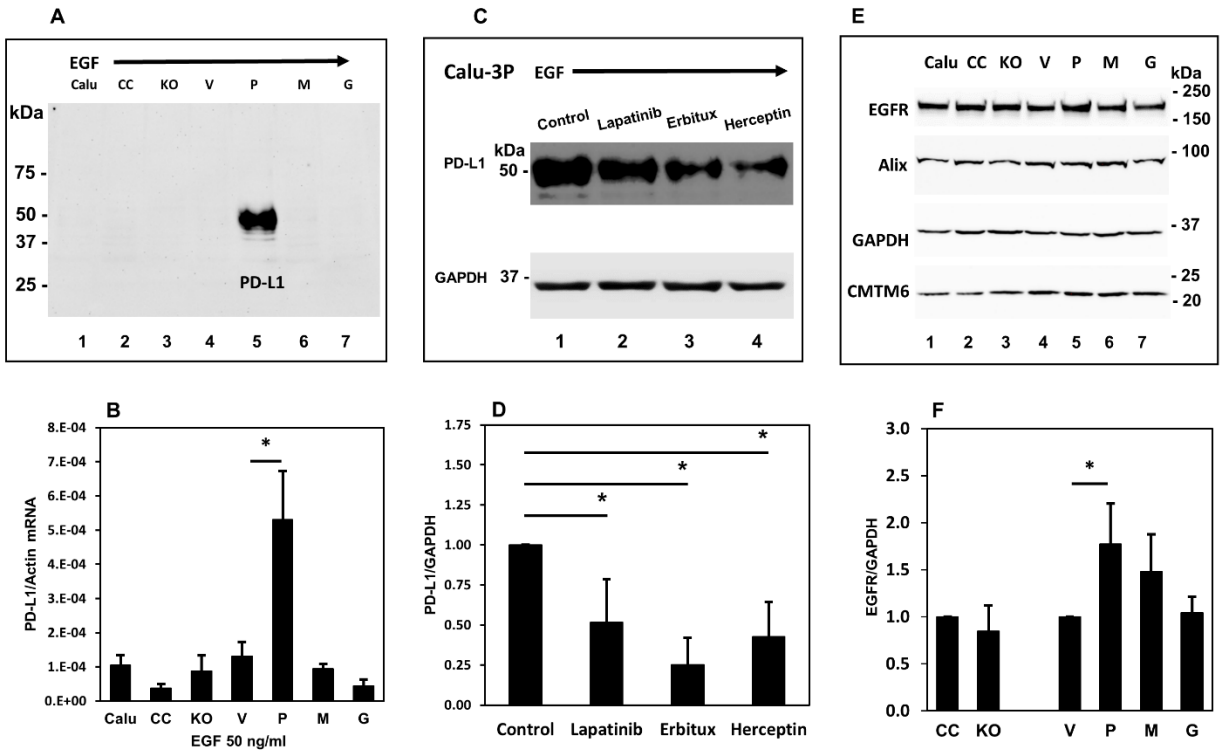

Figure 5. Prostasin up-regulates PD-L1 expression via the EGFR signaling pathway.

A: Immunoblotting of PD-L1 induced by EGF (50 ng/ml for 24 hours) in Calu-3 sublines. **B:** RT-qPCR analysis of PD-L1 expression in Calu-3 sublines treated with EGF (50 ng/ml, n=3, ANOVA $p < 0.05$, * denotes $p < 0.05$ as compared to the vector control (V). **C:** top panel, EGF-induced PD-L1 expression in Calu-3P can be inhibited by an EGFR kinase inhibitor (Lapatinib, 0.2 μM) and antibodies against EGFR (Erbitux, 40 μg/ml) and Her-2 (Herceptin, 40 μg/ml); bottom panel, immunoblotting of GAPDH as a loading control. **D:** Bar graph of C (n=4), * denotes $p < 0.05$ as compared to the control. **E:** Immunoblotting of EGFR, Alix, CMTM6 and GAPDH. **F:** Bar graph of EGFR in E (n=3), * denotes $p < 0.05$, as compared to the vector control (V).

Figure 6

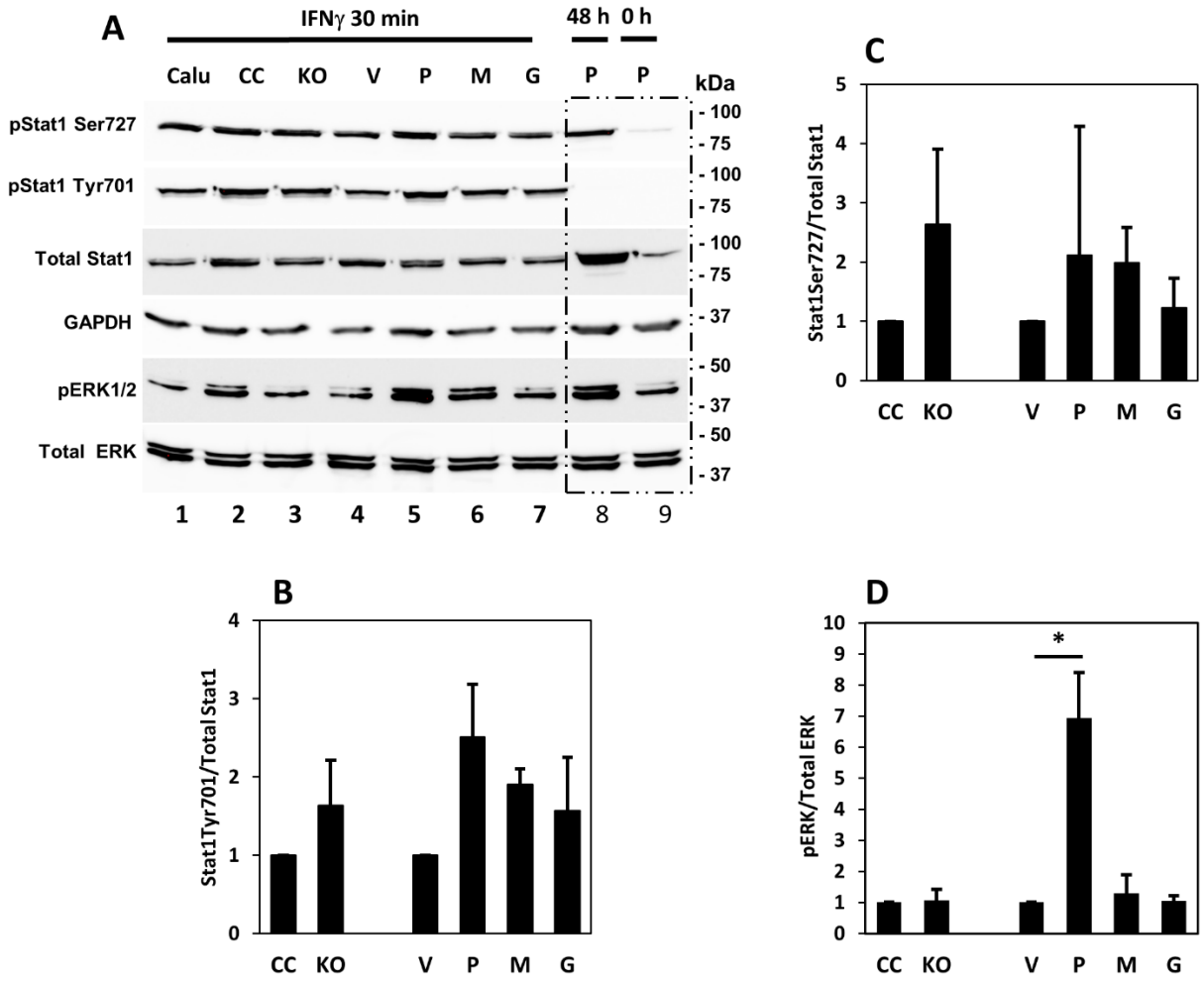

Figure 6. Prostasin activates MAPK pathway manifested by ERK1/2 phosphorylation.

A: Representative images of Western blot analysis on Calu-3 sublines treated with 100 ng/ml IFNγ for 30 minutes. Calu-3P cells without the treatment (0 hour) and with the treatment for 48 hours were used for monitoring protein phosphorylation as indicated. Both pStat1Tyr701 and pStat1Ser727 were increased upon IFNγ treatment, while phosphorylation of Stat1Ser727 sustained for at least 48 hours. **B-D:** Bar graphs of phosphorylated proteins in A, * denotes $p < 0.05$, as compared to the vector control (V).

Figure 7

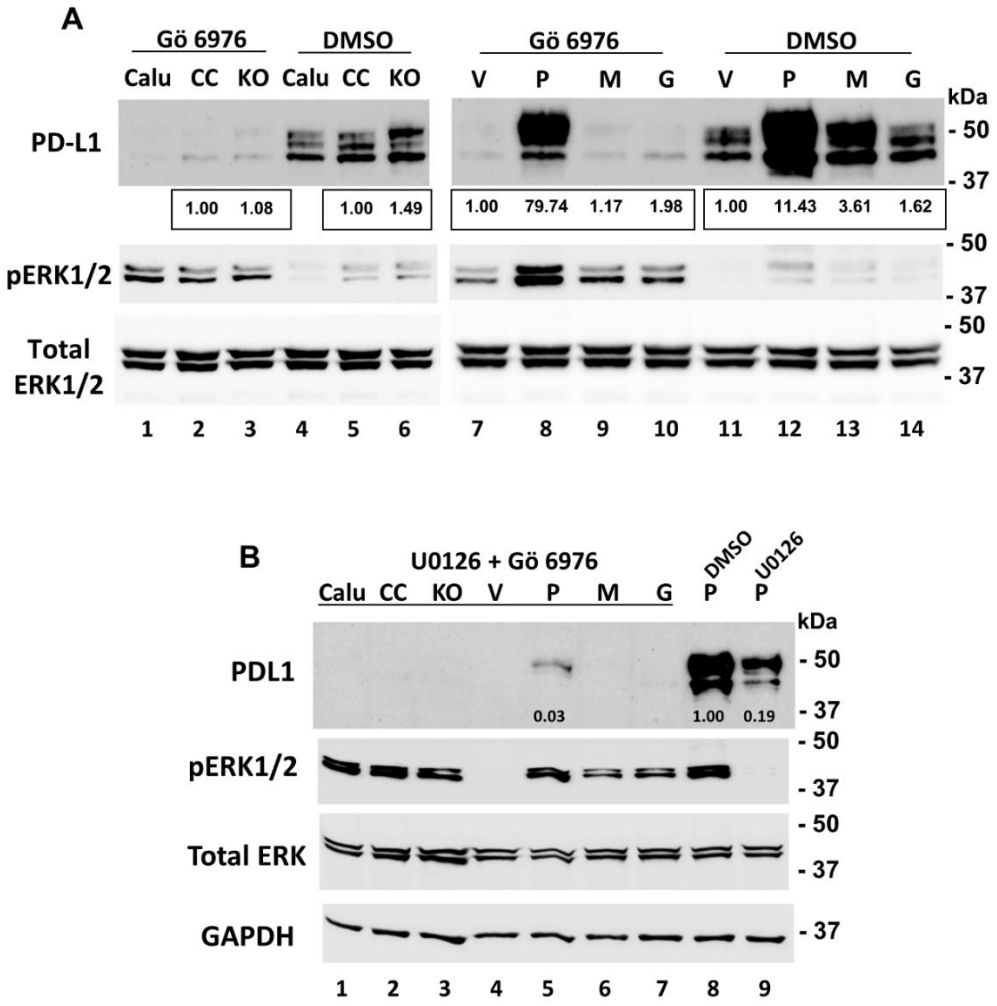

Figure 7. Prostasin up-regulates PD-L1 expression via activation of MAPK/ERK pathways.

A: Cells were treated with the PKCα inhibitor Gö 6976 (4 μM) for 30 minutes followed by IFNγ treatment (100 ng/ml) for 7 hours. Thirty micrograms of total cell lysates from each Calu-3 subline were subjected to Western blot analysis with antibodies as indicated. Inhibition of PKCα increased phosphorylated ERK1/2 content in Calu-3P (lane 8) and sustained the expression of PD-L1 (lane 8). **B:** Cells were analyzed as described in A, except cells were treated with a MEK inhibitor (U0126, 5 μM) for 15 minutes, the PKCα inhibitor Gö 6976 (4 μM) for 45 minutes and then IFNγ (100 ng/ml) for 7 hours. DMSO was used as the vehicle control for the inhibitors. Inhibition of both PKCα and ERK1/2 phosphorylation further reduced PD-L1 expression. Relative densities of the PD-L1 bands normalized against GAPDH are indicated under each band.

Figure 8

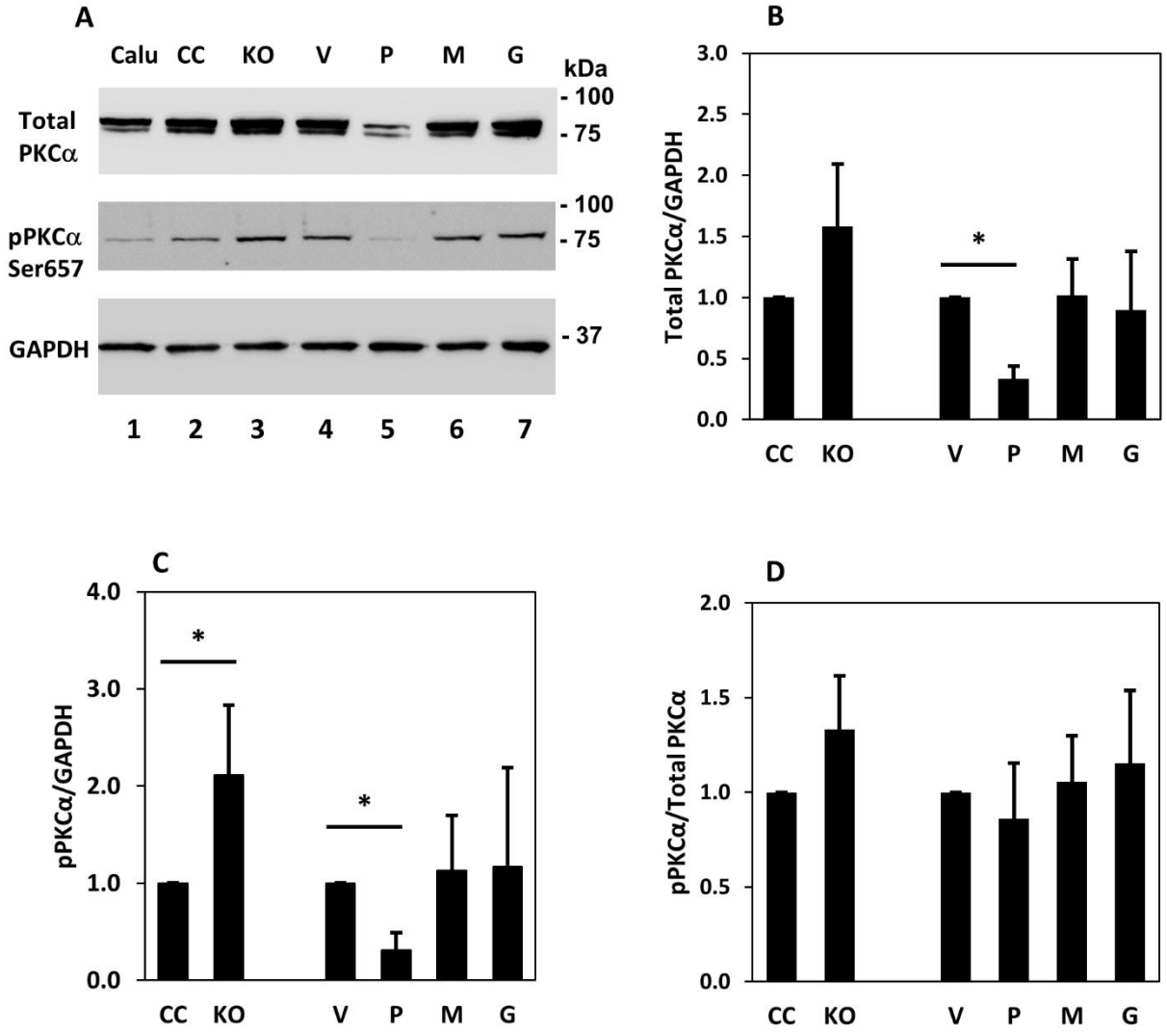

Figure 8. Prostasin down-regulates PKCα expression.

Thirty micrograms of total cell lysates from each Calu-3 subline were subjected to Western blot analysis. **A:** Reduced PKCα expression is seen only in samples over-expressing the wild-type membrane-anchored prostasin (lane 5). **B-D:** Results of four independent experiments were analyzed, quantified and presented as bar graphs: total PKCα normalized against GAPDH (**B**); phosphorylated PKCα normalized against GAPDH (**C**); ratio of phosphorylated PKCα in total PKCα content (**D**). Data are presented as mean ± SD, * denotes $p < 0.05$, as compared to the controls (CC or V).

Figure 9

a. Up-regulated Gene Sets From TCGA LUSC Patients with High PRSS8 or CD274

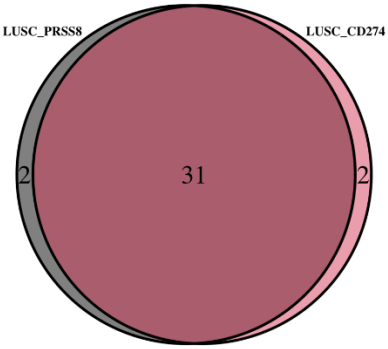

LUSC High PRSS8 Enriched Gene Sets (25% FDR)	NES	FDR q-val
HALLMARK_TNFA_SIGNALING_VIA_NFKB	2.9	0
HALLMARK_INTERFERON_GAMMA_RESPONSE	2.9	0
HALLMARK_INFLAMMATORY_RESPONSE	2.8	0
HALLMARK_IL6_JAK_STAT3_SIGNALING	2.6	0

LUSC High CD274 Enriched Gene Sets (25% FDR)	NES	FDR q-val
HALLMARK_INTERFERON_GAMMA_RESPONSE	3.7	0
HALLMARK_INTERFERON_ALPHA_RESPONSE	3.5	0
HALLMARK_INFLAMMATORY_RESPONSE	3.4	0
HALLMARK_TNFA_SIGNALING_VIA_NFKB	3.2	0

b. Down-regulated Gene Sets From TCGA LUSC Patients with High PRSS8 or CD274

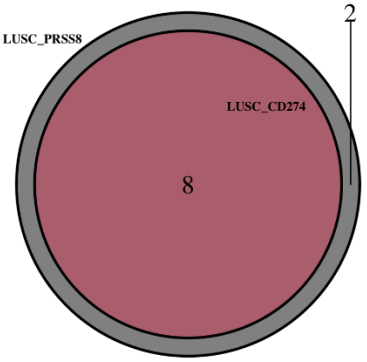

LUSC Low PRSS8 Enriched Gene Sets (25% FDR)	NES	FDR q-val
HALLMARK_E2F_TARGETS	-3.8	0
HALLMARK_G2M_CHECKPOINT	-3.6	0
HALLMARK_MYC_TARGETS_V1	-3.4	0
HALLMARK_MYC_TARGETS_V2	-3.1	0

LUSC Low CD274 Enriched Gene Sets (25% FDR)	NES	FDR q-val
HALLMARK_E2F_TARGETS	-3.0	0
HALLMARK_G2M_CHECKPOINT	-2.9	0
HALLMARK_MYC_TARGETS_V1	-2.8	0
HALLMARK_MYC_TARGETS_V2	-2.4	0

c.

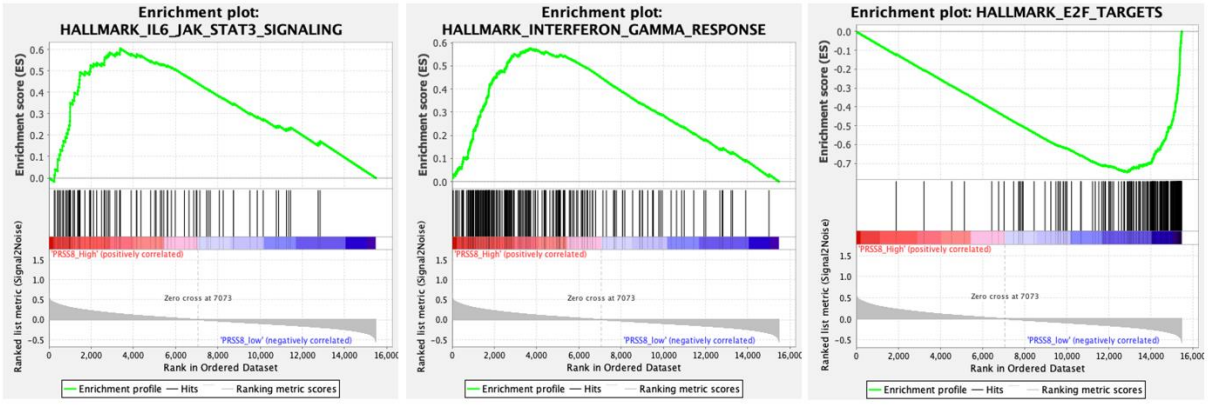

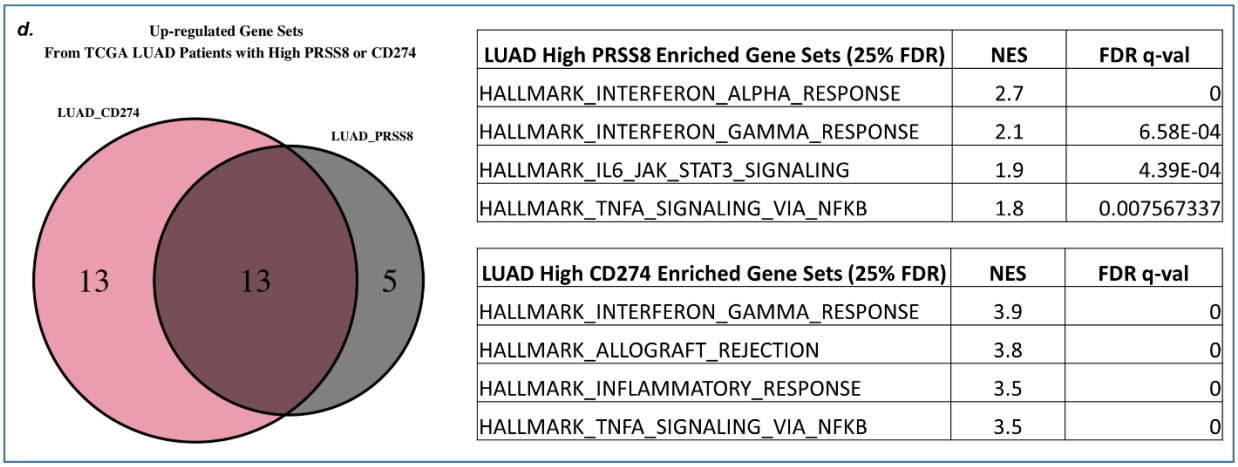

LUAD High PRSS8 Enriched Gene Sets (25% FDR)	NES	FDR q-val
HALLMARK_INTERFERON_ALPHA_RESPONSE	2.7	0
HALLMARK_INTERFERON_GAMMA_RESPONSE	2.1	6.58E-04
HALLMARK_IL6_JAK_STAT3_SIGNALING	1.9	4.39E-04
HALLMARK_TNFA_SIGNALING_VIA_NFKB	1.8	0.007567337

LUAD High CD274 Enriched Gene Sets (25% FDR)	NES	FDR q-val
HALLMARK_INTERFERON_GAMMA_RESPONSE	3.9	0
HALLMARK_ALLOGRAFT_REJECTION	3.8	0
HALLMARK_INFLAMMATORY_RESPONSE	3.5	0
HALLMARK_TNFA_SIGNALING_VIA_NFKB	3.5	0

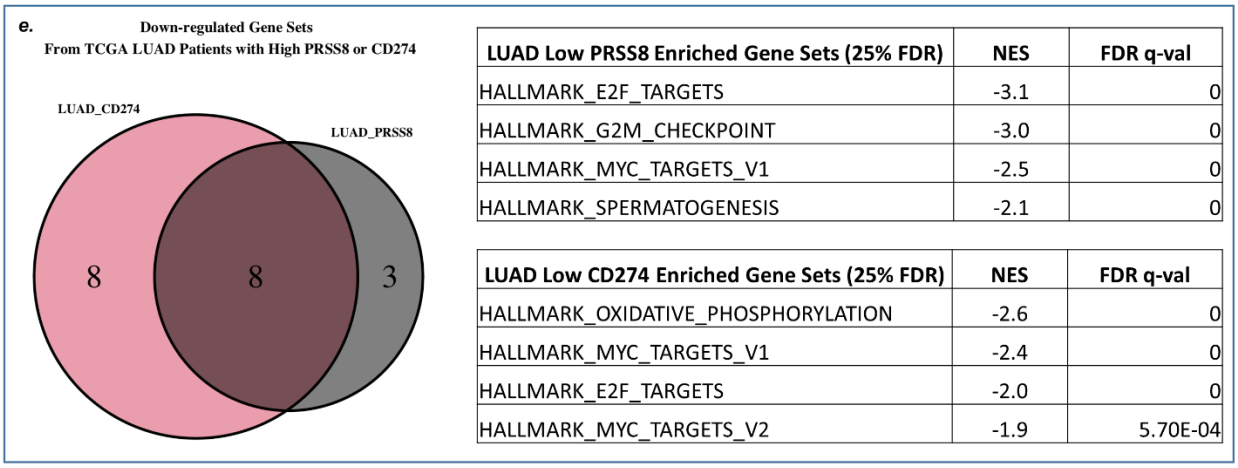

LUAD Low PRSS8 Enriched Gene Sets (25% FDR)	NES	FDR q-val
HALLMARK_E2F_TARGETS	-3.1	0
HALLMARK_G2M_CHECKPOINT	-3.0	0
HALLMARK_MYC_TARGETS_V1	-2.5	0
HALLMARK_SPERMATOGENESIS	-2.1	0

LUAD Low CD274 Enriched Gene Sets (25% FDR)	NES	FDR q-val
HALLMARK_OXIDATIVE_PHOSPHORYLATION	-2.6	0
HALLMARK_MYC_TARGETS_V1	-2.4	0
HALLMARK_E2F_TARGETS	-2.0	0
HALLMARK_MYC_TARGETS_V2	-1.9	5.70E-04

Figure 9. Gene set enrichment analysis for lung squamous cell carcinoma (LUSC, panel a-c) and lung adenocarcinoma (LUAD, panel d-e) from TCGA.

The selected top 4 gene sets are shown. The complete list of enriched gene sets is in Supplementary Figure 3 (a-h). **Panel a:** 31 out of 33 enriched gene sets from the samples with high expressed CD274 were shared with the enriched gene sets from samples with high PRSS8 expression. **Panel b:** 8 out of 8 enriched gene sets from samples with low expressed CD274 were shared with the enriched gene sets from samples with low PRSS8 expression. **Panel c:** The hallmark gene sets from the MSigDB gene sets were used. The hallmark IL6_JAK_Stat3 signaling and interferon gamma response are listed on the top shared enriched gene sets for both PRSS8 and CD274 high expression sample groups. The E2F_targets is listed on the top shared enriched gene sets for both PRSS8 and CD274 low expression sample groups. **Panel d:** 13 out of 18 enriched gene sets from the samples with high expressed PRSS8 were shared with the enriched gene sets from the samples with high CD274 expression. **Panel e:** 8 out of 11 enriched gene sets from samples with low expressed PRSS8 were shared with the enriched gene sets from the samples with low CD274 expression. All significant gene sets are defined with 25% FDR as the threshold.

Figure 10

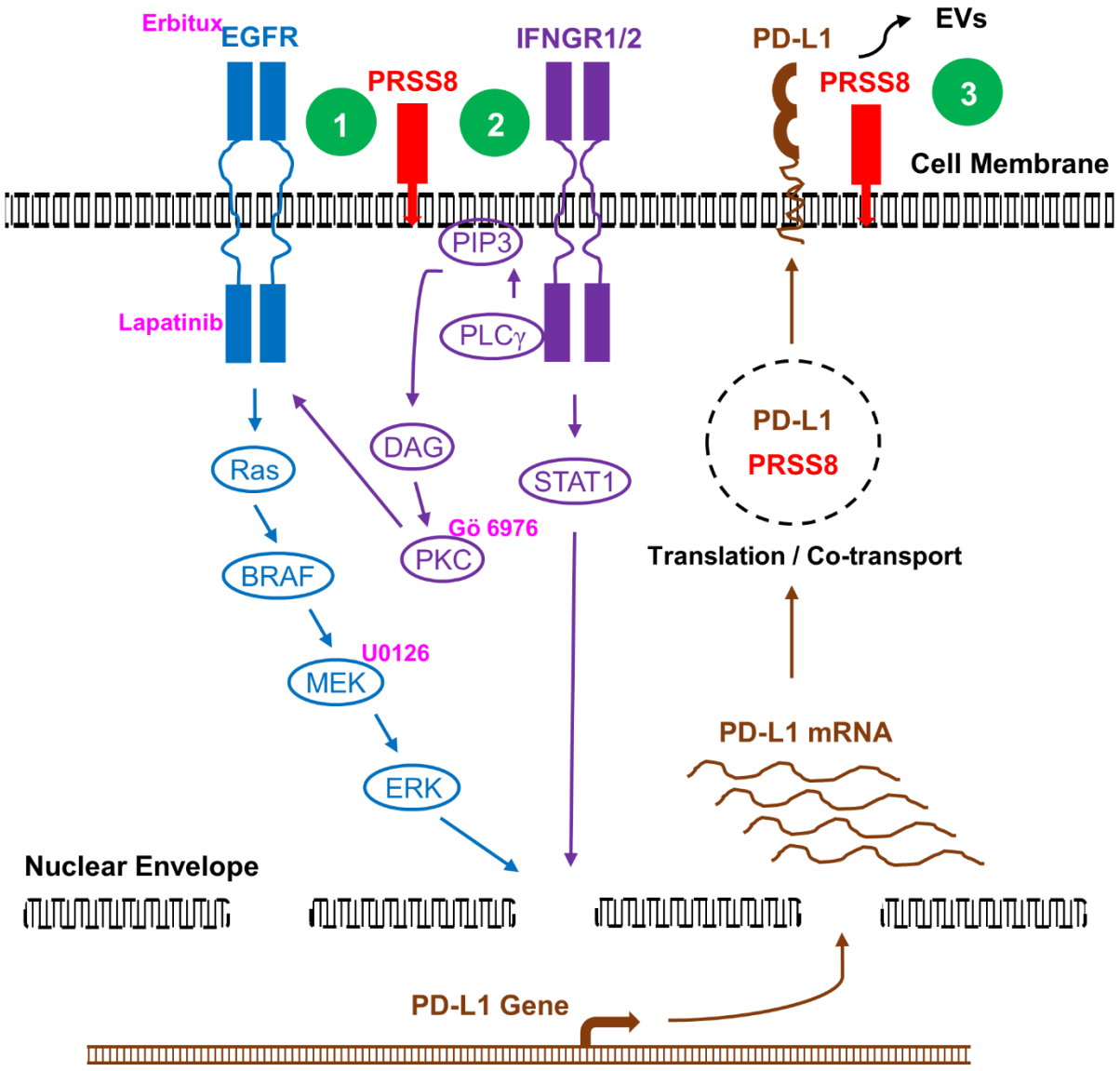

Figure 10. Signaling pathways in prostasin regulation of PD-L1 expression.

(Green) Node 1: EGFR signaling, with Erbitux and lapatinib showing effects on prostasin regulation of PD-L1 expression. **Node 2:** IFNγ signaling via PKCα, with Gö 6976 and U0126 showing effects on the prostasin-mediated potentiation of PD-L1 induction by IFNγ. **Node 3:** Prostasin and PD-L1 co-localization in exosomes.

Supplementary Materials

Supplementary Figure 1

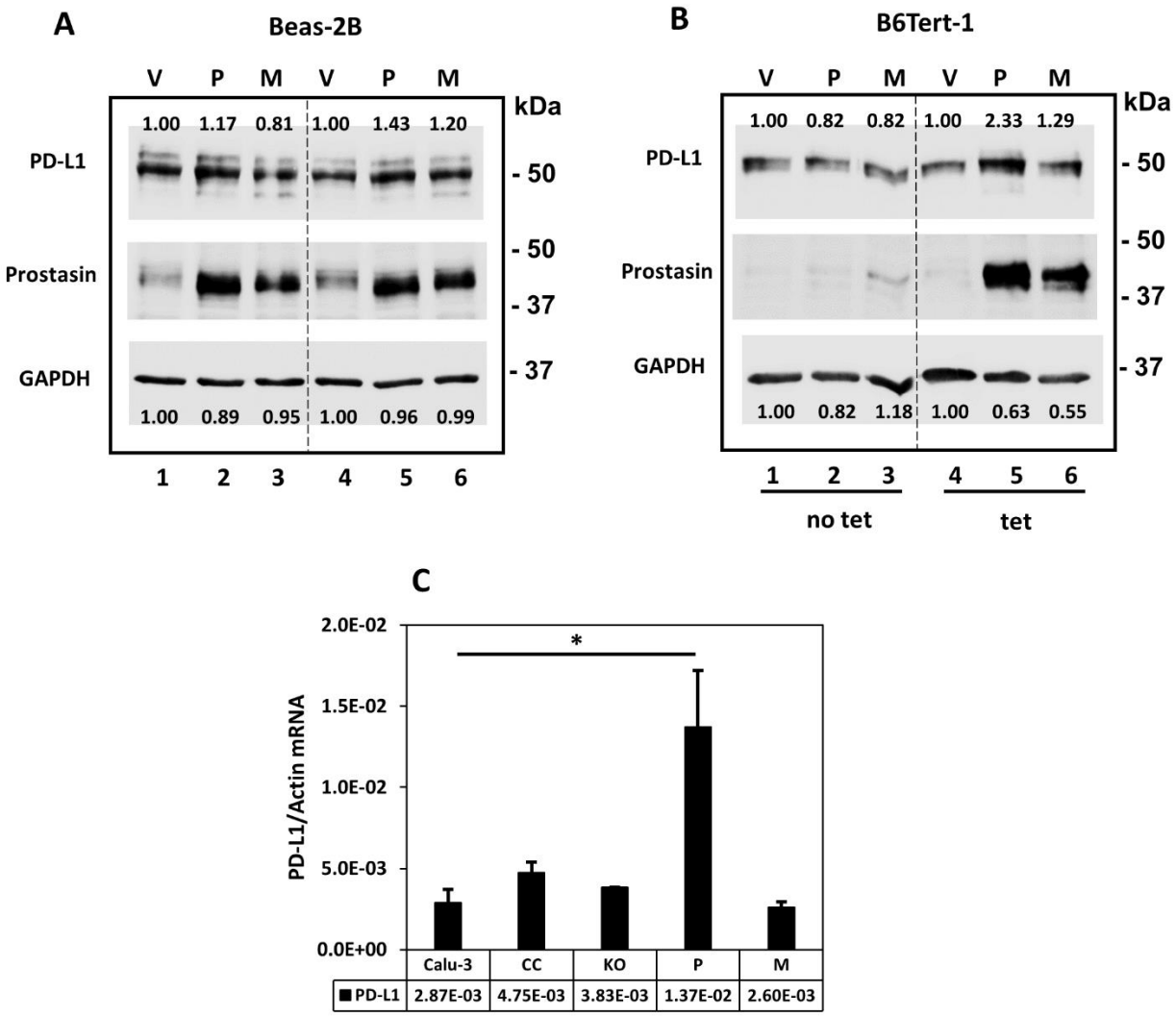

Supplementary Figure 1. Over-expression of prostasin increases PD-L1 in normal epithelial cells.

A: Beas-2B cells over-expressing the wild-type prostasin (P) or an inactive prostasin mutant (M) were analyzed by SDS-PAGE followed by Western blot analysis using various antibodies as indicated. The density of each band was quantified using the vector cells (V) as the control, and the intensity of each band is labeled above or under each band. Prostasin, reduced form, 40 kDa [11]. **B:** B6Tert-1 cells were treated the same as in A, except the expression of prostasin is under the control of tetracycline (tet). Prostasin, reduced form, 40 kDa [11]. **C:** Bar graph of PD-L1 mRNA expression in Calu-3 sublines cultured in Transwells. Data are presented as mean ± SD (n=2), ANOVA $p < 0.05$, * denotes $p < 0.05$ as compared to Calu-3.

Supplementary Figure 2

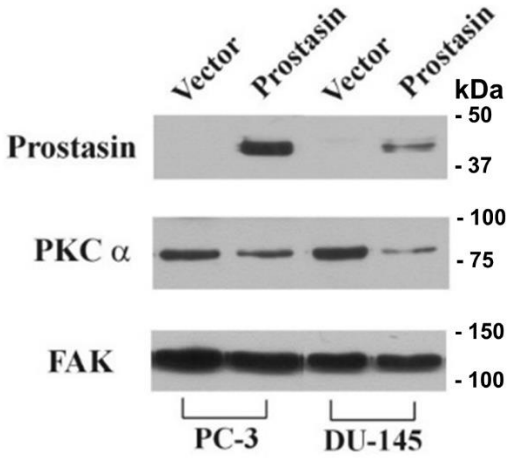

Supplementary Figure 2. Western blot analysis of PKCα expression in prostate cancer cell lines.

Over-expression of prostasin in PC-3 and DU-145 cells reduced PKCα expression in both cell lines as compared to their corresponding vector control cells, while FAK (focal adhesion kinase) expression was not changed. Prostasin, reduced form, 40 kDa [11].

Supplementary Figure 3. The complete list of enriched gene sets.

Gene set enrichment analysis for lung squamous cell carcinoma (LUSC, panel a-d) and lung adenocarcinoma (LUAD, panel e-h) from TCGA.

a. LUSC High PRSS8 Enriched Gene Sets

LUSC High PRSS8 Enriched Gene Sets (25% FDR)	NES	FDR q-val
HALLMARK_TNFA_SIGNALING_VIA_NFKB	2.9	0
HALLMARK_INTERFERON_GAMMA_RESPONSE	2.9	0
HALLMARK_INFLAMMATORY_RESPONSE	2.8	0
HALLMARK_IL6_JAK_STAT3_SIGNALING	2.6	0
HALLMARK_COAGULATION	2.5	0
HALLMARK_COMPLEMENT	2.5	0
HALLMARK_INTERFERON_ALPHA_RESPONSE	2.5	0
HALLMARK_ALLOGRAFT_REJECTION	2.1	0
HALLMARK_IL2_STAT5_SIGNALING	2.1	0
HALLMARK_APICAL_JUNCTION	2.0	0
HALLMARK_TGF_BETA_SIGNALING	2.0	0
HALLMARK_MYOGENESIS	2.0	0
HALLMARK_ESTROGEN_RESPONSE_EARLY	2.0	0
HALLMARK_BILE_ACID_METABOLISM	2.0	0
HALLMARK_APOPTOSIS	2.0	0
HALLMARK_KRAS_SIGNALING_UP	1.9	0
HALLMARK_HYPOXIA	1.8	2.39E-04
HALLMARK_UV_RESPONSE_DN	1.8	3.81E-04
HALLMARK_EPITHELIAL_MESENCHYMAL_TRANSITION	1.8	0.001179557
HALLMARK_XENOBIOTIC_METABOLISM	1.8	0.001188436
HALLMARK_ANGIOGENESIS	1.8	0.001584159
HALLMARK_ADIPOGENESIS	1.7	0.001991312
HALLMARK_P53_PATHWAY	1.7	0.002751719
HALLMARK_HEME_METABOLISM	1.6	0.003917295
HALLMARK_PEROXISOME	1.5	0.009721883
HALLMARK_ESTROGEN_RESPONSE_LATE	1.5	0.011090398
HALLMARK_CHOLESTEROL_HOMEOSTASIS	1.5	0.012853715
HALLMARK_REACTIVE_OXYGEN_SPECIES_PATHWAY	1.4	0.021902649
HALLMARK_ANDROGEN_RESPONSE	1.4	0.022806939
HALLMARK_FATTY_ACID_METABOLISM	1.3	0.055563193
HALLMARK_UV_RESPONSE_UP	1.3	0.06734516
HALLMARK_APICAL_SURFACE	1.2	0.16197442
HALLMARK_KRAS_SIGNALING_DN	1.2	0.20365763

b. LUSC High CD274 Enriched Gene Sets

LUSC High CD274 Enriched Gene Sets (25% FDR)	NES	FDR q-val
HALLMARK_INTERFERON_GAMMA_RESPONSE	3.7	0
HALLMARK_INTERFERON_ALPHA_RESPONSE	3.5	0
HALLMARK_INFLAMMATORY_RESPONSE	3.4	0
HALLMARK_TNFA_SIGNALING_VIA_NFKB	3.2	0
HALLMARK_ALLOGRAFT_REJECTION	3.1	0
HALLMARK_COMPLEMENT	3.0	0
HALLMARK_IL6_JAK_STAT3_SIGNALING	2.9	0
HALLMARK_IL2_STAT5_SIGNALING	2.7	0
HALLMARK_COAGULATION	2.3	0
HALLMARK_KRAS_SIGNALING_UP	2.3	0
HALLMARK_APOPTOSIS	2.2	0
HALLMARK_REACTIVE_OXYGEN_SPECIES_PATHWAY	2.0	2.23E-04
HALLMARK_HYPOXIA	1.9	2.06E-04
HALLMARK_XENOBIOTIC_METABOLISM	1.9	6.14E-04
HALLMARK_HEME_METABOLISM	1.8	6.55E-04
HALLMARK_TGF_BETA_SIGNALING	1.8	7.09E-04
HALLMARK_MYOGENESIS	1.8	8.09E-04
HALLMARK_UV_RESPONSE_DN	1.8	9.02E-04
HALLMARK_BILE_ACID_METABOLISM	1.8	0.001168116
HALLMARK_APICAL_JUNCTION	1.8	0.001406594
HALLMARK_UV_RESPONSE_UP	1.7	0.002580947
HALLMARK_ESTROGEN_RESPONSE_EARLY	1.7	0.003043273
HALLMARK_EPITHELIAL_MESENCHYMAL_TRANSITION	1.6	0.009378419
HALLMARK_ADIPOGENESIS	1.5	0.012899715
HALLMARK_P53_PATHWAY	1.5	0.020130154
HALLMARK_ANDROGEN_RESPONSE	1.4	0.038793676
HALLMARK_FATTY_ACID_METABOLISM	1.4	0.03879502
HALLMARK_APICAL_SURFACE	1.4	0.038254187
HALLMARK_PROTEIN_SECRETION	1.4	0.050922032
HALLMARK_ESTROGEN_RESPONSE_LATE	1.3	0.07497506
HALLMARK_KRAS_SIGNALING_DN	1.2	0.14584666
HALLMARK_CHOLESTEROL_HOMEOSTASIS	1.2	0.1506702
HALLMARK_PI3K_AKT_MTOR_SIGNALING	1.2	0.19768856

c. LUSC Low PRSS8 Enriched Gene Sets

LUSC Low PRSS8 Enriched Gene Sets (25% FDR)	NES	FDR q-val
HALLMARK_E2F_TARGETS	-3.8	0
HALLMARK_G2M_CHECKPOINT	-3.6	0
HALLMARK_MYC_TARGETS_V1	-3.4	0
HALLMARK_MYC_TARGETS_V2	-3.1	0
HALLMARK_MITOTIC_SPINDLE	-2.1	1.04E-04
HALLMARK_SPERMATOGENESIS	-2.0	8.70E-05
HALLMARK_MTORC1_SIGNALING	-1.9	1.60E-04
HALLMARK_OXIDATIVE_PHOSPHORYLATION	-1.8	4.34E-04
HALLMARK_DNA_REPAIR	-1.8	3.86E-04
HALLMARK_UNFOLDED_PROTEIN_RESPONSE	-1.7	0.001982023

d. LUSC Low CD274 Enriched Gene Sets

LUSC Low CD274 Enriched Gene Sets (25% FDR)	NES	FDR q-val
HALLMARK_E2F_TARGETS	-3.0	0
HALLMARK_G2M_CHECKPOINT	-2.9	0
HALLMARK_MYC_TARGETS_V1	-2.8	0
HALLMARK_MYC_TARGETS_V2	-2.4	0
HALLMARK_OXIDATIVE_PHOSPHORYLATION	-1.9	9.45E-04
HALLMARK_DNA_REPAIR	-1.8	0.00147399
HALLMARK_SPERMATOGENESIS	-1.8	0.001415876
HALLMARK_MITOTIC_SPINDLE	-1.3	0.060848035

e. LUAD High PRSS8 Enriched Gene Sets

LUAD High PRSS8 Enriched Gene Sets (25% FDR)	NES	FDR q-val
HALLMARK_INTERFERON_ALPHA_RESPONSE	2.7	0
HALLMARK_INTERFERON_GAMMA_RESPONSE	2.1	6.58E-04
HALLMARK_IL6_JAK_STAT3_SIGNALING	1.9	4.39E-04
HALLMARK_TNFA_SIGNALING_VIA_NFKB	1.8	0.007567337
HALLMARK_P53_PATHWAY	1.7	0.007077679
HALLMARK_INFLAMMATORY_RESPONSE	1.7	0.009387618
HALLMARK_APICAL_JUNCTION	1.6	0.010865434
HALLMARK_CHOLESTEROL_HOMEOSTASIS	1.6	0.01064314
HALLMARK_ALLOGRAFT_REJECTION	1.4	0.06476901
HALLMARK_PEROXISOME	1.4	0.08273839
HALLMARK_GLYCOLYSIS	1.3	0.08865474
HALLMARK_COMPLEMENT	1.3	0.09164486
HALLMARK_COAGULATION	1.3	0.10120447
HALLMARK_APOPTOSIS	1.3	0.09475186
HALLMARK_IL2_STAT5_SIGNALING	1.2	0.15677549
HALLMARK_ESTROGEN_RESPONSE_EARLY	1.2	0.17921966
HALLMARK_NOTCH_SIGNALING	1.2	0.2382772
HALLMARK_KRAS_SIGNALING_DN	1.2	0.2343269

f. LUAD High CD274 Enriched Gene Sets

LUAD High CD274 Enriched Gene Sets (25% FDR)	NES	FDR q-val
HALLMARK_INTERFERON_GAMMA_RESPONSE	3.9	0
HALLMARK_ALLOGRAFT_REJECTION	3.8	0
HALLMARK_INFLAMMATORY_RESPONSE	3.5	0
HALLMARK_TNFA_SIGNALING_VIA_NFKB	3.5	0
HALLMARK_INTERFERON_ALPHA_RESPONSE	3.4	0
HALLMARK_IL6_JAK_STAT3_SIGNALING	3.2	0
HALLMARK_COMPLEMENT	2.9	0
HALLMARK_IL2_STAT5_SIGNALING	2.7	0
HALLMARK_KRAS_SIGNALING_UP	2.7	0
HALLMARK_APOPTOSIS	2.5	0
HALLMARK_APICAL_JUNCTION	2.4	0
HALLMARK_TGF_BETA_SIGNALING	2.2	0
HALLMARK_EPITHELIAL_MESENCHYMAL_TRANSITION	2.1	0
HALLMARK_HYPOXIA	1.9	1.02E-04
HALLMARK_COAGULATION	1.9	3.24E-04
HALLMARK_UV_RESPONSE_DN	1.8	5.87E-04
HALLMARK_APICAL_SURFACE	1.7	0.003995385
HALLMARK_ANGIOGENESIS	1.6	0.006372829
HALLMARK_P53_PATHWAY	1.5	0.012783593
HALLMARK_PI3K_AKT_MTOR_SIGNALING	1.5	0.023198167
HALLMARK_MYOGENESIS	1.4	0.030198675
HALLMARK_HEME_METABOLISM	1.4	0.047247607
HALLMARK_HEDGEHOG_SIGNALING	1.4	0.050490916
HALLMARK_MITOTIC_SPINDLE	1.3	0.08157678
HALLMARK_CHOLESTEROL_HOMEOSTASIS	1.2	0.15549049
HALLMARK_UV_RESPONSE_UP	1.2	0.1805793

g. LUAD Low PRSS8 Enriched Gene Sets

LUAD Low PRSS8 Enriched Gene Sets (25% FDR)	NES	FDR q-val
HALLMARK_E2F_TARGETS	-3.1	0
HALLMARK_G2M_CHECKPOINT	-3.0	0
HALLMARK_MYC_TARGETS_V1	-2.5	0
HALLMARK_SPERMATOGENESIS	-2.1	0
HALLMARK_MITOTIC_SPINDLE	-2.0	0
HALLMARK_EPITHELIAL_MESENCHYMAL_TRANSITION	-2.0	1.16E-04
HALLMARK_MYC_TARGETS_V2	-1.9	5.12E-04
HALLMARK_MTORC1_SIGNALING	-1.8	0.001880215
HALLMARK_UV_RESPONSE_DN	-1.5	0.034481023
HALLMARK_UNFOLDED_PROTEIN_RESPONSE	-1.3	0.12530452
HALLMARK_OXIDATIVE_PHOSPHORYLATION	-1.3	0.16235016

h. LUAD Low CD274 Enriched Gene Sets

LUAD Low CD274 Enriched Gene Sets (25% FDR)	NES	FDR q-val
HALLMARK_OXIDATIVE_PHOSPHORYLATION	-2.6	0
HALLMARK_MYC_TARGETS_V1	-2.4	0
HALLMARK_E2F_TARGETS	-2.0	0
HALLMARK_MYC_TARGETS_V2	-1.9	5.70E-04
HALLMARK_UNFOLDED_PROTEIN_RESPONSE	-1.7	0.004312027
HALLMARK_FATTY_ACID_METABOLISM	-1.6	0.010758515
HALLMARK_G2M_CHECKPOINT	-1.6	0.012803096
HALLMARK_SPERMATOGENESIS	-1.6	0.011908125
HALLMARK_GLYCOLYSIS	-1.5	0.02734927
HALLMARK_DNA_REPAIR	-1.4	0.033594772
HALLMARK_ADIPOGENESIS	-1.4	0.042960566
HALLMARK_MTORC1_SIGNALING	-1.3	0.079123646
HALLMARK_XENOBIOTIC_METABOLISM	-1.3	0.09165737
HALLMARK_PANCREAS_BETA_CELLS	-1.3	0.12316957
HALLMARK_PEROXISOME	-1.2	0.16723569
HALLMARK_ESTROGEN_RESPONSE_LATE	-1.2	0.19401155

Supplementary Figure 4

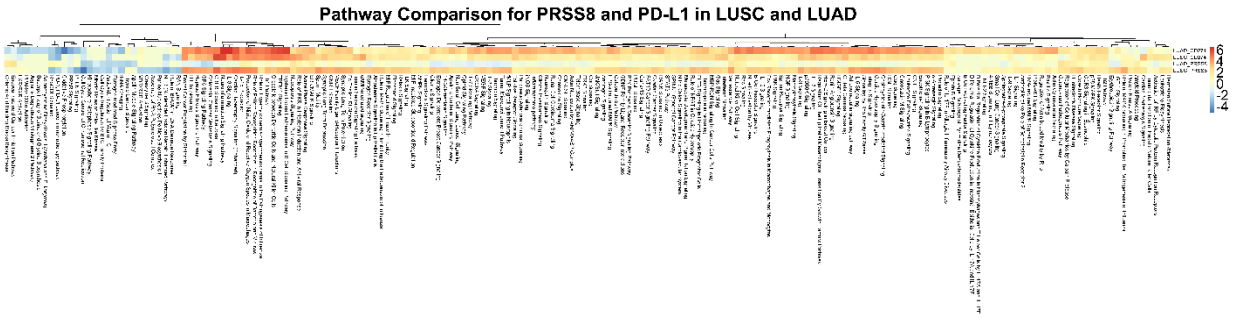

Supplementary Figure 4. The hierarchical clustering heatmap.

The identified pathways were generated by means of the Ingenuity Pathway Analysis (IPA) using the rank ordered gene lists from GSEA. Z-score cutoff = 2.

Supplementary Figure 5 (Uncropped Western blot images)

All images are overlays of ink-stained membrane (with molecular weight markers) and the corresponding chemiluminescent blot

Figure 1, uncropped images

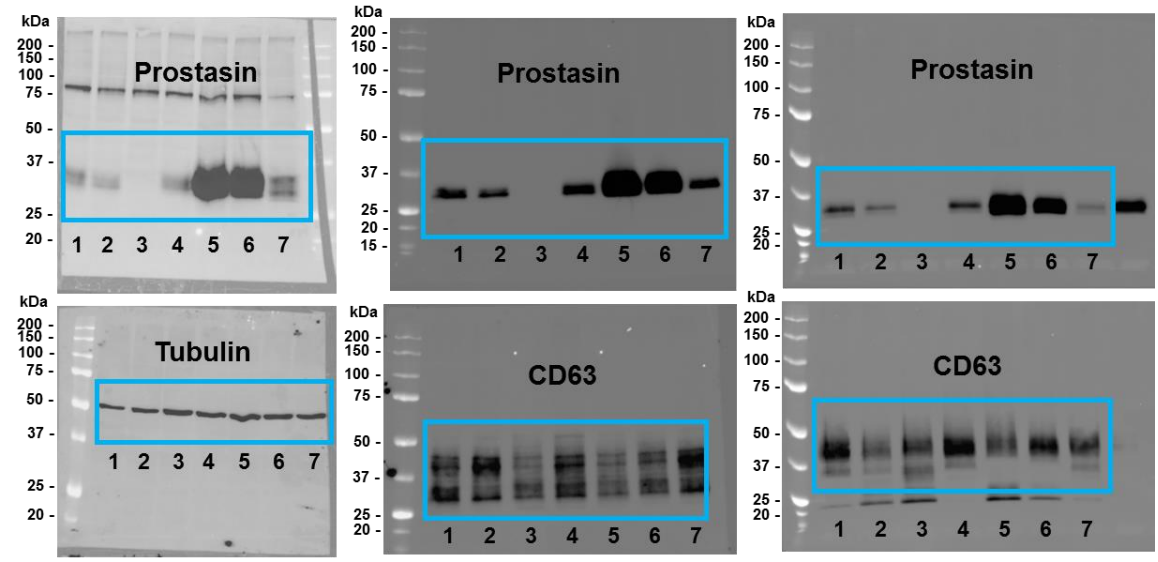

Figure 2, uncropped images

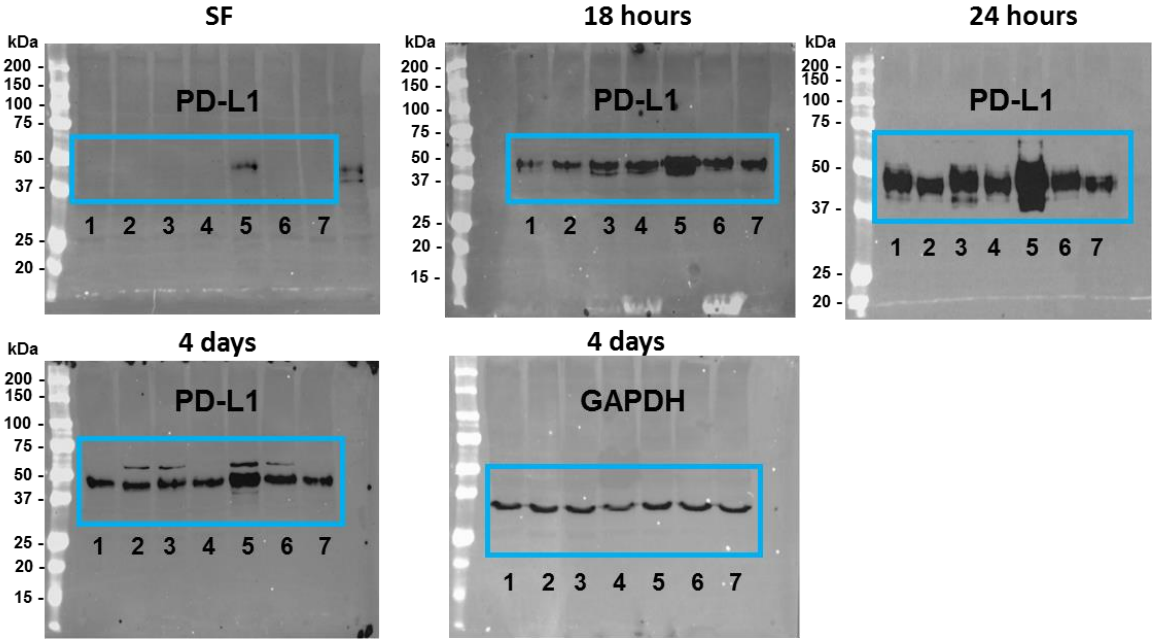

Figure 4, uncropped images

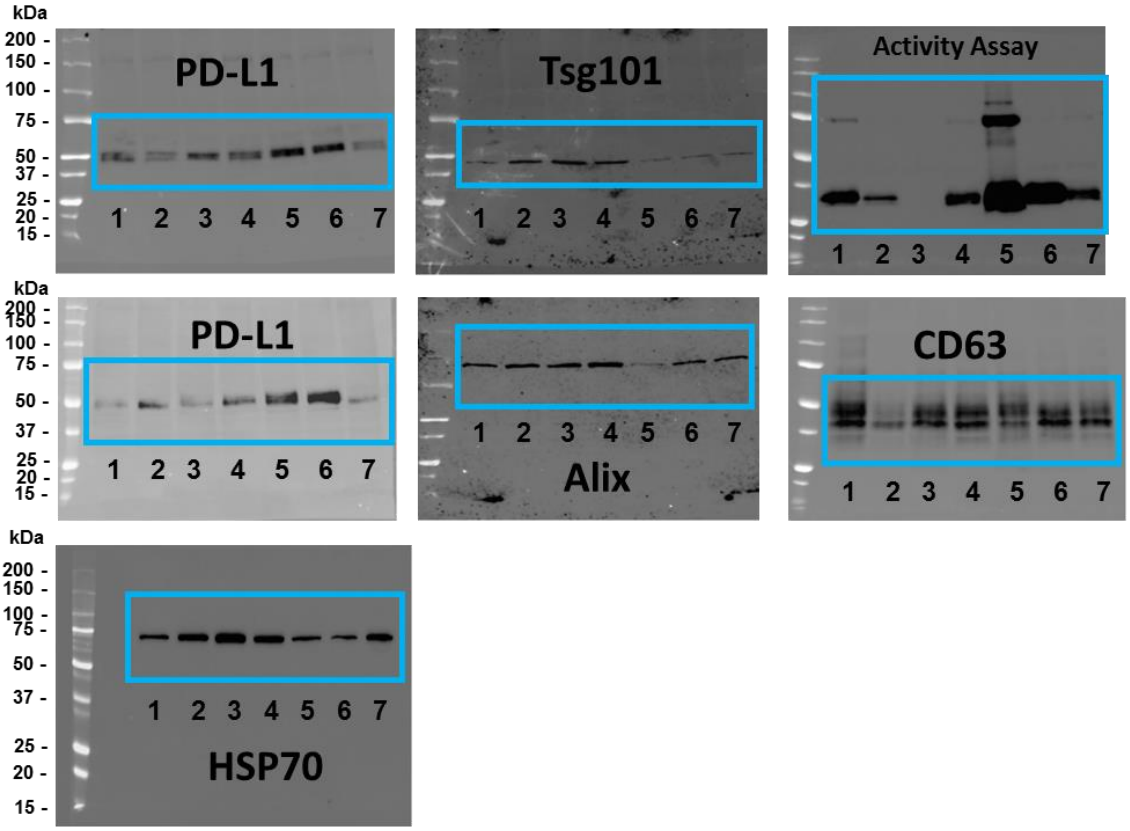

Figure 5, uncropped images

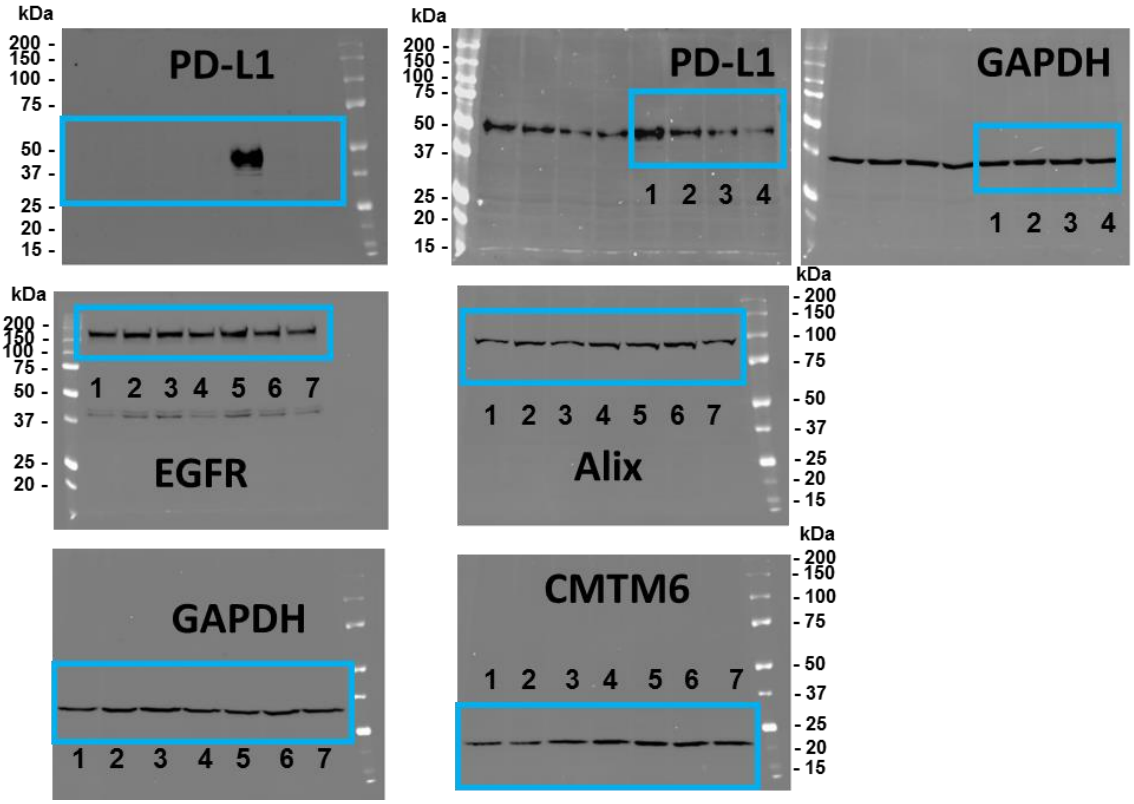

Figure 6, uncropped images

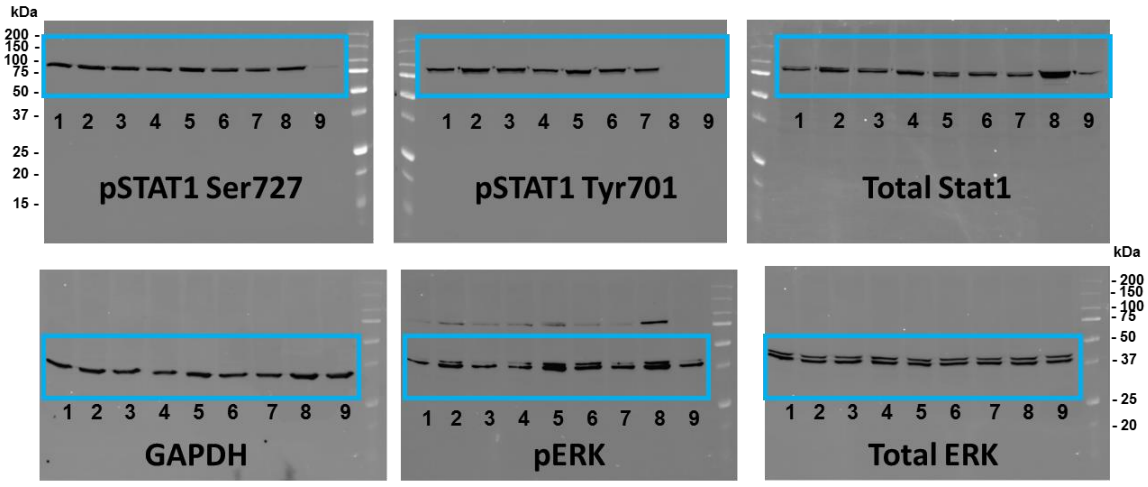

Figure 7, uncropped images

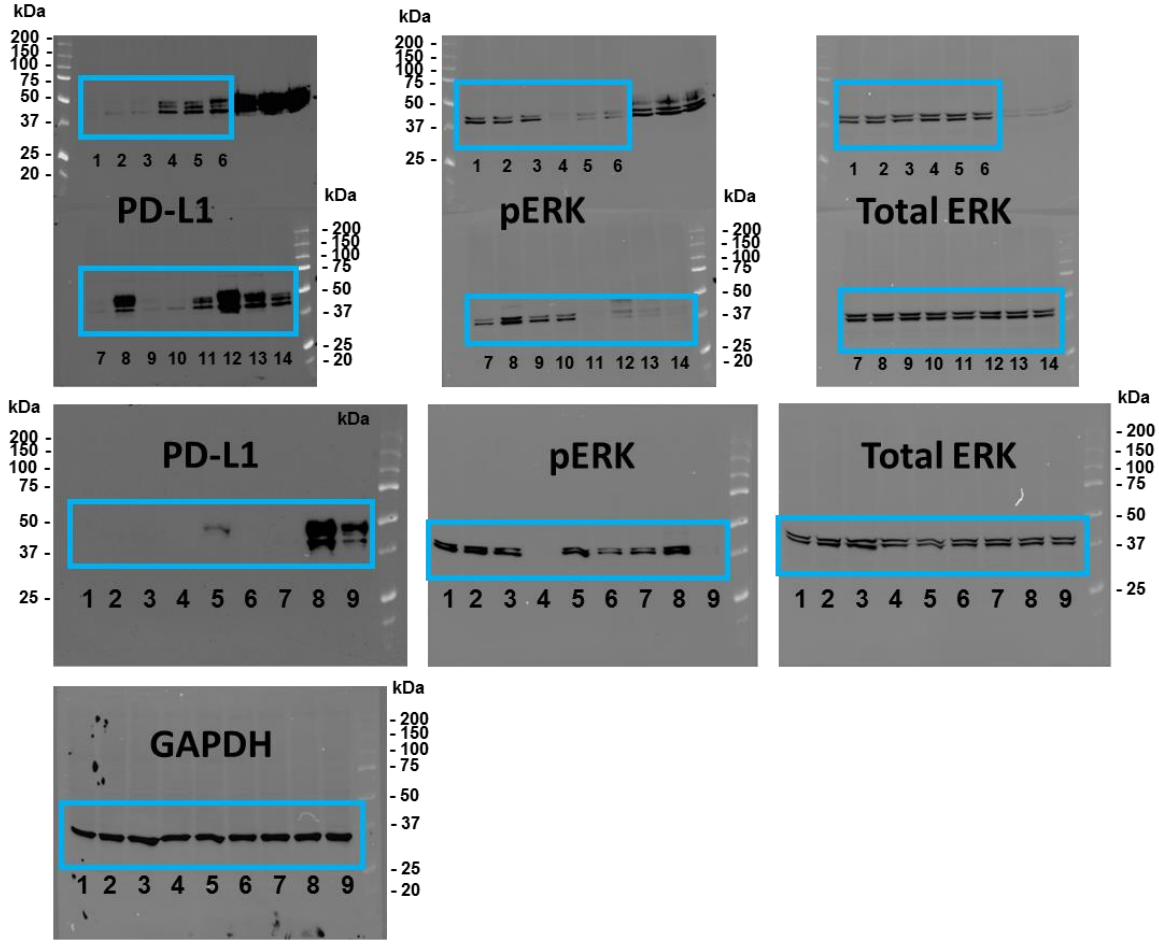

Figure 8, uncropped images

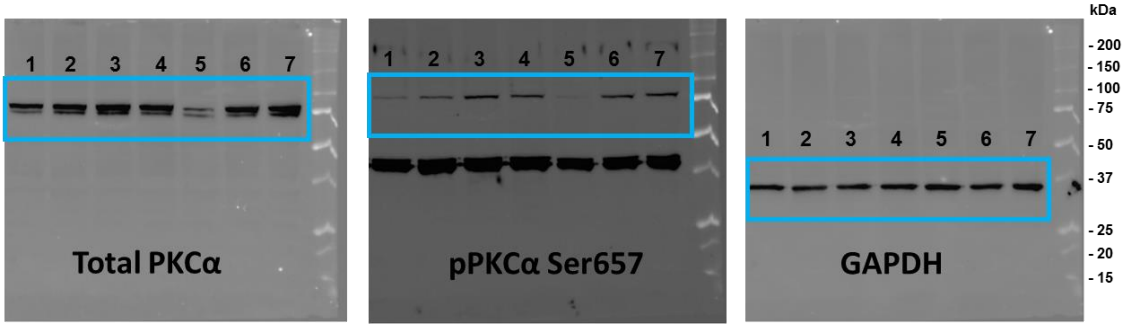

Figure 1

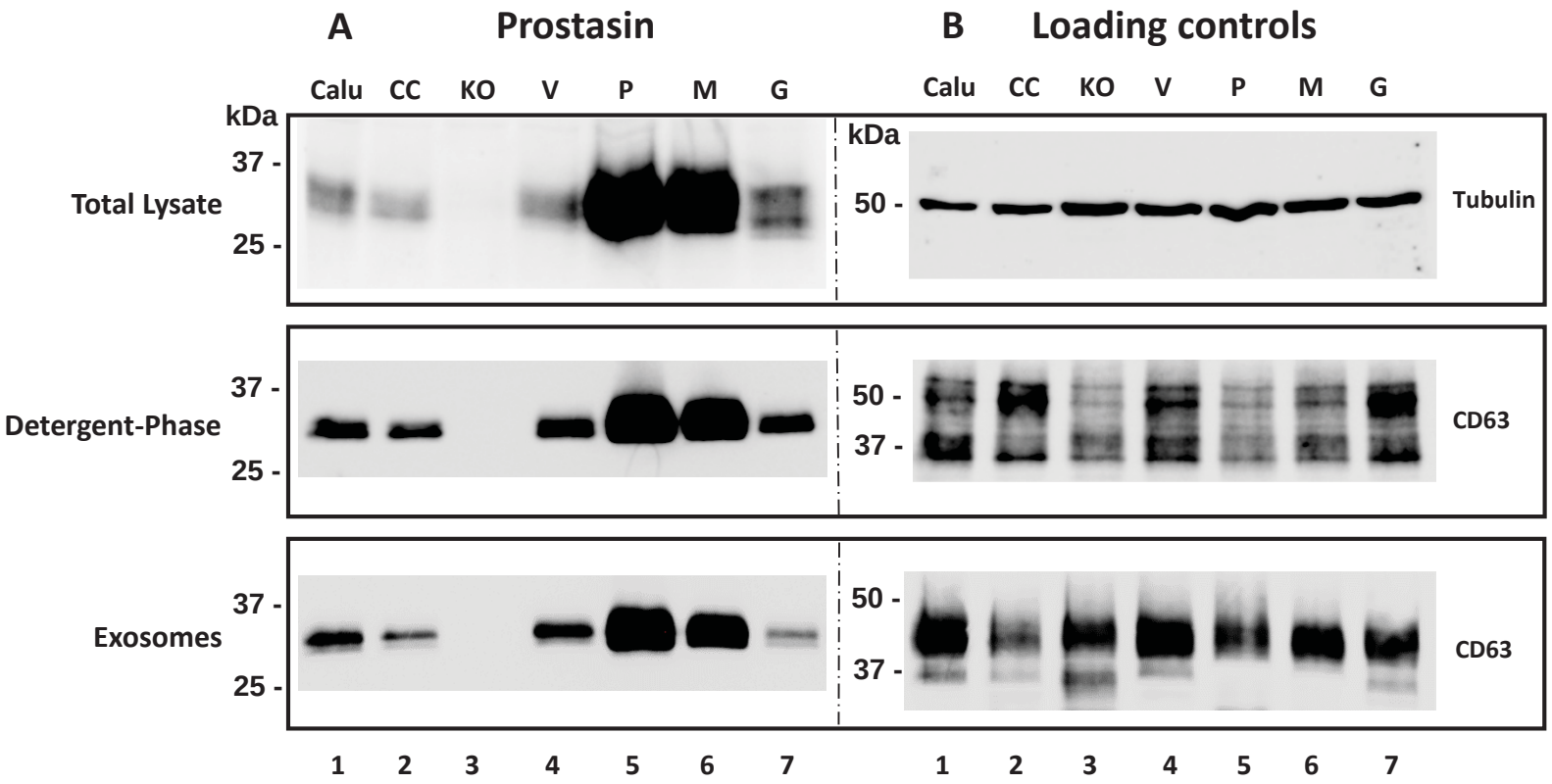

Figure 2

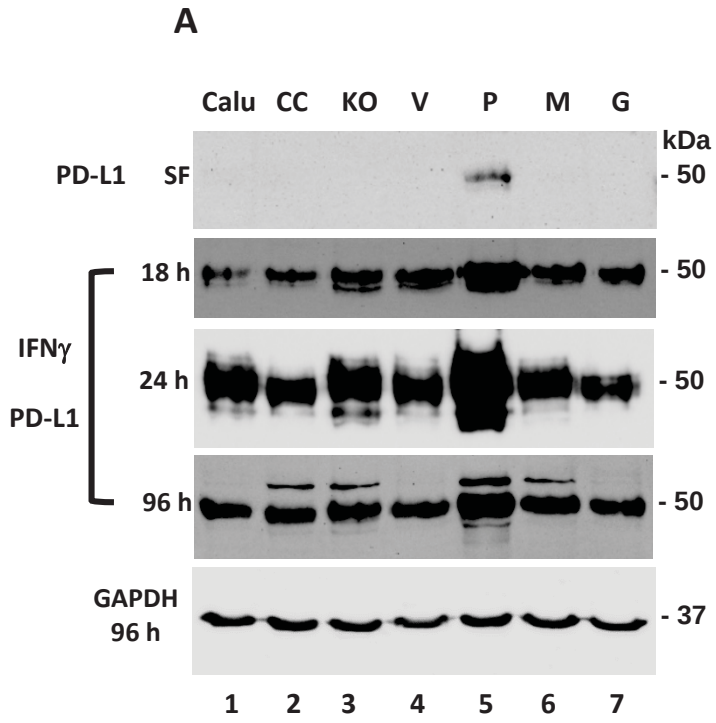

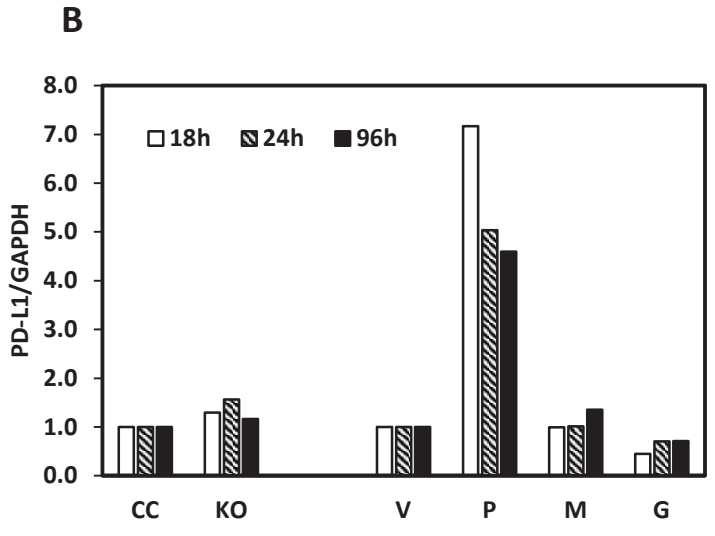

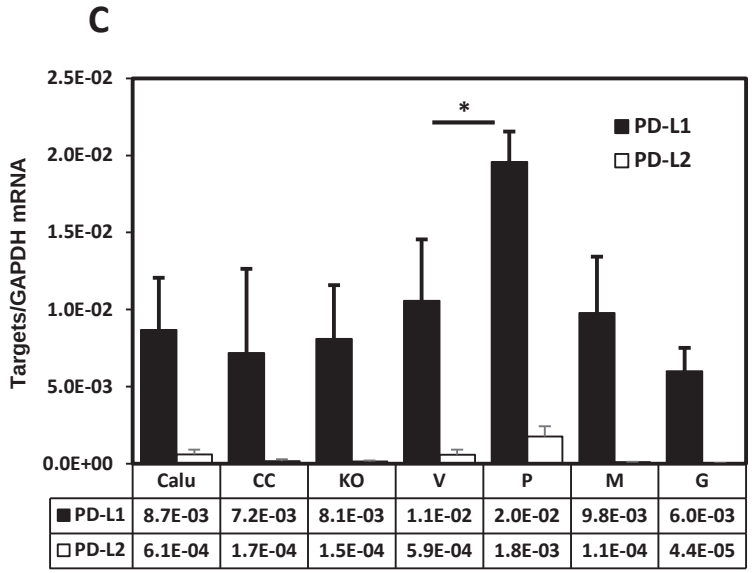

	Calu	CC	KO	V	P	M	G
PD-L1	8.7E-03	7.2E-03	8.1E-03	1.1E-02	2.0E-02	9.8E-03	6.0E-03
PD-L2	6.1E-04	1.7E-04	1.5E-04	5.9E-04	1.8E-03	1.1E-04	4.4E-05

Figure 3

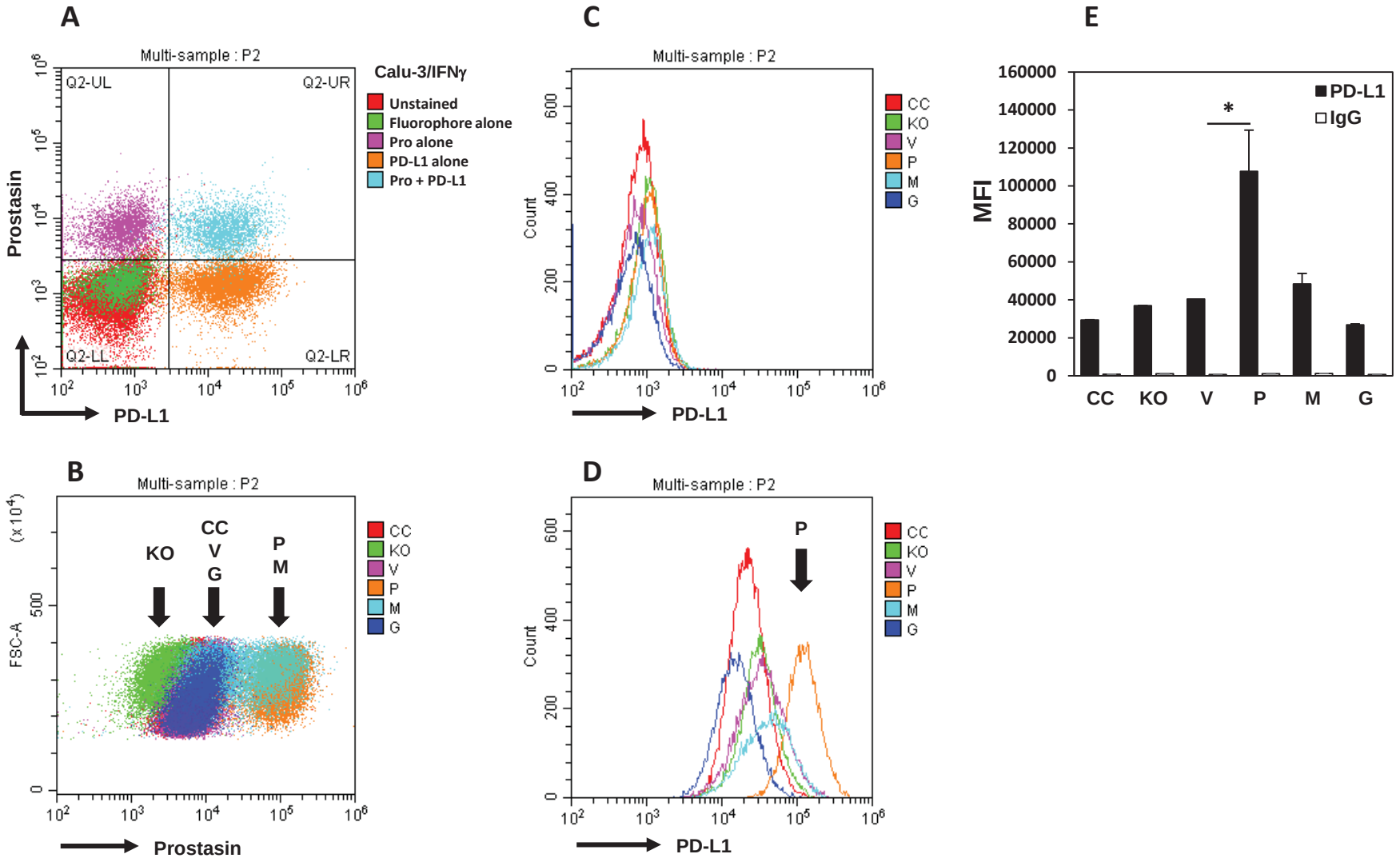

Figure 4

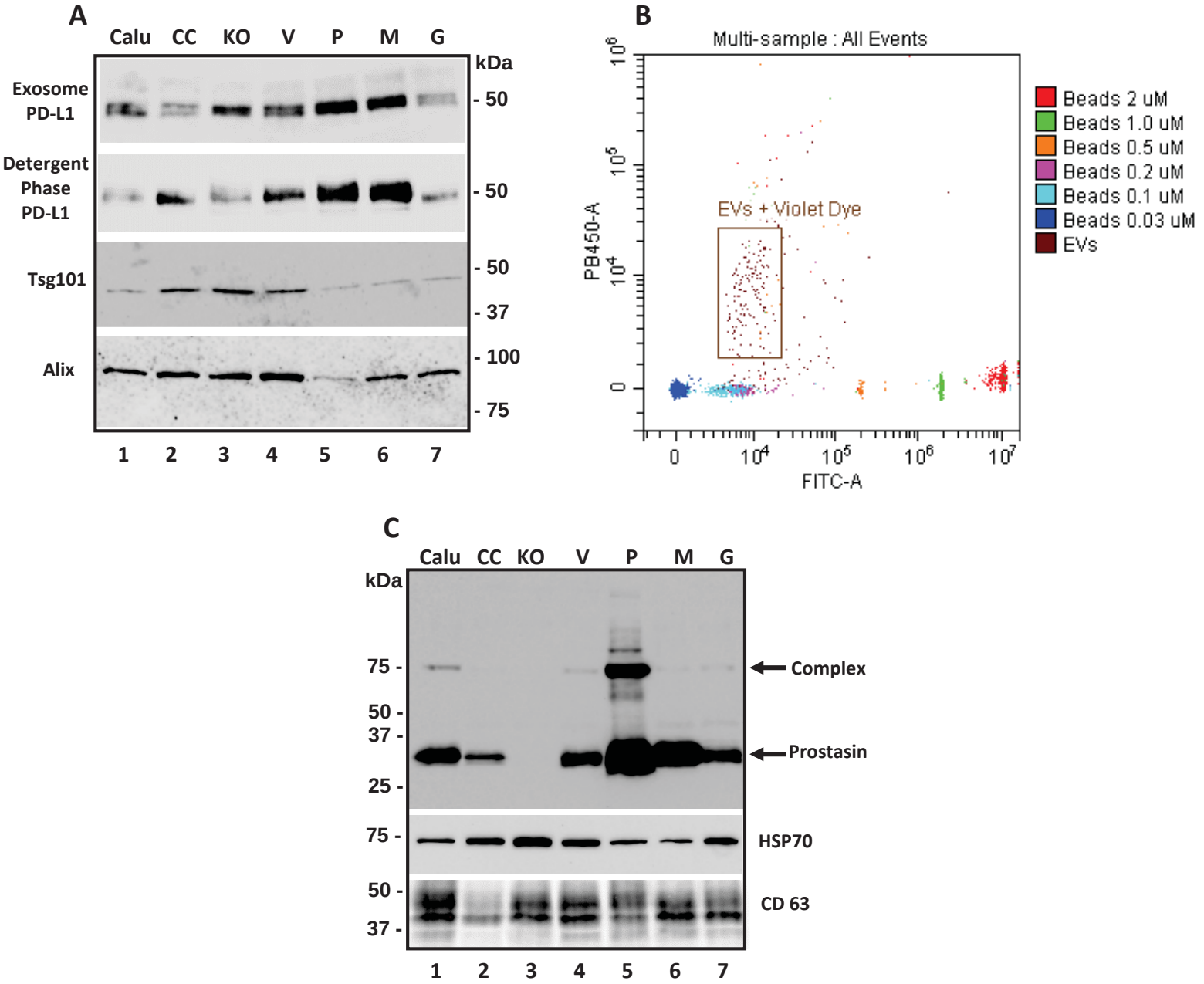

Figure 5

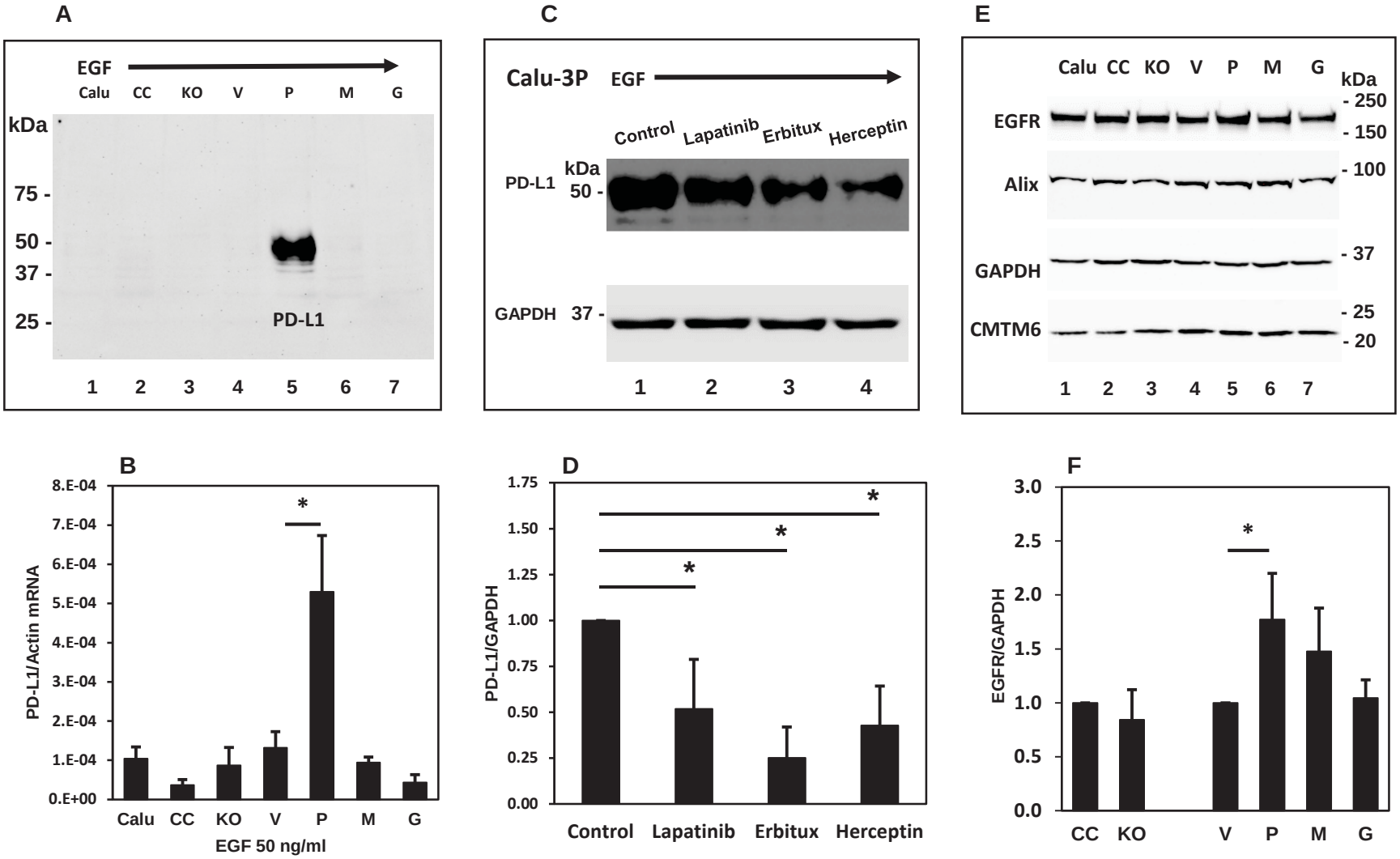

Figure 6

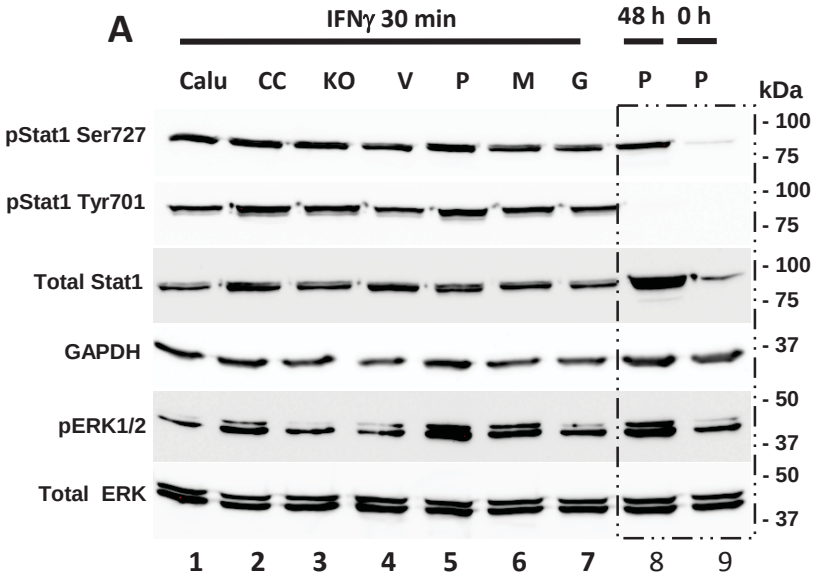

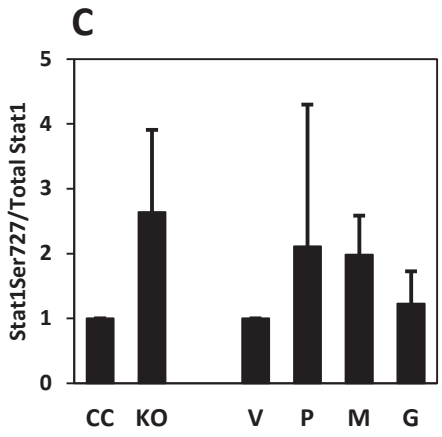

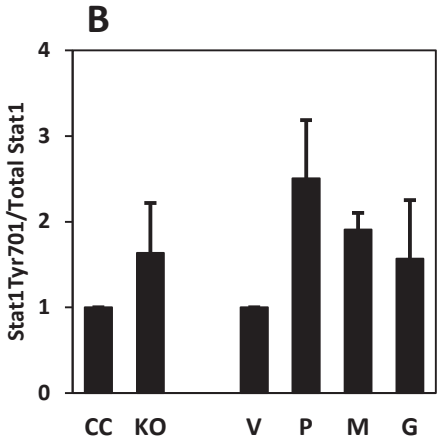

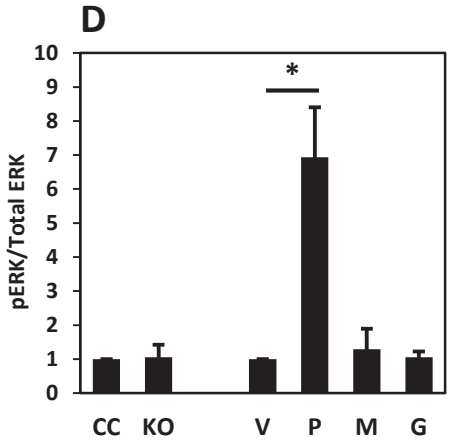

Figure 7

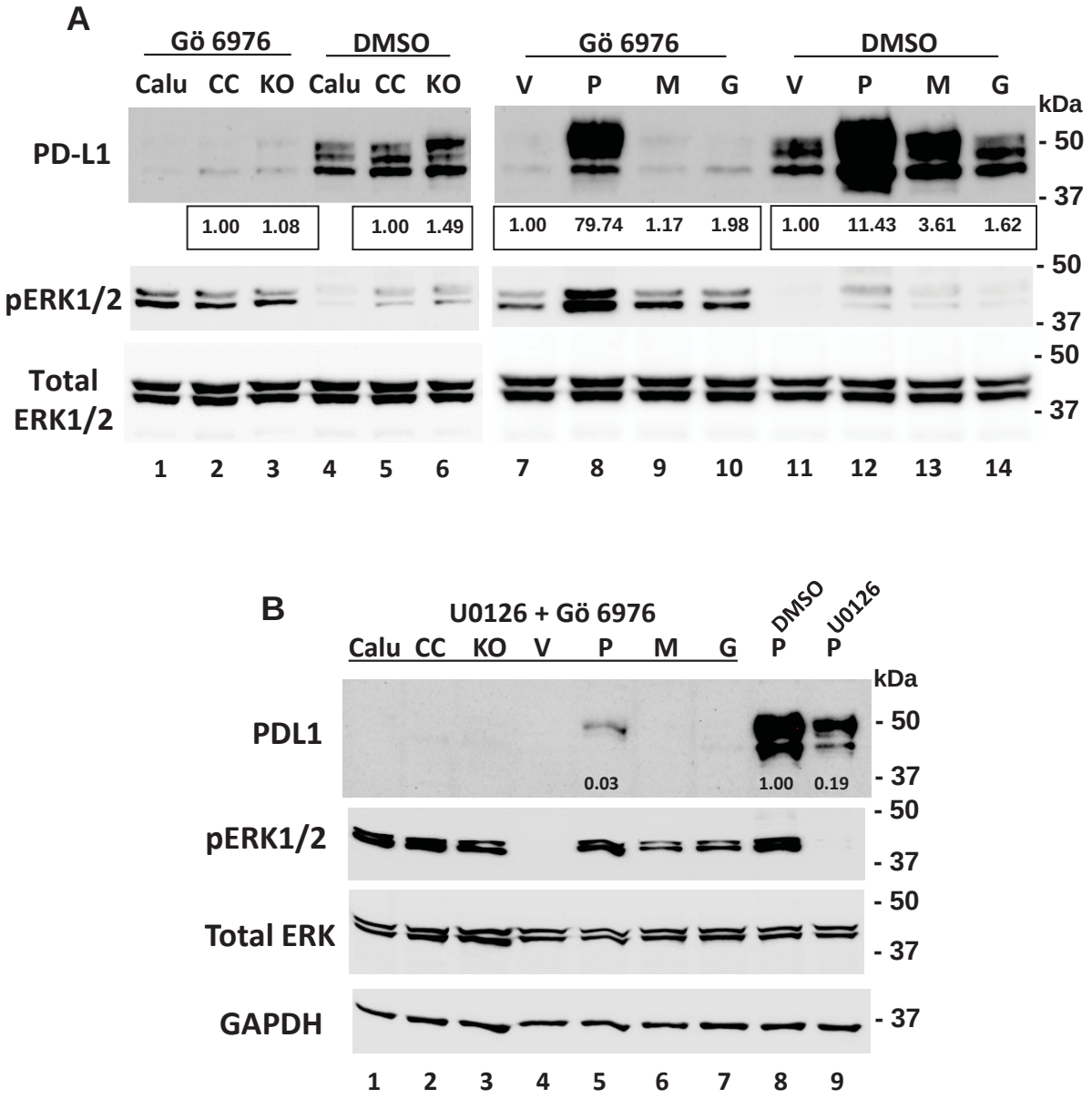

Figure 8

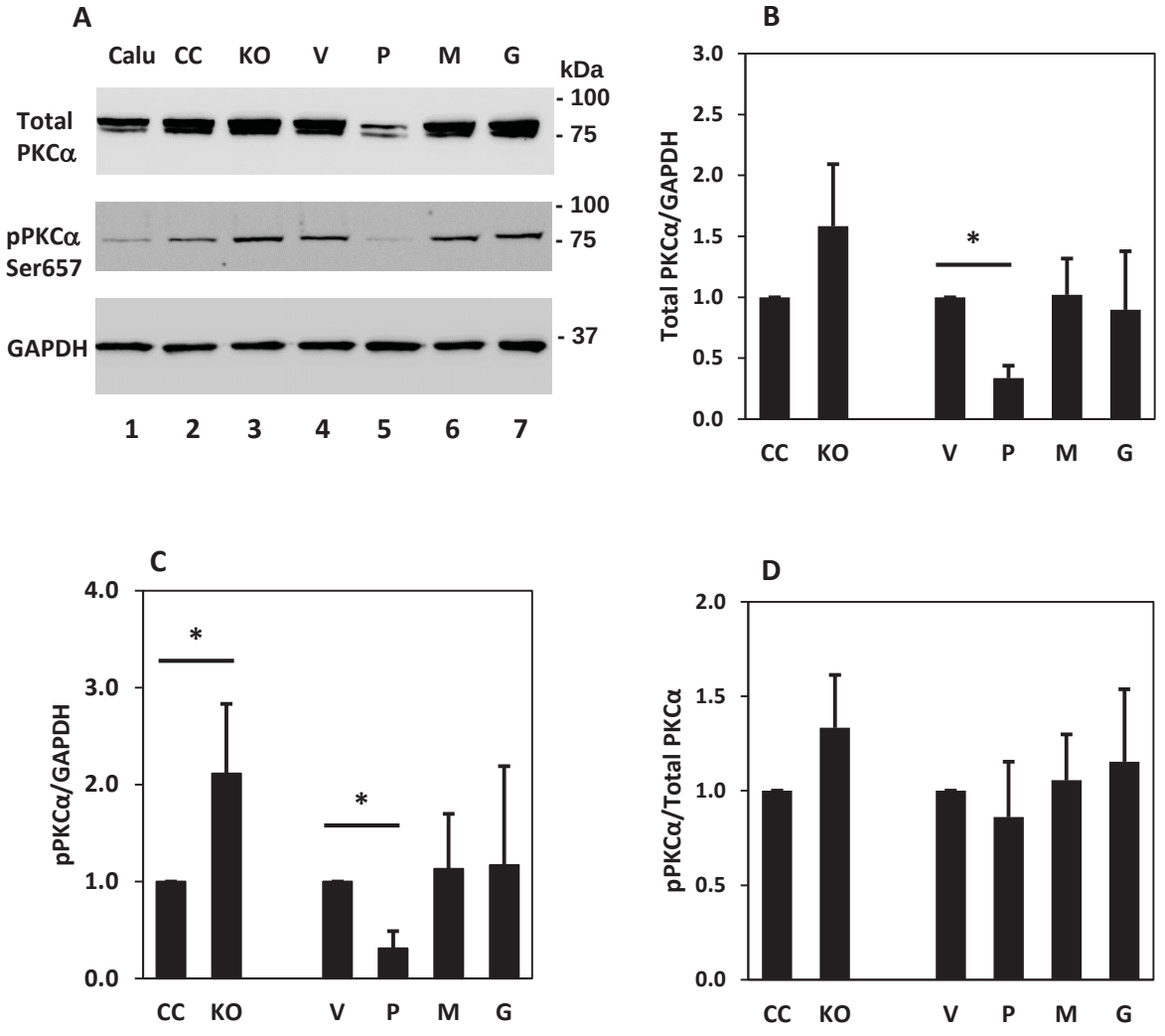

Figure 9

a. Up-regulated Gene Sets From TCGA LUSC Patients with High PRSS8 or CD274

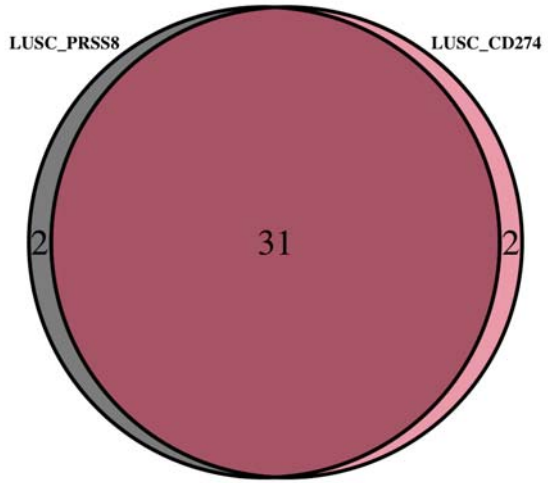

LUSC High PRSS8 Enriched Gene Sets (25% FDR)	NES	FDR q-val
HALLMARK_TNFA_SIGNALING_VIA_NFKB	2.9	0
HALLMARK_INTERFERON_GAMMA_RESPONSE	2.9	0
HALLMARK_INFLAMMATORY_RESPONSE	2.8	0
HALLMARK_IL6_JAK_STAT3_SIGNALING	2.6	0

LUSC High CD274 Enriched Gene Sets (25% FDR)	NES	FDR q-val
HALLMARK_INTERFERON_GAMMA_RESPONSE	3.7	0
HALLMARK_INTERFERON_ALPHA_RESPONSE	3.5	0
HALLMARK_INFLAMMATORY_RESPONSE	3.4	0
HALLMARK_TNFA_SIGNALING_VIA_NFKB	3.2	0

b. Down-regulated Gene Sets From TCGA LUSC Patients with High PRSS8 or CD274

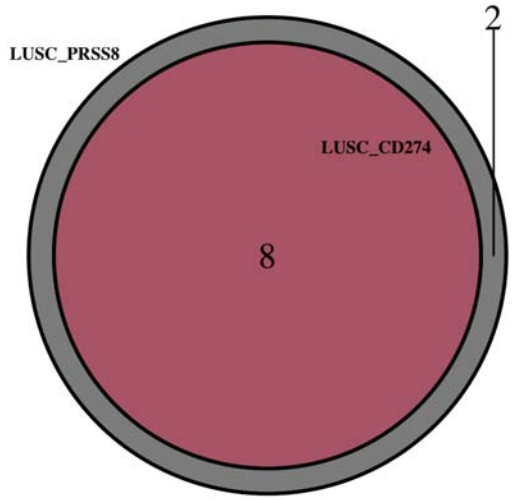

LUSC Low PRSS8 Enriched Gene Sets (25% FDR)	NES	FDR q-val
HALLMARK_E2F_TARGETS	-3.8	0
HALLMARK_G2M_CHECKPOINT	-3.6	0
HALLMARK_MYC_TARGETS_V1	-3.4	0
HALLMARK_MYC_TARGETS_V2	-3.1	0

LUSC Low CD274 Enriched Gene Sets (25% FDR)	NES	FDR q-val
HALLMARK_E2F_TARGETS	-3.0	0
HALLMARK_G2M_CHECKPOINT	-2.9	0
HALLMARK_MYC_TARGETS_V1	-2.8	0
HALLMARK_MYC_TARGETS_V2	-2.4	0

c.

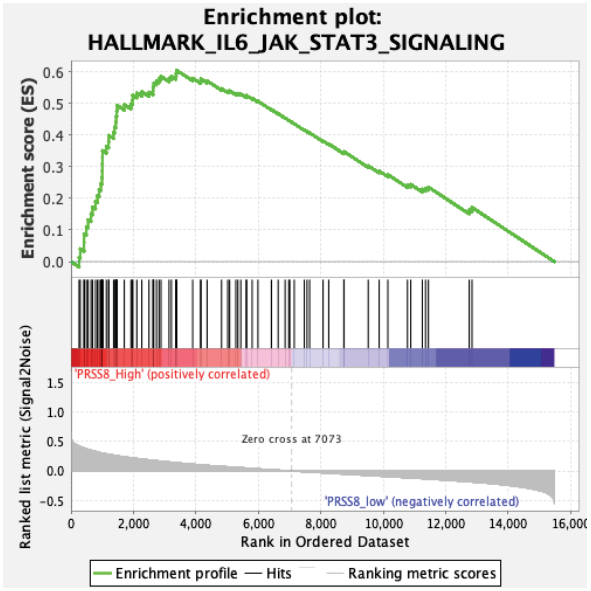

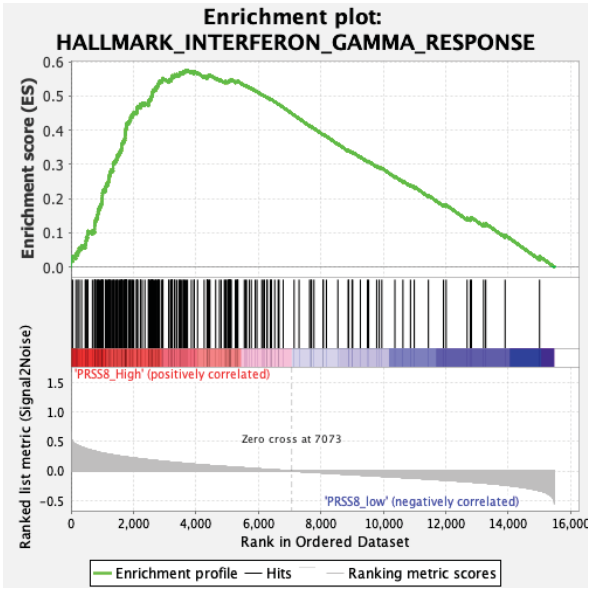

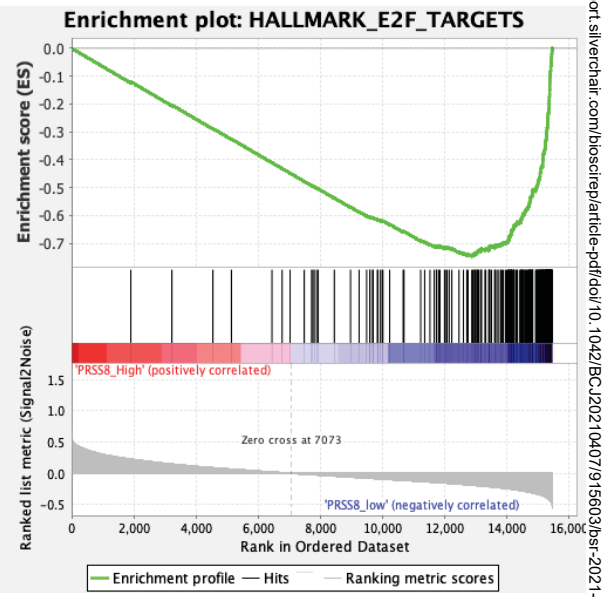

d.

Up-regulated Gene Sets From TCGA LUAD Patients with High PRSS8 or CD274

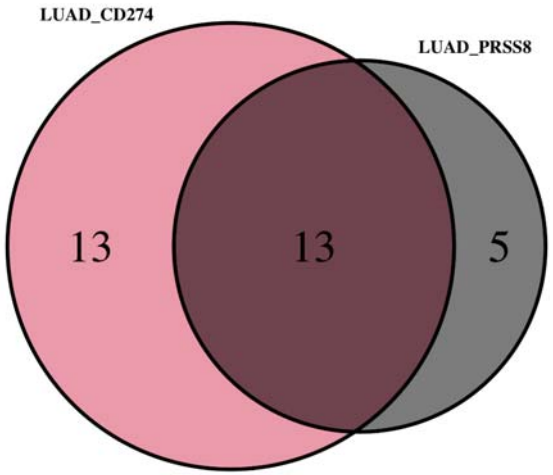

LUAD High PRSS8 Enriched Gene Sets (25% FDR)	NES	FDR q-val
HALLMARK_INTERFERON_ALPHA_RESPONSE	2.7	0
HALLMARK_INTERFERON_GAMMA_RESPONSE	2.1	6.58E-04
HALLMARK_IL6_JAK_STAT3_SIGNALING	1.9	4.39E-04
HALLMARK_TNFA_SIGNALING_VIA_NFKB	1.8	0.007567337

LUAD High CD274 Enriched Gene Sets (25% FDR)	NES	FDR q-val
HALLMARK_INTERFERON_GAMMA_RESPONSE	3.9	0
HALLMARK_ALLOGRAFT_REJECTION	3.8	0
HALLMARK_INFLAMMATORY_RESPONSE	3.5	0
HALLMARK_TNFA_SIGNALING_VIA_NFKB	3.5	0

e.

Down-regulated Gene Sets From TCGA LUAD Patients with High PRSS8 or CD274

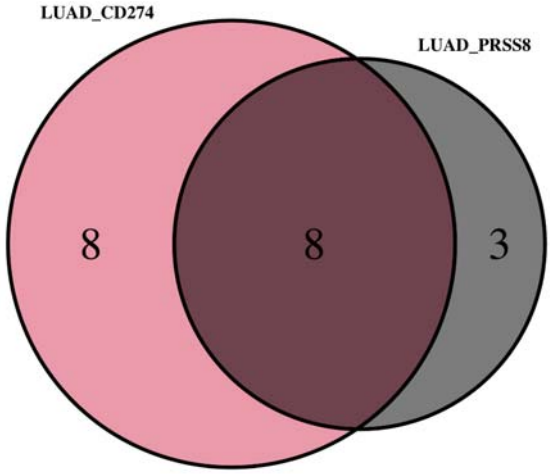

LUAD Low PRSS8 Enriched Gene Sets (25% FDR)	NES	FDR q-val
HALLMARK_E2F_TARGETS	-3.1	0
HALLMARK_G2M_CHECKPOINT	-3.0	0
HALLMARK_MYC_TARGETS_V1	-2.5	0
HALLMARK_SPERMATOGENESIS	-2.1	0

LUAD Low CD274 Enriched Gene Sets (25% FDR)	NES	FDR q-val
HALLMARK_OXIDATIVE_PHOSPHORYLATION	-2.6	0
HALLMARK_MYC_TARGETS_V1	-2.4	0
HALLMARK_E2F_TARGETS	-2.0	0
HALLMARK_MYC_TARGETS_V2	-1.9	5.70E-04

Figure 10

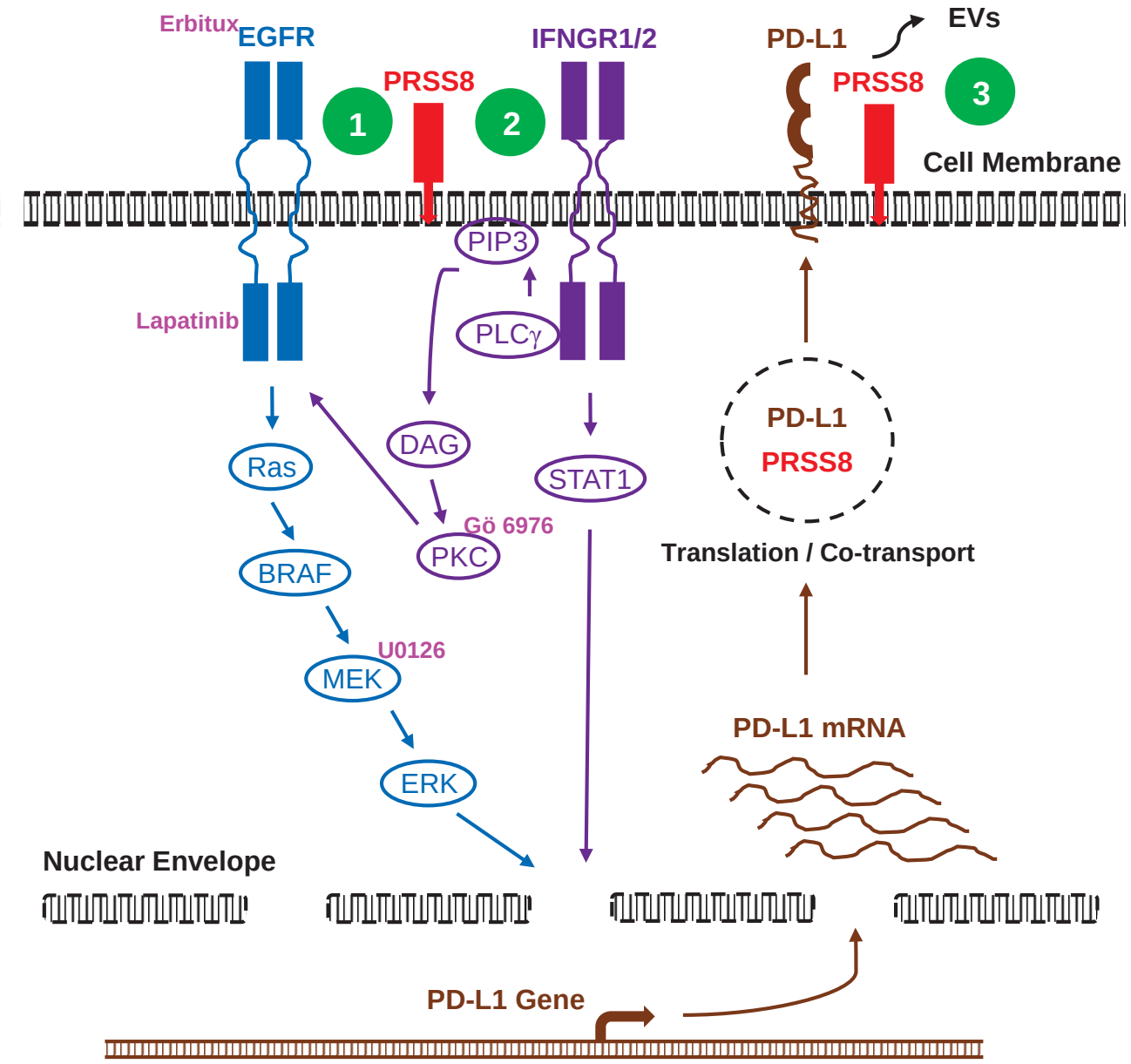

Supplementary Figure 1

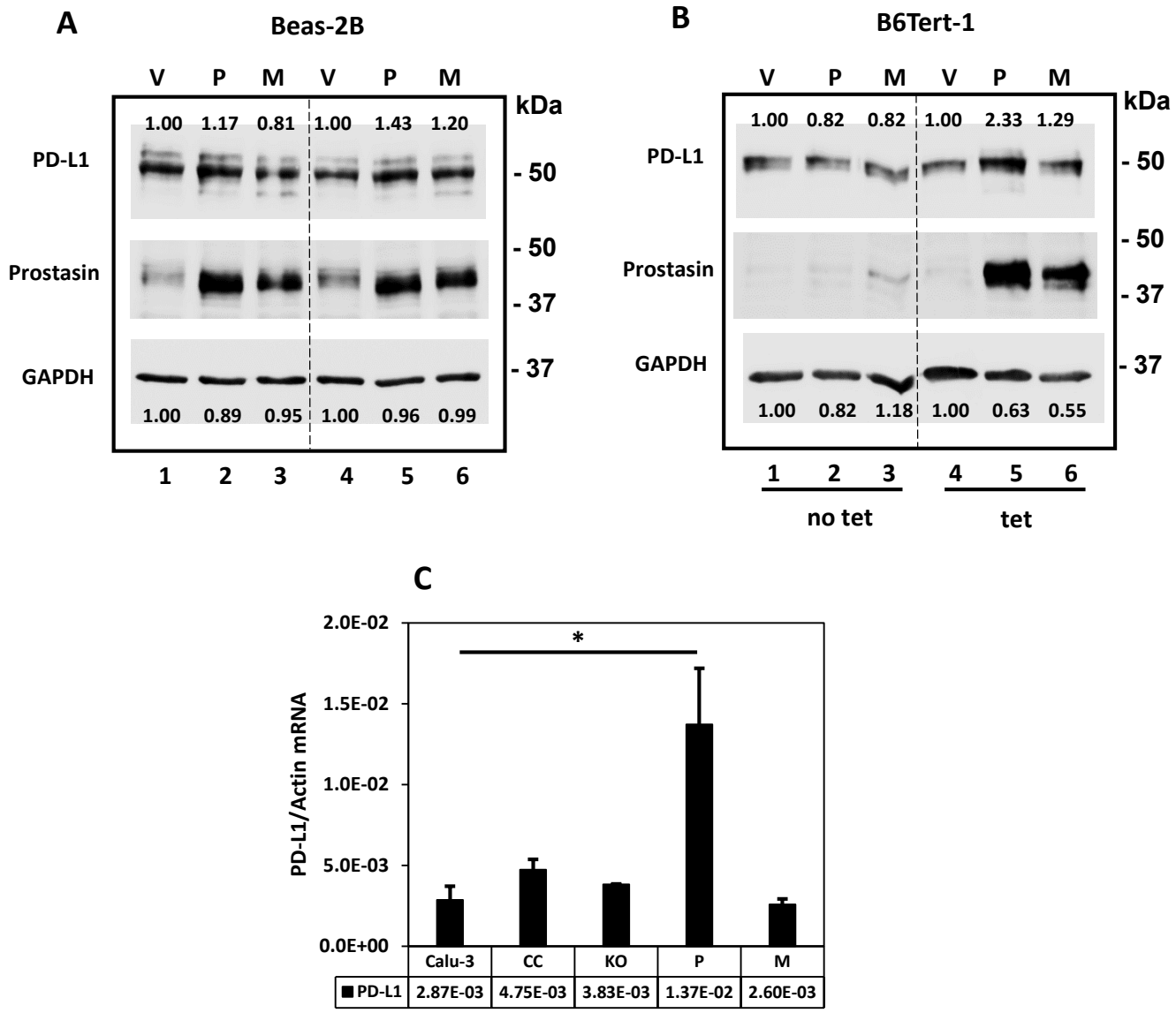

Supplementary Figure 2

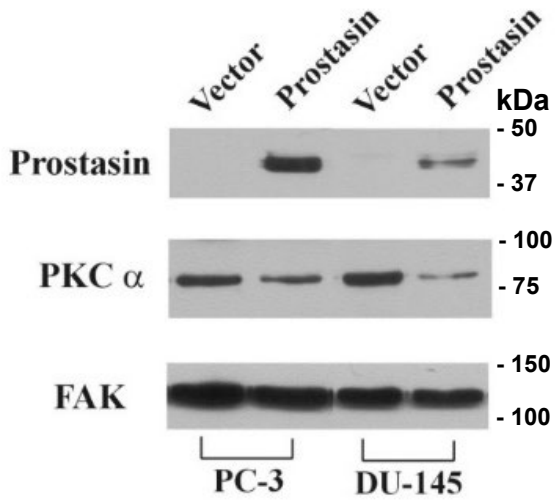

Supplementary Figure 3 (a-h)

a. LUSC High PRSS8 Enriched Gene Sets

LUSC High PRSS8 Enriched Gene Sets (25% FDR)	NES	FDR q-val
HALLMARK_TNFA_SIGNALING_VIA_NFKB	2.9	0
HALLMARK_INTERFERON_GAMMA_RESPONSE	2.9	0
HALLMARK_INFLAMMATORY_RESPONSE	2.8	0
HALLMARK_IL6_JAK_STAT3_SIGNALING	2.6	0
HALLMARK_COAGULATION	2.5	0
HALLMARK_COMPLEMENT	2.5	0
HALLMARK_INTERFERON_ALPHA_RESPONSE	2.5	0
HALLMARK_ALLOGRAFT_REJECTION	2.1	0
HALLMARK_IL2_STAT5_SIGNALING	2.1	0
HALLMARK_APICAL_JUNCTION	2.0	0
HALLMARK_TGF_BETA_SIGNALING	2.0	0
HALLMARK_MYOGENESIS	2.0	0
HALLMARK_ESTROGEN_RESPONSE_EARLY	2.0	0
HALLMARK_BILE_ACID_METABOLISM	2.0	0
HALLMARK_APOPTOSIS	2.0	0
HALLMARK_KRAS_SIGNALING_UP	1.9	0
HALLMARK_HYPOXIA	1.8	2.39E-04
HALLMARK_UV_RESPONSE_DN	1.8	3.81E-04
HALLMARK_EPITHELIAL_MESENCHYMAL_TRANSITION	1.8	0.001179557
HALLMARK_XENOBIOTIC_METABOLISM	1.8	0.001188436
HALLMARK_ANGIOGENESIS	1.8	0.001584159
HALLMARK_ADIPOGENESIS	1.7	0.001991312
HALLMARK_P53_PATHWAY	1.7	0.002751719
HALLMARK_HEME_METABOLISM	1.6	0.003917295
HALLMARK_PEROXISOME	1.5	0.009721883
HALLMARK_ESTROGEN_RESPONSE_LATE	1.5	0.011090398
HALLMARK_CHOLESTEROL_HOMEOSTASIS	1.5	0.012853715
HALLMARK_REACTIVE_OXYGEN_SPECIES_PATHWAY	1.4	0.021902649
HALLMARK_ANDROGEN_RESPONSE	1.4	0.022806939
HALLMARK_FATTY_ACID_METABOLISM	1.3	0.055563193
HALLMARK_UV_RESPONSE_UP	1.3	0.06734516
HALLMARK_APICAL_SURFACE	1.2	0.16197442
HALLMARK_KRAS_SIGNALING_DN	1.2	0.20365763

b. LUSC High CD274 Enriched Gene Sets

LUSC High CD274 Enriched Gene Sets (25% FDR)	NES	FDR q-val
HALLMARK_INTERFERON_GAMMA_RESPONSE	3.7	0
HALLMARK_INTERFERON_ALPHA_RESPONSE	3.5	0
HALLMARK_INFLAMMATORY_RESPONSE	3.4	0
HALLMARK_TNFA_SIGNALING_VIA_NFKB	3.2	0
HALLMARK_ALLOGRAFT_REJECTION	3.1	0
HALLMARK_COMPLEMENT	3.0	0
HALLMARK_IL6_JAK_STAT3_SIGNALING	2.9	0
HALLMARK_IL2_STAT5_SIGNALING	2.7	0
HALLMARK_COAGULATION	2.3	0
HALLMARK_KRAS_SIGNALING_UP	2.3	0
HALLMARK_APOPTOSIS	2.2	0
HALLMARK_REACTIVE_OXYGEN_SPECIES_PATHWAY	2.0	2.23E-04
HALLMARK_HYPOXIA	1.9	2.06E-04
HALLMARK_XENOBIOTIC_METABOLISM	1.9	6.14E-04
HALLMARK_HEME_METABOLISM	1.8	6.55E-04
HALLMARK_TGF_BETA_SIGNALING	1.8	7.09E-04
HALLMARK_MYOGENESIS	1.8	8.09E-04
HALLMARK_UV_RESPONSE_DN	1.8	9.02E-04
HALLMARK_BILE_ACID_METABOLISM	1.8	0.001168116
HALLMARK_APICAL_JUNCTION	1.8	0.001406594
HALLMARK_UV_RESPONSE_UP	1.7	0.002580947
HALLMARK_ESTROGEN_RESPONSE_EARLY	1.7	0.003043273
HALLMARK_EPITHELIAL_MESENCHYMAL_TRANSITION	1.6	0.009378419
HALLMARK_ADIPOGENESIS	1.5	0.012899715
HALLMARK_P53_PATHWAY	1.5	0.020130154
HALLMARK_ANDROGEN_RESPONSE	1.4	0.038793676
HALLMARK_FATTY_ACID_METABOLISM	1.4	0.03879502
HALLMARK_APICAL_SURFACE	1.4	0.038254187
HALLMARK_PROTEIN_SECRETION	1.4	0.050922032
HALLMARK_ESTROGEN_RESPONSE_LATE	1.3	0.07497506
HALLMARK_KRAS_SIGNALING_DN	1.2	0.14584666
HALLMARK_CHOLESTEROL_HOMEOSTASIS	1.2	0.1506702
HALLMARK_PI3K_AKT_MTOR_SIGNALING	1.2	0.19768856

c. LUSC Low PRSS8 Enriched Gene Sets

LUSC Low PRSS8 Enriched Gene Sets (25% FDR)	NES	FDR q-val
HALLMARK_E2F_TARGETS	-3.8	0
HALLMARK_G2M_CHECKPOINT	-3.6	0
HALLMARK_MYC_TARGETS_V1	-3.4	0
HALLMARK_MYC_TARGETS_V2	-3.1	0
HALLMARK_MITOTIC_SPINDLE	-2.1	1.04E-04
HALLMARK_SPERMATOGENESIS	-2.0	8.70E-05
HALLMARK_MTORC1_SIGNALING	-1.9	1.60E-04
HALLMARK_OXIDATIVE_PHOSPHORYLATION	-1.8	4.34E-04
HALLMARK_DNA_REPAIR	-1.8	3.86E-04
HALLMARK_UNFOLDED_PROTEIN_RESPONSE	-1.7	0.001982023

d. LUSC Low CD274 Enriched Gene Sets

LUSC Low CD274 Enriched Gene Sets (25% FDR)	NES	FDR q-val
HALLMARK_E2F_TARGETS	-3.0	0
HALLMARK_G2M_CHECKPOINT	-2.9	0
HALLMARK_MYC_TARGETS_V1	-2.8	0
HALLMARK_MYC_TARGETS_V2	-2.4	0
HALLMARK_OXIDATIVE_PHOSPHORYLATION	-1.9	9.45E-04
HALLMARK_DNA_REPAIR	-1.8	0.00147399
HALLMARK_SPERMATOGENESIS	-1.8	0.001415876
HALLMARK_MITOTIC_SPINDLE	-1.3	0.060848035

e. LUAD High PRSS8 Enriched Gene Sets

LUAD High PRSS8 Enriched Gene Sets (25% FDR)	NES	FDR q-val
HALLMARK_INTERFERON_ALPHA_RESPONSE	2.7	0
HALLMARK_INTERFERON_GAMMA_RESPONSE	2.1	6.58E-04
HALLMARK_IL6_JAK_STAT3_SIGNALING	1.9	4.39E-04
HALLMARK_TNFA_SIGNALING_VIA_NFKB	1.8	0.007567337
HALLMARK_P53_PATHWAY	1.7	0.007077679
HALLMARK_INFLAMMATORY_RESPONSE	1.7	0.009387618
HALLMARK_APICAL_JUNCTION	1.6	0.010865434
HALLMARK_CHOLESTEROL_HOMEOSTASIS	1.6	0.01064314
HALLMARK_ALLOGRAFT_REJECTION	1.4	0.06476901
HALLMARK_PEROXISOME	1.4	0.08273839
HALLMARK_GLYCOLYSIS	1.3	0.08865474
HALLMARK_COMPLEMENT	1.3	0.09164486
HALLMARK_COAGULATION	1.3	0.10120447
HALLMARK_APOPTOSIS	1.3	0.09475186
HALLMARK_IL2_STAT5_SIGNALING	1.2	0.15677549
HALLMARK_ESTROGEN_RESPONSE_EARLY	1.2	0.17921966
HALLMARK_NOTCH_SIGNALING	1.2	0.2382772
HALLMARK_KRAS_SIGNALING_DN	1.2	0.2343269

f. LUAD High CD274 Enriched Gene Sets

LUAD High CD274 Enriched Gene Sets (25% FDR)	NES	FDR q-val
HALLMARK_INTERFERON_GAMMA_RESPONSE	3.9	0
HALLMARK_ALLOGRAFT_REJECTION	3.8	0
HALLMARK_INFLAMMATORY_RESPONSE	3.5	0
HALLMARK_TNFA_SIGNALING_VIA_NFKB	3.5	0
HALLMARK_INTERFERON_ALPHA_RESPONSE	3.4	0
HALLMARK_IL6_JAK_STAT3_SIGNALING	3.2	0
HALLMARK_COMPLEMENT	2.9	0
HALLMARK_IL2_STAT5_SIGNALING	2.7	0
HALLMARK_KRAS_SIGNALING_UP	2.7	0
HALLMARK_APOPTOSIS	2.5	0
HALLMARK_APICAL_JUNCTION	2.4	0
HALLMARK_TGF_BETA_SIGNALING	2.2	0
HALLMARK_EPITHELIAL_MESENCHYMAL_TRANSITION	2.1	0
HALLMARK_HYPOXIA	1.9	1.02E-04
HALLMARK_COAGULATION	1.9	3.24E-04
HALLMARK_UV_RESPONSE_DN	1.8	5.87E-04
HALLMARK_APICAL_SURFACE	1.7	0.003995385
HALLMARK_ANGIOGENESIS	1.6	0.006372829
HALLMARK_P53_PATHWAY	1.5	0.012783593
HALLMARK_PI3K_AKT_MTOR_SIGNALING	1.5	0.023198167
HALLMARK_MYOGENESIS	1.4	0.030198675
HALLMARK_HEME_METABOLISM	1.4	0.047247607
HALLMARK_HEDGEHOG_SIGNALING	1.4	0.050490916
HALLMARK_MITOTIC_SPINDLE	1.3	0.08157678
HALLMARK_CHOLESTEROL_HOMEOSTASIS	1.2	0.15549049
HALLMARK_UV_RESPONSE_UP	1.2	0.1805793

g. LUAD Low PRSS8 Enriched Gene Sets

LUAD Low PRSS8 Enriched Gene Sets (25% FDR)	NES	FDR q-val
HALLMARK_E2F_TARGETS	-3.1	0
HALLMARK_G2M_CHECKPOINT	-3.0	0
HALLMARK_MYC_TARGETS_V1	-2.5	0
HALLMARK_SPERMATOGENESIS	-2.1	0
HALLMARK_MITOTIC_SPINDLE	-2.0	0
HALLMARK_EPITHELIAL_MESENCHYMAL_TRANSITION	-2.0	1.16E-04
HALLMARK_MYC_TARGETS_V2	-1.9	5.12E-04
HALLMARK_MTORC1_SIGNALING	-1.8	0.001880215
HALLMARK_UV_RESPONSE_DN	-1.5	0.034481023
HALLMARK_UNFOLDED_PROTEIN_RESPONSE	-1.3	0.12530452
HALLMARK_OXIDATIVE_PHOSPHORYLATION	-1.3	0.16235016

h. LUAD Low CD274 Enriched Gene Sets

LUAD Low CD274 Enriched Gene Sets (25% FDR)	NES	FDR q-val
HALLMARK_OXIDATIVE_PHOSPHORYLATION	-2.6	0
HALLMARK_MYC_TARGETS_V1	-2.4	0
HALLMARK_E2F_TARGETS	-2.0	0
HALLMARK_MYC_TARGETS_V2	-1.9	5.70E-04
HALLMARK_UNFOLDED_PROTEIN_RESPONSE	-1.7	0.004312027
HALLMARK_FATTY_ACID_METABOLISM	-1.6	0.010758515
HALLMARK_G2M_CHECKPOINT	-1.6	0.012803096
HALLMARK_SPERMATOGENESIS	-1.6	0.011908125
HALLMARK_GLYCOLYSIS	-1.5	0.02734927
HALLMARK_DNA_REPAIR	-1.4	0.033594772
HALLMARK_ADIPOGENESIS	-1.4	0.042960566
HALLMARK_MTORC1_SIGNALING	-1.3	0.079123646
HALLMARK_XENOBIOTIC_METABOLISM	-1.3	0.09165737
HALLMARK_PANCREAS_BETA_CELLS	-1.3	0.12316957
HALLMARK_PEROXISOME	-1.2	0.16723569
HALLMARK_ESTROGEN_RESPONSE_LATE	-1.2	0.19401155

Supplementary Figure 4

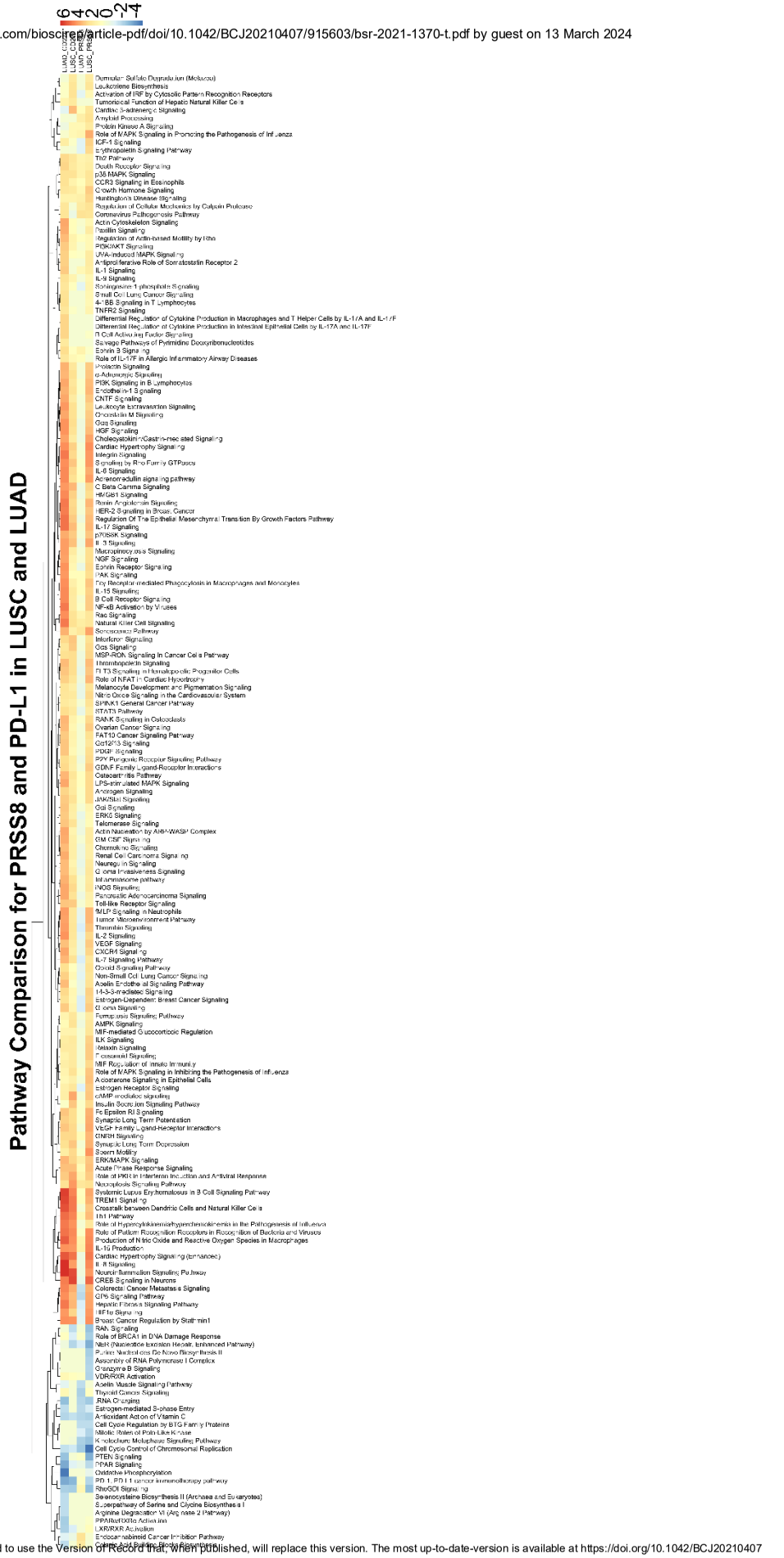

Supplementary Figure 5 (a-g, uncropped Western blot images)

All images are overlays of ink-stained membrane (with molecular weight markers) and the corresponding chemiluminescent blot.

Supplementary Figure 5a: Figure 1_uncropped images

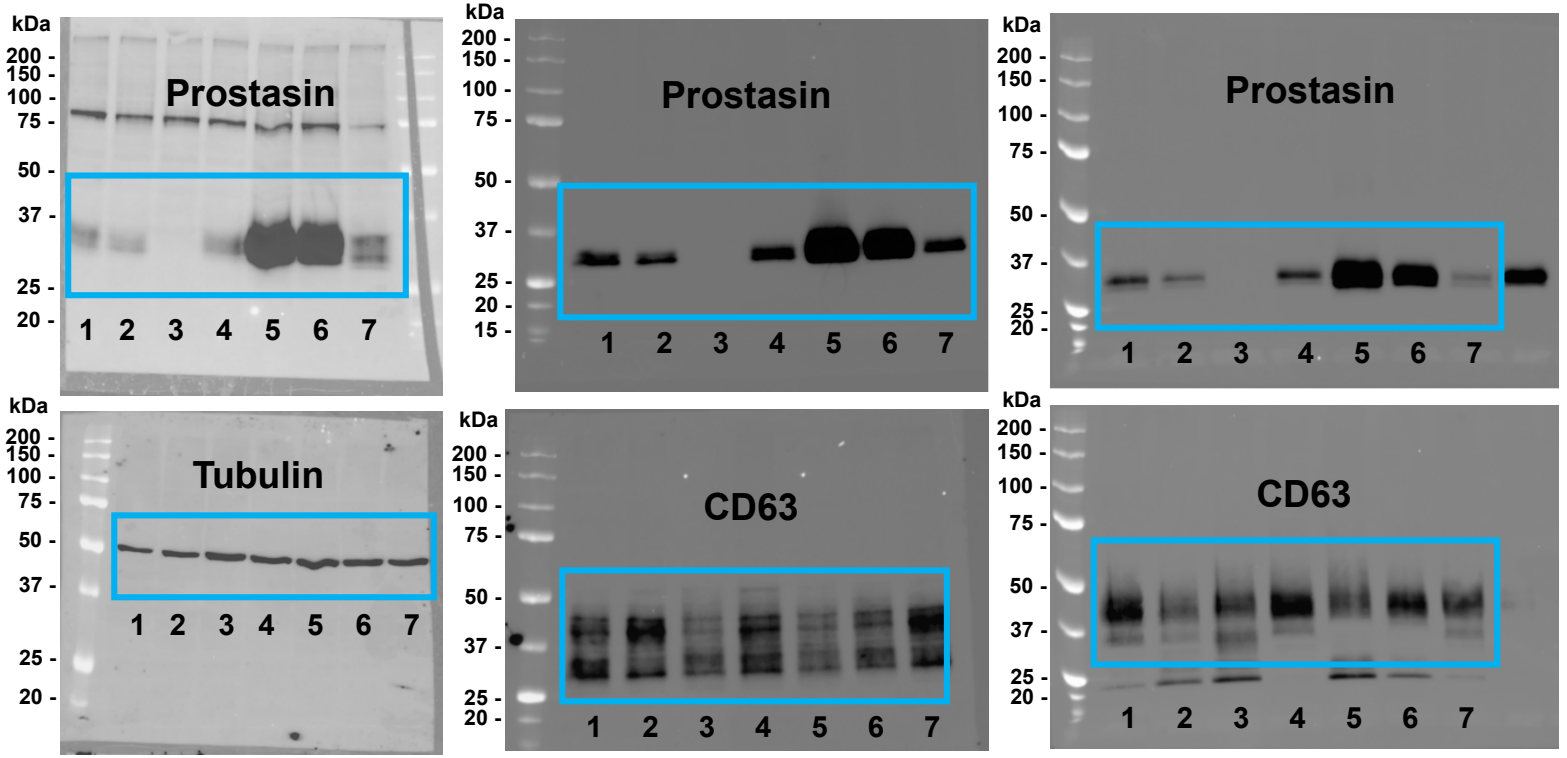

Supplementary Figure 5b: Figure 2_uncropped images

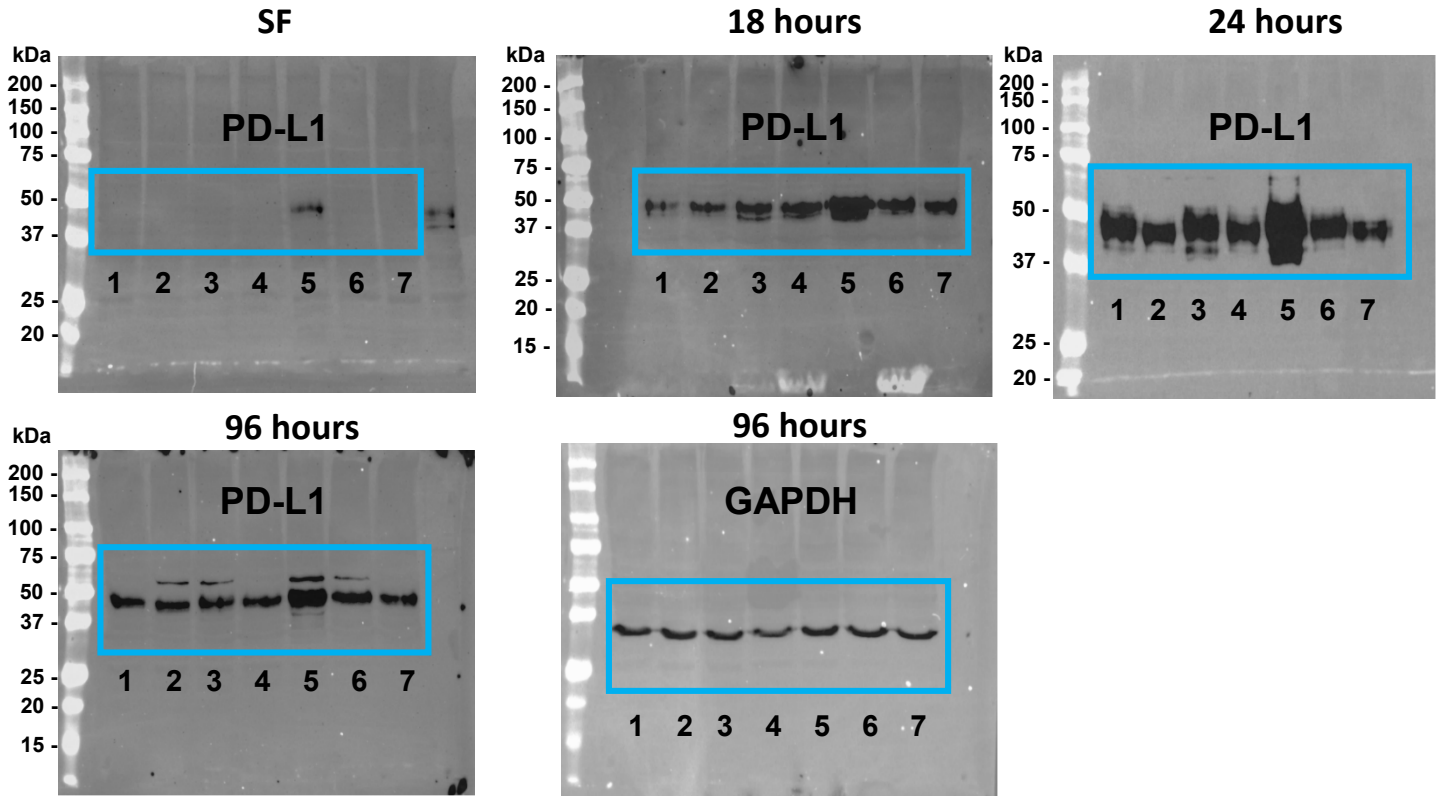

Supplementary Figure 5c: Figure 4_uncropped images

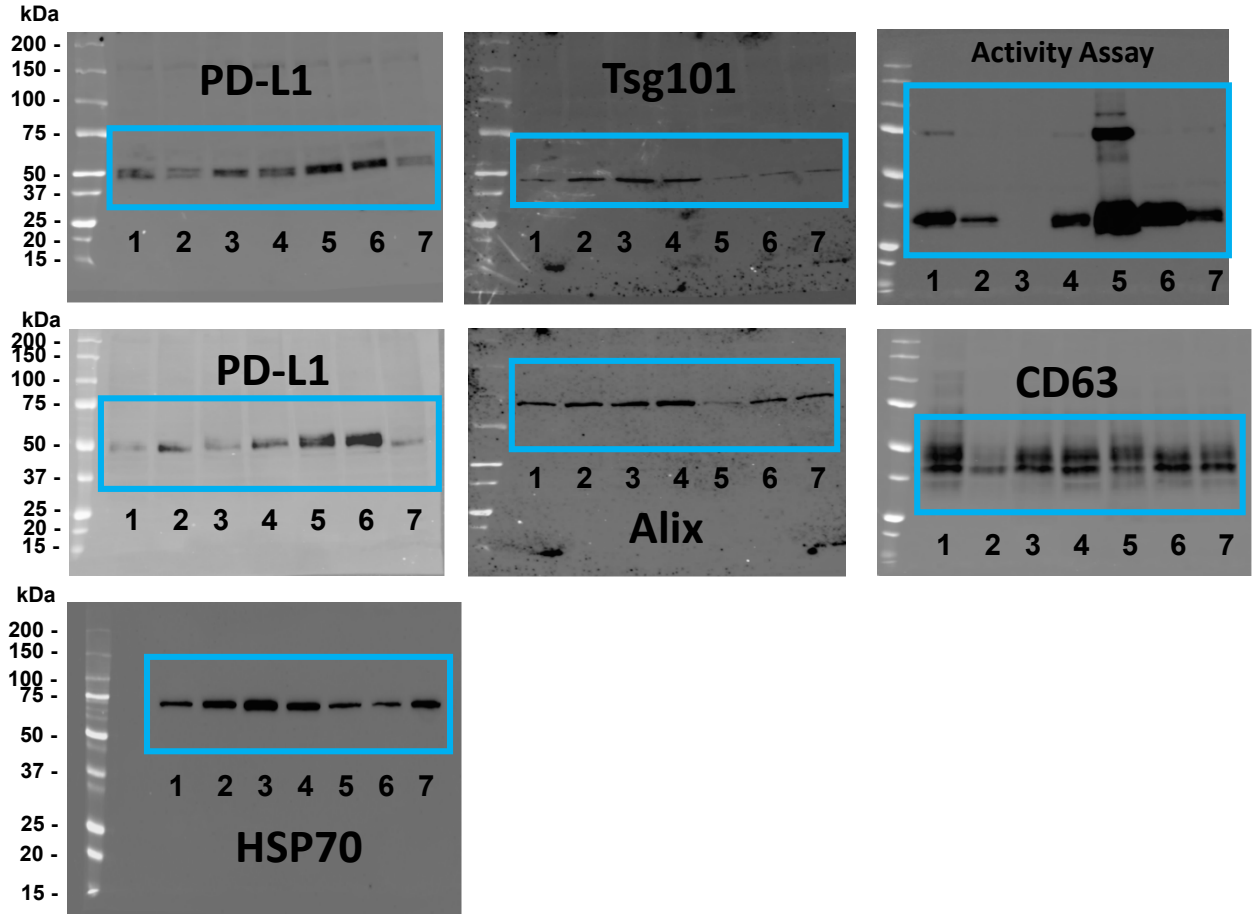

Supplementary Figure 5d: Figure 5_uncropped images

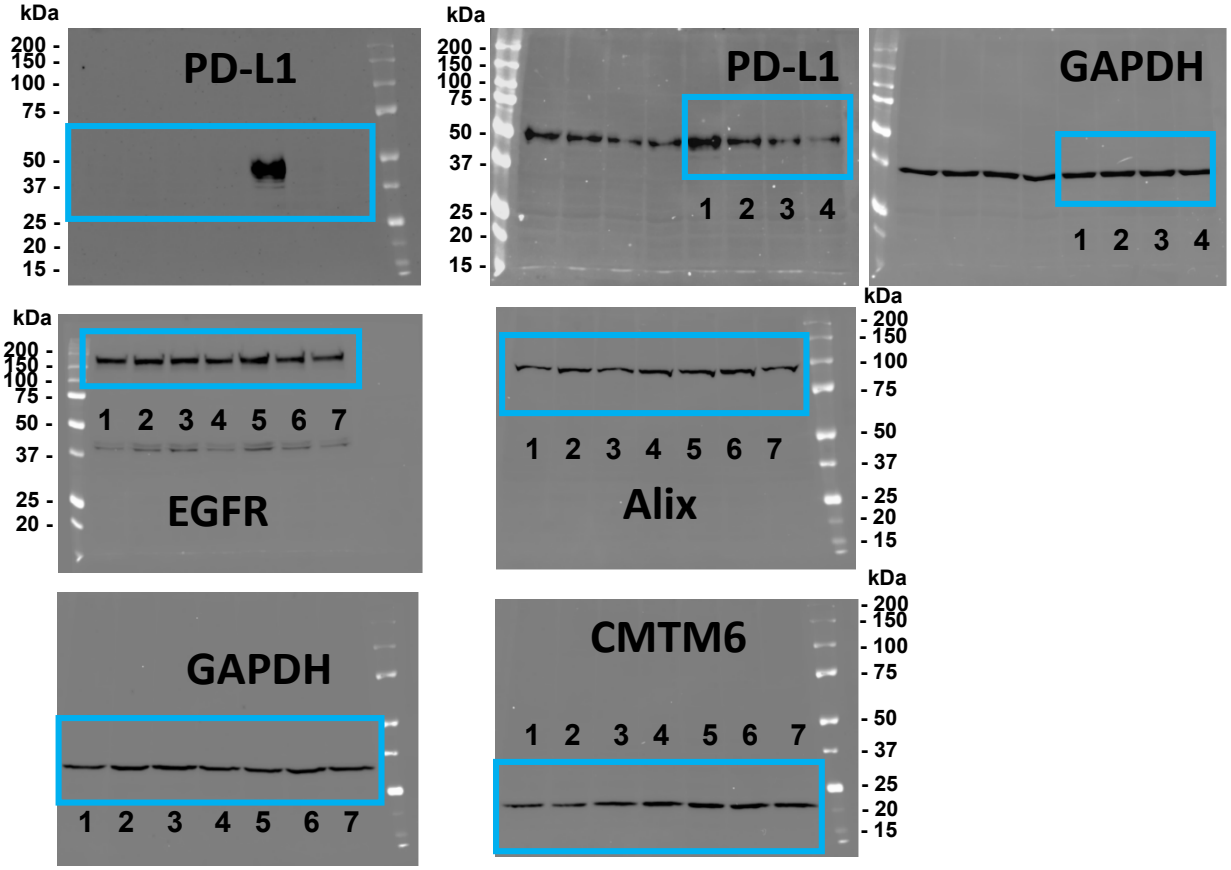

Supplementary Figure 5e: Figure 6_uncropped images

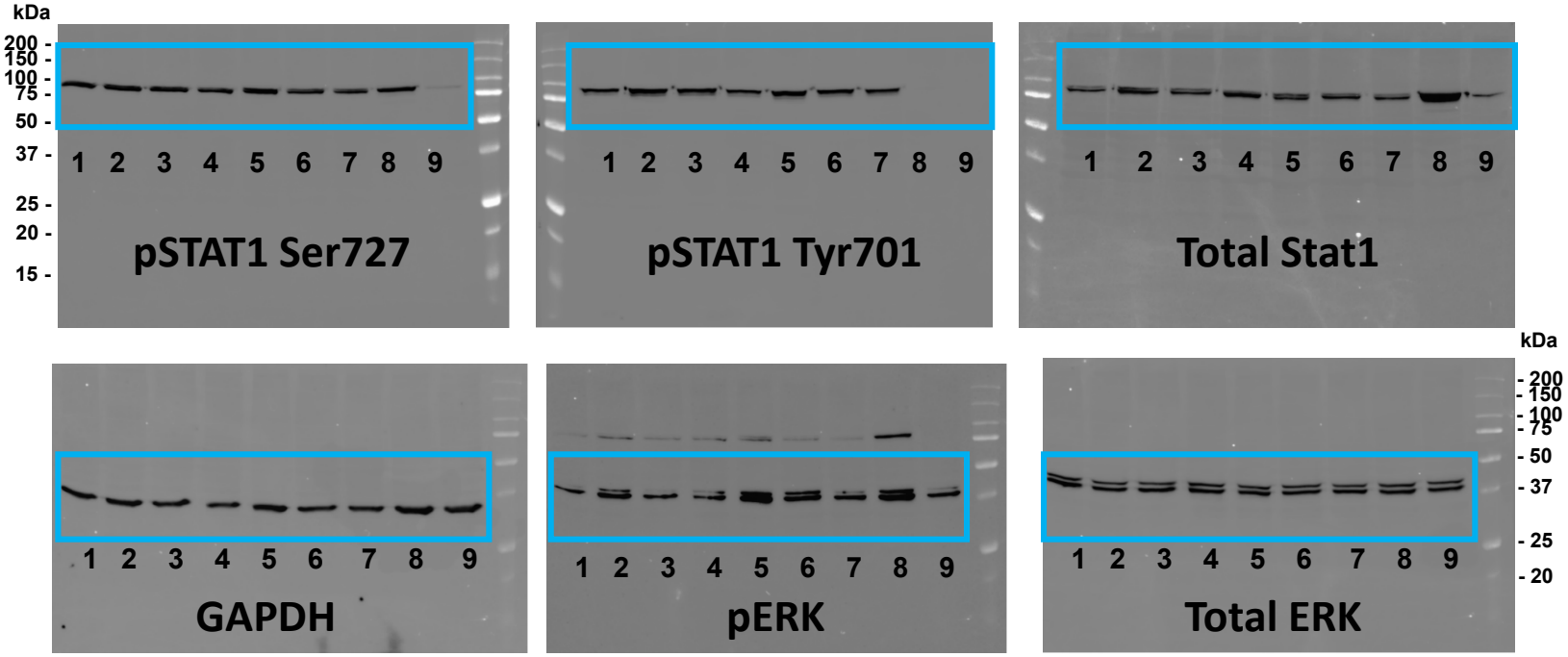

Supplementary Figure 5f: Figure 7_uncropped images

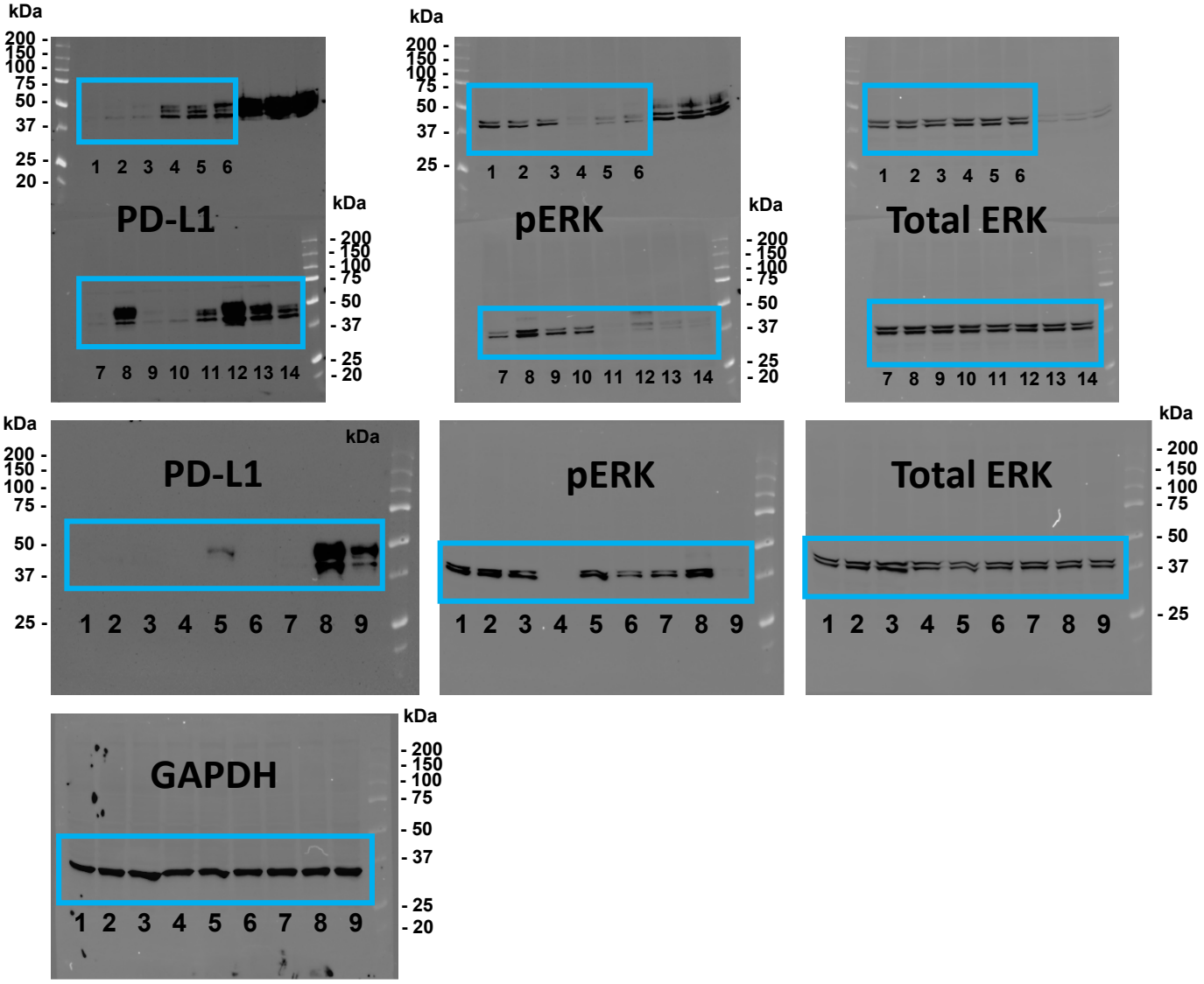

Supplementary Figure 5g: Figure 8_uncropped images